TKK Dissertations 114
Espoo 2008

MONITORING DEPTH OF ANESTHESIA WITH ELECTROENCEPHALOGRAM: METHODS AND PERFORMANCE EVALUATION

Doctoral Dissertation

Mika Särkelä

Helsinki University of Technology
Faculty of Information and Natural Sciences
Department of Biomedical Engineering and Computational Science

TKK Dissertations 114
Espoo 2008

MONITORING DEPTH OF ANESTHESIA WITH ELECTROENCEPHALOGRAM: METHODS AND PERFORMANCE EVALUATION

Doctoral Dissertation

Mika Särkelä

Dissertation for the degree of Doctor of Science in Technology to be presented with due permission of the Faculty of Information and Natural Sciences for public examination and debate in Auditorium TU1 at Helsinki University of Technology (Espoo, Finland) on the 18th of April, 2008, at 12 noon.

Helsinki University of Technology
Faculty of Information and Natural Sciences
Department of Biomedical Engineering and Computational Science

Teknillinen korkeakoulu
Informaatio- ja luonnontieteiden tiedekunta
Lääketieteellisen tekniikan ja laskennallisen tieteen laitos

Distribution:
Helsinki University of Technology
Faculty of Information and Natural Sciences
Department of Biomedical Engineering and Computational Science
P.O. Box 3310
FI - 02015 TKK
FINLAND
URL: http://www.becs.tkk.fi/
Tel. +358-9-451 3172
Fax +358-9-451 3182
E-mail: mika.sarkela@ge.com

ISBN 978-951-22-9288-2
ISBN 978-951-22-9289-9 (PDF)
ISSN 1795-2239
ISSN 1795-4584 (PDF)
URL: http://lib.tkk.fi/Diss/2008/isbn9789512292899/

TKK-DISS-2451

Picaset Oy
Helsinki 2008

ABSTRACT OF DOCTORAL DISSERTATION	HELSINKI UNIVERSITY OF TECHNOLOGY P. O. BOX 1000, FI-02015 TKK http://www.tkk.fi

Author Mika Särkelä

Name of the dissertation

Monitoring depth of anesthesia with electroencephalogram: Methods and performance evaluation

Manuscript submitted Dec. 11, 2007	Manuscript revised Mar. 10, 2008
Date of the defence Apr. 18, 2008	
☐ Monograph	☒ Article dissertation (summary + original articles)

Faculty	Faculty of Information and Natural Sciences
Department	Department of Biomedical Engineering and Computational Science
Field of research	Biomedical Engineering
Opponent(s)	Professor Guy Dumont, University of British Columbia
Supervisor	Professor Pekka Meriläinen
Instructor	Hanna Viertiö-Oja, D.Sc. (Tech.)

Abstract

In monitoring depth of anesthesia, use of electroencephalogram (EEG) signal data helps to prevent intraoperative awareness and reduces the costs of anesthesia. Modern depth-of-anesthesia monitors use frontal EEG signal to derive an index value, which decreases monotonically with increasing anesthetic drug levels. In this study, electroencephalogram signal processing methods for depth-of-anesthesia monitoring were developed.

The first aim was to develop a method for burst suppression detection and integrate it into the anesthetic depth monitor. Accurate detection of burst suppression improves the accuracy of depth-of-anesthesia monitoring at deep levels of anesthesia. The method developed utilizes a nonlinear energy operator and is based on adaptive segmentation. The developed monitor has been proven accurate in several scientific studies.

A second aim was to develop a depth-of-anesthesia monitor that utilizes both cortical and subcortical information and is applicable with most commonly used anesthetics. The method developed is based on the spectral entropy of EEG and facial electromyogram (EMG) signals. In the method, two spectral entropy variables are derived, aiming to differentiate the cortical state of the patient and subcortical responses during surgery. The concept has been confirmed in the scientific studies conducted during surgery.

Another aim was to develop a method for monitoring epileptiform activity during anesthesia. The method developed is based on a novel EEG-derived quantity, wavelet subband entropy (WSE), which followed the time evolution of epileptiform activity in anesthesia with prediction probability of 0.8 and recognized misleading readings of the depth-of-anesthesia monitor during epileptiform activity with event-sensitivity of 97%.

The fourth aim was to investigate the monitoring technique developed, called Entropy, in S-ketamine anesthesia and in dexmedetomidine sedation. In S-ketamine anesthesia, high-frequency EEG oscillations turned out to be the reason for the high entropy values seen despite deep anesthesia. In dexmedetomidine sedation, Entropy proved a rapid indicator of transition phases from conscious and unconscious states.

Keywords anesthesia, burst suppression, EEG, entropy, wavelet	
ISBN (printed) 978-951-22-9288-2	ISSN (printed) 1795-2239
ISBN (pdf) 978-951-22-9289-9	ISSN (pdf) 1795-4584
Language English	Number of pages 118 + 57 (app)
Publisher Department of Biomedical Engineering and Computational Science, Helsinki University of Technology	
Print distribution Department of Biomedical Engineering and Computational Science	
☒ The dissertation can be read at http://lib.tkk.fi/Diss/2008/isbn9789512292899/	

VÄITÖSKIRJAN TIIVISTELMÄ	TEKNILLINEN KORKEAKOULU PL 1000, 02015 TKK http://www.tkk.fi

Tekijä Mika Särkelä

Väitöskirjan nimi

Anestesian syvyyden monitoroiminen aivosähkökäyrän avulla: Menetelmät sekä menetelmien suorituskyvyn arviointi

Käsikirjoituksen päivämäärä 11.12.2007	Korjatun käsikirjoituksen päivämäärä 10.3.2008
Väitöstilaisuuden ajankohta 18.4.2008	
☐ Monografia	☒ Yhdistelmäväitöskirja (yhteenveto + erillisartikkelit)

Tiedekunta	Informaatio- ja luonnontieteiden tiedekunta
Laitos	Lääketieteellisen tekniikan ja laskennallisen tieteen laitos
Tutkimusala	Lääketieteellinen tekniikka
Vastaväittäjä(t)	Professori Guy Dumont, University of British Columbia
Työn valvoja	Professori Pekka Meriläinen
Työn ohjaaja	TkT Hanna Viertiö-Oja

Tiivistelmä

Anestesian syvyyttä monitoroitaessa aivosähkökäyrä (EEG) auttaa välttämään potilaan kirurgian aikaisen tietoisuuden tunteen sekä pienentämään anestesian kustannuksia. Anestesian syvyyden monitorit laskevat otsalta mitatusta EEG-signaalista numeroarvon, joka pienenee monotonisesti anestesialääkityksen kasvaessa. Tässä työssä kehitettiin EEG-signaalinkäsittelymenetelmiä anestesian syvyyden monitorointiin.

Työn ensimmäinen tavoite oli kehittää menetelmä purskevaimentuman ilmaisemiseksi ja yhdistää tämä osaksi anestesian syvyyden monitoria, parantaen monitoroinnin tarkkuutta syvässä anestesiassa. Kehitetty menetelmä perustuu adaptiiviseen segmentointiin, jossa hyödynnetään epälineaarista energiaoperaattoria. Kehitetty monitori on osoittautunut tarkaksi menetelmäksi lukuisissa tieteellisissä tutkimuksissa.

Toinen tavoite oli kehittää menetelmä anestesian syvyyden monitorointiin, joka hyödyntää sekä aivokuorelta peräisin olevaa EEG-signaalia, että osittain aivorungosta peräisin olevaa kasvolihasten lihassähkökäyrää (EMG). Kehitetty menetelmä perustuu EEG- ja EMG-signaaleista laskettavaan spektraaliseen entropiaan. Menetelmä tuottaa kaksi muuttujaa, joiden avulla pyritään erottamaan potilaan aivokuoren tila sekä kirurgian aiheuttamat aivorunkovasteet. Tieteeliset tutkimukset ovat osoittaneet konseptin toimivuuden kirurgian aikaiseen monitorointiin.

Kolmas tavoite oli kehittää menetelmä anestesian aikaisen epileptiformisen aivotoiminnan monitorointiin. Työssä kehitettiin täysin uusi EEG-signaalista johdettu suure; aallokemuunnoksen osakaistan entropia (WSE). WSE kykeni seuraaman epileptiformisen toiminnan kehitystä ennustetodennäköisyydellä 0,8 sekä tunnisti 97 %:sti tämän aiheuttamat harhaanjohtavat tapaukset anestesian syvyyden monitorin lukemissa.

Lisäksi työssä arvioitiin kehitetyn Entropia-monitorin suorituskykyä S-ketamiinianestesiassa sekä deksmedetomidiinisedaatiossa. S-ketamiinianestesiassa korkeataajuiset EEG-oskillaatiot olivat syynä korkeille Entropia-arvoille huolimatta syvästä anestesiasta. Deksmedetomidiinisedaatiossa Entropia-monitori kykeni seuraamaan nopeita muutoksia tajuisuuden ja tajuttomuuden välillä.

Asiasanat	aalloke, anestesia, EEG, entropia, purskevaimentuma		
ISBN (painettu)	978-951-22-9288-2	ISSN (painettu)	1795-2239
ISBN (pdf)	978-951-22-9289-9	ISSN (pdf)	1795-4584
Kieli	englanti	Sivumäärä	118 + 57 (liitteet)
Julkaisija	Lääketieteellisen tekniikan ja laskennallisen tieteen laitos, Teknillinen korkeakoulu		
Painetun väitöskirjan jakelu	Lääketieteellisen tekniikan ja laskennallisen tieteen laitos		
☒ Luettavissa verkossa osoitteessa http://lib.tkk.fi/Diss//2008/isbn9789512292899/			

Preface

This thesis is a result of a long journey. The work has been mostly carried out in Research Unit of GE Healthcare Finland Oy during 2000-07. The first steps of this work was already taken in Department of Anesthesiology, Oulu University Hospital, Finland in 1999-2000.

I wish to express my gratitude to professor Pekka Meriläinen for providing me the opportunity for this thesis work and for his support during all these years. Pekka has been acting as my manager in GE Healthcare as well as my supervisor in Helsinki University of Technology. Hanna Viertiö-Oja, D.Sc. (Tech.), is appreciated of instruction she has offered in the scientific field of anesthetic depth monitoring as well as significant help in the final steps of this thesis. Pre-examiners professor Pasi Karjalainen and docent Ilkka Korhonen are appreciated for their valuable comments.

From the years in Oulu, professor Tapio Seppänen is acknowledged for introducing me the interesting world of signal processing and docent Ville Jäntti for familiarizing me with the odd-looking waveforms called EEG. I am grateful to professor Seppo Alahuhta, head of Department of Anesthesiology for his positive attitude toward this thesis project.

Anne Vakkuri, M.D., Ph.D., is appreciated for her significant role in the development of Entropy monitor as well as scientific advises considering the publication of wavelet subband entropy. Professor Arvi Yli-Hankala is acknowledged for his pioneering work in the field of anesthesia EEG that, among others results, led to the development of Entropy monitor and wavelet subband entropy. Docent Mark van Gils and mr. Miikka Ermes, M.Sc. (Tech.), both from VTT Technical Research Centre of Finland are appreciated for the co-operation in the development of wavelet subband entropy.

Part of this thesis work has been conducted in collaboration with Turku PET Centre and Turku University Hospital, Finland. It was pleasure to work with this enthusiastic research group that has offered in-depth understanding of anesthesia mechanisms. Especially, I wish to express my gratitude to professor Harry Scheinin, docent Satu Jääskeläinen, and mrs. Anu Maksimow, M.D., Ph.D. Anu has a major contribution for this thesis as being the first author of two publications.

I express my special gratitude to all 30 co-authors of the five publications constituting this thesis. This work is a result of several projects carried out in industry, research institutes, central hospital, and in four of the total five university hospitals in Finland. It has been a rewarding experience to work with all these people each representing top knowledge in their own speciality.

My colleagues in GE Healthcare and Oulu University Hospital are appreciated for their support during this almost endless thesis project. Especially, I wish to thank mr. Matti Huiku, D.Sc. (Tech.), for his guidance and encouragement during the last few years. Mr. Petteri Lapinlampi, M.Sc. (Tech.), is acknowledged for guiding me in the practicality of Helsinki University of Technology and support with LaTeX typesetting.

I wish to thank my parents, Anja and Sakari Särkelä for their support. Finally, I would like to thank my dear Sirkku for her love, patience, and understanding.

Helsinki, 10th of March, 2008

Contents

List of Publications

This thesis consists of an overview and of the following publications, which are referred to in the text by their Roman numerals.

I M. Särkelä, S. Mustola, T. Seppänen, M. Koskinen, P. Lepola, K. Suominen, T. Juvonen, H. Tolvanen-Laakso, V. Jäntti. 2002. Automatic analysis and monitoring of burst suppression in anesthesia. Journal of Clinical Monitoring and Computing 17, no. 2, pages 125-134.

II H. Viertiö-Oja, V. Maja, M. Särkelä, P. Talja, N. Tenkanen, H. Tolvanen-Laakso, M. Paloheimo, A. Vakkuri, A. Yli-Hankala, P. Meriläinen. 2004. Description of the Entropy$^{\text{TM}}$ algorithm as applied in the Datex-Ohmeda S/5$^{\text{TM}}$ Entropy module. Acta Anaesthesiologica Scandinavica 48, no. 2, pages 154-161.

III M.O.K. Särkelä, M.J. Ermes, M.J. van Gils, A.M. Yli-Hankala, V.H. Jäntti, A.P. Vakkuri. 2007. Quantification of epileptiform electroencephalographic activity during sevoflurane mask induction. Anesthesiology 107, no. 6, pages 928-938.

IV A. Maksimow, M. Särkelä, J.W. Långsjö, E. Salmi, K.K. Kaisti, A. Yli-Hankala, S. Hinkka-Yli-Salomäki, H. Scheinin, S.K. Jääskeläinen. 2006. Increase in high frequency EEG activity explains the poor performance of EEG spectral entropy monitor during S-ketamine anesthesia. Clinical Neurophysiology 117, no. 8, pages 1660-1668.

V A. Maksimow, A. Snapir, M. Särkelä, E. Kentala, J. Koskenvuo, J. Posti, S.K. Jääskeläinen, S. Hinkka-Yli-Salomäki, M. Scheinin, H. Scheinin. 2007. Assessing the depth of dexmedetomidine-induced sedation with electroencephalogram (EEG)-based spectral entropy. Acta Anaesthesiologica Scandinavica 51, no. 1, pages 22-31.

Author's contribution

In Publication **I**, the author describes methods developed for the detection and representation of burst suppression patterns. The author compares the performance of the detection method developed against the earlier method. The author had primary responsibility for the manuscript's production.

Publication **II** describes the algorithm of the commercially available Entropy™ monitor. The author developed the burst suppression detection method further and integrated it into the Entropy monitor, contributing to the development of the Entropy monitor also by developing the front-line measurement and signal processing software for the device.

Publication **III** describes a method the author developed for the monitoring of epileptiform electroencephalographic activity. The author identified the demand for the application and established the structure of the study. The author participated in the performance evaluation work and had primary responsibility for the manuscript's production.

For the work described in Publication **IV**, the author conducted performance evaluations for the Entropy monitor during S-ketamine anesthesia. The author investigated reasons for poor performance and conducted quantitative electroencephalogram analysis for the subjects in S-ketamine and propofol anesthesia.

In the work covered by Publication **V**, the author conducted performance evaluation for the Entropy monitor during dexmedetomidine sedation and quantitative electroencephalogram analysis.

List of Abbreviations

AW	Awake electroencephalographic activity
BcSEF	Burst-compensated spectral edge frequency
BcSpEn	Burst-compensated spectral entropy
Bic	Bicoherence index
BIS	Bispectral Index Scale
BIS-XP	Dual-channel XP-level version of BIS
BS	Burst suppression electroencephalographic activity
BSR	Burst suppression ratio
CUP	Canonical univariate parameter
cWSE	Combined wavelet subband entropy
CWT	Continuous wavelet transform
D	Delta electroencephalographic activity
DC	Direct current
DFT	Discrete Fourier transform
DS	Slow delta electroencephalographic activity
DSM	Slow-delta monophasic electroencephalographic activity
DSMS	Slow-delta monophasic electroencephalographic activity with spikes
DWT	Discrete wavelet transform
EEG	Electroencephalogram
EMG	Electromyogram
FFT	Fast Fourier transform
FN	Number of false negative classifications
FP	Number of false positive classifications
FWT	Fast wavelet transform
GABA	Gamma-aminobutyric acid
$GABA_A$	Gamma-aminobutyric acid receptor subtype A
ICU	Intensive care unit
LOC	Loss of consciousness
MAP	Mean arterial pressure
MF	Median frequency, 50% spectral edge frequency
NLEO	Nonlinear energy operator
NMDA	*N*-methyl-D-aspartate

NPV	Negative predictive value
OAAS	Observer's assessment of alertness/sedation scale
PD	Periodic electroencephalographic discharges
PK–PD	Pharmacokinetic–pharmacodynamic
PPV	Positive predictive value
PSD	Power spectral density
qEEG	Quantitative electroencephalogram
RE	Response entropy
RWE	Relative wavelet energy
ROC	Return of consciousness
ROC	Receiver operating characteristics
SBS	Burst suppression electroencephalographic activity with spikes
SD	Standard deviation
SE	State entropy
SEF	Spectral edge frequency
SpEn	Spectral entropy
TEO	Teager's energy operator
TN	Number of true negative classifications
TP	Number of true positive classifications
WE	Wavelet entropy
WSE	Wavelet subband entropy
WSMF	Weighted spectral median frequency

List of Symbols

B	Cross-biperiodogram, an estimate of bispectrum
C_e	Effect-site concentration
C_{et}	End-tidal concentration
C_p	Plasma concentration
E	Energy
$E\{\cdot\}$	Expected value of the estimate
E_{max}	The maximum possible drug effect
E_0	The effect in baseline conditions, without drug
EC_{50}	The effect-site concentration associated with 50% of maximal drug effect
H	Shannon entropy
H_{rel}	Relative form of Shannon entropy
I	Self-information
P	Periodogram, an estimate of power spectrum
P_c	Probability of concordance
P_d	Probability of disconcordance
P_K	Prediction probability
P_{tx}	Probability of indicator-only tie
R	Correlation coefficient
R^2	Coefficient of determination
X	Fourier transform of signal x
$\overline{X}$	Vector of random variables x_i
W	Fourier transform of window function w
W	Wavelet transform of signal x
Ψ	Operator
Ψ	Fourier transform of the wavelet function ψ
a_j	Approximation coefficient of scale j
d_j	Detail coefficient of scale j
e	Neper's value
f	Spline function
h_ψ	Wavelet filter coefficients
h_φ	Scaling coefficients
j	Imaginary unit

j	Fixed value scale of the discrete wavelet transform
k	Translation index of the discrete wavelet transform
k_{e0}	Rate constant
m_j	Running index in wavelet decomposition scale j
p_j	Relative wavelet energy of fixed scale j
$\tilde{p}_j$	Relative coefficient energy of fixed scale j
p_k	Frequency bin of normalized power spectrum
$p(x_i)$	Probability of an event x_i
s	Continuous value scale of the wavelet transform
t	Time
x	Signal
x_j	Approximation signal of scale j
y_j	Detail signal of scale j
w	Window function
w	White Gaussian noise
γ	Steepness of the concentration-versus-response relation
γ_k	Weighting factor of normalized frequency bin p_k
σ	Standard error
τ	Continuous value translation of the wavelet transform
φ	Scaling function
ψ	Wavelet function
ω	Frequency in radians

List of Figures

List of Tables

1 Introduction

Anesthesia is drug-induced nonresponsiveness which can be defined by its hypnotic (unconsciousness) and analgesic (pain relief) components. Today, depth of anesthesia or of hypnosis is defined as a continuum or progressive central nervous system depression and decreased responsiveness to stimulation [169].

Anesthetics affect the central nervous system, producing a state of reversible coma or anesthesia. It is known that most hypnotic drugs in current use have their effect via gamma-aminobutyric acid (GABA) subtype A ($GABA_A$) receptors. The vast majority of neurons have $GABA_A$ receptors, and there is debate concerning whether the main effect of anesthesia-induced unconsciousness is within the cerebral cortex [184], in the thalamus [6], or in thalamocortical interactions [73]. In clinical monitoring practice, neither the main effect site nor the anesthetics' concentrations at the effect site(s) is known.

One of the main effects of general anesthetics is the suppression of consciousness – i.e., prevention of awareness. The most convenient approach to prevent patient awareness and to get an indication of the temporal effect and potency of anesthetics is to monitor electroencephalogram (EEG) activity and surrogate measures derived therefrom. Electroencephalogram activity is known to be generated by cortical nerve cell inhibitory and excitatory postsynaptic potentials. These postsynaptic potentials summate in the cortex and extend to the scalp surface. In addition to postsynaptic potentials, intrinsic cell currents produced by activation of ionic channels probably also contribute to the EEG. Electroencephalogram measurements are commonly taken as potential difference over time between two electrodes attached to the scalp. These are referred to a third electrode.[37]

Electroencephalogram activity was first measured in humans by Hans Berger in the 1920s, and in the 1930s the method's sensitivity to anesthetic agents had already been observed [124]. The effects of deepening anesthesia on EEG activity, according to the classic definition of Stockard & Bickford (1975), are [158, 201]:

1. Disorganized high-frequency activity
2. Organized activity with an increase in rhythmicity and voltage, especially delta activity
3. Mixtures of lower frequencies with the higher frequencies, with increased delta activity at deeper levels
4. Burst suppression, with the duration of suppression becoming longer with deeper levels
5. Suppression with isoelectric EEG

In the late 1990s, the EEG experienced a renaissance of interest as a clinical monitoring tool for anesthesia. This revival was the result of two events: first, the use of the EEG was retargeted from confirming deep surgical anesthesia to the assessment of lighter or sedative levels, and, second, technological developments led to the creation of a means of monitoring anesthetic depth.[124]

The process resulted in the commercialization of the Bispectral Index® monitor (BIS®, from Aspect Medical Systems of Norwood, MA, in the USA). However, in the early 1990s the developers of BIS were unclear about their goal, as the following statement indicates [79]: "Any useful EEG measure of adequate anesthetic depth should correlate with the absence of patient movement to skin incision." It took some years before the developers realized that patient movement in response to skin incision is merely a spinal cord reflex [9, 123, 127] and therefore not predictable from the cortical electroencephalogram.

Bispectral Index was followed by other EEG-based depth-of-anesthesia monitors: Narcotrend® (from MonitorTechnik of Bad Branstedt, Germany), Patient State Analyzer (or PSA, from Hospira, Inc., of Lake Forest, IL, in the USA), Cerebral State Monitor™ (from Danmeter A/S of Odense, Denmark), and the AAI™ index which is partly derived from auditory evoked potentials (AEP Monitor/2™, Danmeter).

Modern anesthetic depth monitors utilize only one or two electroencephalogram channels, measured from the forehead of the patient, and are able to produce an EEG-derived index value ranging from 0 to 100, where low index values denote deep anesthesia and high values indicate a conscious patient. Ideally a monitor of anesthetic depth should aim to [28, 41]:

1. achieve a perfect correlation between the drug effect and the value obtained by the monitor,
2. where this correlation is independent of the drug administered, and
3. there should be no inter-patient variability.

None of the monitors meet these criteria; however, they have been proven to be useful in the prevention of intraoperative awareness and in generation of cost savings during anesthesia. Intraoperative awareness occurs when a patient becomes conscious during a procedure performed under general anesthesia and subsequently has recall of these events. In this context, recall refers to explicit memory; i.e., the patient recalls specific events that took place during general anesthesia [40, 169]. Post-traumatic stress disorder may occur as a result of intraoperative awareness, and affected patients may remain severely disabled for extended periods of time [21]. The incidence of awareness during general anesthesia is 0.1–0.2% [40, 107, 139, 150]. However, the incidence is greater during cardiac surgery, Caesarean section, and trauma surgery [40, 107]. With high-risk patients, the use of an anesthetic depth monitor has been shown to reduce the risk of awareness by 82% [107]. However, in another study, conducted with a common patient population, the use of an anesthetic depth monitor did not have an effect on the incidence of awareness [150].

While the effect of anesthetic depth monitoring for intraoperative awareness has not been unambiguously demonstrated, several studies have shown an influence on anesthetic drug consumption and in some instances on recovery after anesthesia. Reduction of anesthetic drug consumption has been shown with propofol [39, 177], isoflurane [47], desflurane [88], and sevoflurane [3]. Faster emergence after surgery [39, 161, 177] and improved recovery, manifested as wellbeing in the postanesthesia care unit [39] and sooner readiness to return home [39], have been reported. However, in some studies no difference was seen in the emergence time after surgery [3, 88], nor in the time spent in the postanesthesia care unit [115, 177] between the

group monitored with an anesthetic depth monitor and the control group.

Applied in conjunction, the methods developed in this thesis aim to enable accurate and reliable monitoring of anesthesia depth.

1.1 Burst suppression

Burst suppression is an EEG pattern that can be produced with large doses of the most commonly used anesthetics. In burst suppression, the EEG is characterized by suppression periods with intermediating bursts. As anesthesia deepens, EEG suppression periods start to lengthen in time. In burst suppression, the cerebral metabolic rate is maximally reduced; therefore, burst suppression can be used as a reference point during cerebro-protective treatment, such as in cases of intracranial hypertension or status epilepticus. In comatose intensive care patients, burst suppression is a typical EEG pattern that can have various etiologies, and burst suppression monitoring has great value in the intensive care setting [201]. In deep anesthesia, variables derived from burst suppression can be used to monitor anesthetic depth, and interpretation of burst suppression is an integral part of all depth-of-anesthesia monitors.

Thus, the first aim of the thesis project was to develop a method for burst suppression detection in surgical anesthesia and to integrate it into the depth-of-anesthesia monitor, enabling accurate monitoring of anesthetic depth in deep anesthesia.

1.2 Facial electromyographic activity

Facial electromyographic (EMG) activity occurs in the frequency range of 0 to >200 Hz, whereas most of the EEG signal occupies the frequency range from 0 to 70 Hz. The EMG amplitude in the frontal area is greatest in the range 20–30 Hz, and in the temporal area 40–80 Hz. Facial EMG activity attenuates and broadens centrally. Both frontal and temporal EMG activity have substantial inter-individual variation.[42] Because of the frequency spectra overlapping the EEG signal, the EMG is a relevant artifact source for depth-of-anesthesia monitors when the cortical state of the patient is of interest.

On the other hand, facial EMG activity can be used to monitor adequacy of anesthe-

sia. During surgery, increased EMG activity indicates enhanced patient responsiveness and possible impending arousal. Facial muscles are innervated by both cortical motor pathways and brain-stem emotive pathways. Furthermore, facial muscles are more resistant to neuromuscular blockade than are hand muscles, commonly used for neuromuscular transmission monitoring. However, the frontal EMG does not have predictive value in monitoring loss or return of consciousness.[164]

The second aim of the research for this thesis was to develop an anesthetic depth monitor capable of utilizing both cortical information from the EEG signal and subcortical information from the facial EMG signal – thus differentiating it from the other available anesthetic depth monitors, and potentially enabling faster response to impending arousal.

1.3 Epileptiform activity

Epilepsy is the most common neurological disorder. The prevalence of epileptic seizures has been estimated to be between 0.5% and 5% [110]. Epileptiform electroencephalographic activity can be induced by anesthetic agents even in patients without diagnosed epilepsy.

Drugs can be roughly divided into two groups, depending on their effect on the central nervous system. Depressant drugs produce electrocerebral silence and are used for intentional metabolic suppression of the central nervous system, which is related to EEG activity. The drugs that produce marked activation have been used to enhance spike activity in electrocorticography for seizure focus ablation. Differences in neural depression and excitation correlate with changes in EEG patterns with increasing doses of anesthetics. Because of the differences between agents, the effect of each agent must be considered in the choice of anesthetic techniques. When anesthesia is administered to induce burst suppression and electrocerebral silence, the most depressant drugs are usually chosen (propofol or thiopental). For localization of seizure foci, most anesthetic drugs must be avoided since they suppress seizure activity.[158]

Epileptiform EEG activity in sevoflurane anesthesia has been described on several occasions; the first seizure with confirmed EEG was reported on in a 1997 publication [198]. That was followed by studies conducted in sevoflurane mask induction eliciting

epileptiform EEG activity [176, 178, 200]. Epileptiform EEG and seizures have also been observed and systematically reported in deep steady-state sevoflurane anesthesia [68]. These studies were conducted with neurologically healthy subjects.

With epileptic patients, sevoflurane evokes epileptiform activity more often than isoflurane [65]. Patients with brain lesions are at risk of seizure activity during sevoflurane anesthesia [58]. In a recent study female sex, short delay to onset of anesthesia, and high alveolar sevoflurane concentration were identified as risk factors for epileptiform activity in sevoflurane induction with nonepileptic patients [75].

From the other anesthetics, there exist several reports of seizure activity during propofol anesthesia [191]. Propofol can also enhance interictal activity in some patients, and, despite its suppressive activity, it is used for identifying and ablating seizure foci. Nitrous oxide can be either proconvulsant or anticonvulsant. Of the opioids, alfentanil can be used to enhance epileptic spikes. Ketamine has been reported to evoke seizure activity in epileptic patients but not in patients without epilepsy. Etomidate can enhance epileptic activity at low doses and may produce seizures in epilepsy patients.[158]

With all of these considerations factored in, it appears that epileptiform activity and seizures in paralyzed surgical patients may be more common than one might expect. With sevoflurane alone or used in association with other drugs, transient cognitive impairment has been observed. Subclinical epileptiform discharges may explain this [75]. Because current EEG monitors used in operating rooms do not include seizure detectors, the majority of seizures remain undetected and untreated.

Additionally, if depth-of-anesthesia monitors are used without simultaneous EEG waveform examination, epileptiform activity may result in too deep anesthesia because of the misleading readings in the anesthetic depth index [23, 77]. Epileptiform EEG in sevoflurane anesthesia, although generalized, has been shown to be predominant in the frontal region [75], thus making depth-of-anesthesia monitors especially vulnerable to these waveforms.

The third aim in the thesis work was to develop a method for the monitoring of epileptiform activity during anesthesia. Anesthesia is a challenging situation, with a wide range of EEG activity, from awake activity to burst suppression. Therefore, an important goal was for the method developed to be specific to epileptiform activity

only, and not to react to any other EEG change occurring during anesthesia. The method is aimed at improving the reliability of anesthetic depth monitoring and helping to avoid adverse seizure activity.

1.4 Anesthetic drugs

Propofol is the most commonly used intravenous anesthetic agent, achieving its effect primarily through the GABAergic transmitter system [137]. The main advantages of propofol are favorable operating conditions and rapid recovery. On the other side of the coin, incidence of apnea is relatively high and there are occasional reductions in blood pressure. Propofol is used as a hypnotic agent; it has mild antinociceptive effects.

Thiopental is an intravenously used barbiturate that is especially suitable for anesthetic induction. Its advantages are prompt onset, smooth induction, and relatively rapid emergence. Thiopental does not possess analgesic properties.[104]

Ketamine is an intravenously used noncompetitive antagonist of the NMDA receptor. It produces so-called dissociative anesthesia characterized by analgesia, amnesia, hallucinations, and catalepsy [83]. Commercially available ketamine is a racemic mixture of two optical enantiomers, R(-) and S(+) ketamine. Pure S-ketamine is approved for clinical use in some countries. The analgesic and anesthetic potency of S-ketamine is greater than that of R-ketamine, enabling an approximately 50% reduction in dosage from the racemate level. Compared to racemic ketamine, S-ketamine has similar anesthetic properties, but it is associated with less marked tachycardia and smoother recovery, with less undesirable excitement or delirium during emergence.[195] Use of ketamine in single-agent anesthesia is rare; the drug is currently used at low doses as an adjunct to improve analgesia and to prevent opioid tolerance.

Dexmedetomidine is an intravenously applied potent, highly selective adrenergic α_2-receptor agonist. It is approved for short-term sedation of patients undergoing mechanical ventilation in the intensive care unit (ICU). Dexmedetomidine has no clinically significant adverse effects on respiration [31, 52, 61] and has been shown to provide effective post-surgical analgesia [2, 186]. Patients sedated with dexmedetomidine remain cooperative and can be aroused easily for clinical testing and other

procedures [52, 185].

Halogenated ether anesthetics are in common use for anesthetic purposes. These drugs have a strong hypnotic effect and a stronger antinociceptive effect than propofol. Today's most widely used halogenated ether anesthetics are sevoflurane, desflurane, and isoflurane. Advantages of sevoflurane include its fast inhaled induction, favorable cardiovascular effects, absence of respiratory irritation, and low solubility (contributing to fast emergence). It is assumed that sevoflurane produces anesthesia by enhancing the inhibitory GABA transmitter system [137]. Desflurane is a derivative of isoflurane that has lower solubility than isoflurane and therefore more rapid pharmacokinetics.

Nitrous oxide is among the most commonly used anesthetic and sedative agents. In addiction to being an important adjuvant during general anesthesia, it is widely administered in combination with oxygen for obstetric analgesia and for sedation in dental and medical procedures.[125] Nitrous oxide acts by inhibiting the NMDA receptors [138].

Xenon is a noble gas with anesthetic properties believed to be mediated via antagonism of the NMDA receptors. Xenon is hypnotic, exhibiting also potent analgesic action. It has been used experimentally in clinical practice for more than 50 years, with only its high cost precluding more widespread clinical use. Concerns over its cost have begun to be mitigated by technological developments in the delivery and recycling of xenon that should permit much less total gas to be expended in each anesthetic administration. Xenon is a potential substitute for nitrous oxide as an analgesic agent, since nitrous oxide has caused environmental concerns because of its ozone-depleting properties.[138] Xenon has recently been granted marketing authorization for anesthetic maintenance in Germany [91].

Neuromuscular blockers, administered to provide relaxation of skeletal muscles, are valuable adjuncts to general anesthesia, and their use in the operating room is quite common [104]. However, strong scientific evidence supports avoidance of imprudent use of neuromuscular blocking agents, because of the risk of anaphylactic reactions and postoperative residual curarization [12, 108]. Among the most commonly used neuromuscular blocking agents are succinylcholine, pancuroniun, mivacurium, atracurium, and rocuronium.

The term “opioid” refers broadly to all compounds related to opium. Opiates are drugs derived from opium; these include the natural products morphine, codeine, and thepaine, as well as many semisynthetic products derived from them. Synthetic opioids, such as fentanyl and remifentanil, have been developed in order to provide more potent and specific effect. In humans, morphine-like drugs produce analgesia, drowsiness, changes in mood, and mental clouding. A significant feature of opioid analgesia is that it is not associated with loss of consciousness. Although unconsciousness in humans can be produced with high doses of opioids alone, opioid anesthesia can be unpredictable and inconsistent.[104] In today’s anesthesia practice, opioids are used for analgesia.

As another goal, the anesthetic depth monitor developed in the thesis project shall be applicable with most commonly used hypnotic drugs. A fourth aim of the work was to investigate the applicability of the anesthetic depth monitor developed in single-agent S-ketamine anesthesia and in dexmedetomidine sedation.

1.5 Aims of the thesis

	Aim	Publication
1.	To develop a method for the detection of the burst suppression pattern and to incorporate it as part of a depth-of-anesthesia monitor.	**I, II**
2.	To develop a depth-of-anesthesia monitor utilizing both cortical and subcortical information and that can be applied with most commonly used anesthetic agents.	**II**
3.	To develop a method for the monitoring of epileptiform electroencephalographic waveforms and to demonstrate the effects of epileptiform activity on the anesthetic depth monitor.	**III**
4.	To investigate the monitor developed in S-ketamine anesthesia and in dexmedetomidine sedation.	**IV, V**

This thesis focuses on the commercially available depth-of-anesthesia monitor Entropy^{TM} (from GE Healthcare of Helsinki, Finland), which was developed in this project. The performance of Entropy is compared to that of BIS, which was the first monitor on the market and has achieved a state as de facto standard. The mathematical methodologies of these two monitors are presented, and their performance with different anesthetic drugs is discussed, including their limitations with some specific drugs and epileptiform EEG waveforms.

In view of the research aims, the thesis does not cover the other depth-of-anesthesia monitors: Narcotrend, Patient State Analyzer, Cerebral State Monitor, and AEP Monitor/2. These monitors are far less studied than BIS [169] and only two studies have compared AAI to BIS and Entropy [182, 188]. Examples of reviews of these monitors are found in other sources [169]. Applicability of middle-latency auditory evoked potentials to monitor depth of anesthesia is discussed in the work of Drummond, for example [28]. Some non-commercial methods using complexity variables derived from the time-domain EEG also exist, the most well known being approximate entropy [19]. Although these may have similar characteristics to spectral entropy [36, 131], which is the mathematical core of the Entropy monitor, they are not discussed in this thesis.

2 Electroencephalogram signal processing in anesthesia

This chapter describes key signal processing methods used in anesthesia monitoring practice. The methods developed in this work – detection of burst suppression, time-frequency balanced spectral entropy, and wavelet subband entropy – are presented in their own sections. Burst suppression detection and time-frequency balanced spectral entropy are described in greater detail in the corresponding works, publications **I** and **II**. Wavelet subband entropy is unique in its form, and therefore its mathematical background is presented here in more depth than in Publication **III**. Bispectral analysis and Bispectral Index are presented on account of their prominence in depth-of-anesthesia monitoring.

The basics of spectrum estimation with Fourier transforms are presented, because this constitutes the basis for the spectral entropy and Bispectral Index. The Fourier transform was also used for EEG spectral analysis in publications **IV** and **V**. The description of the spectrum estimation is based on that in the books *Statistical Digital Signal Processing and Modeling* by Hayes [56] and *Higher-Order Spectral Analysis Toolbox User's Guide* of Swami, Mendel, & Nikias [167]. The wavelet theory material presented here is based on Sörnmo & Laguna's book *Bioelectrical Signal Processing in Cardiac and Neurological Applications* [162]. These books are recommended reading for further information.

2.1 Time-domain analysis

The EEG is a stochastic, nonstationary signal. In practice, this imposes limits on the signal processing techniques utilized. However, with certain assumptions, EEG can be treated as a stationary signal within certain predefined short epochs. To assure stationarity of the EEG before further signal processing, segmentation of the signal into stationary epochs is required. This can be carried out with adaptive segmentation. To localize segment boundaries precisely, methods employing fixed-duration segments cannot be applied. In adaptive segmentation, segment boundaries can occur at arbitrary positions, depending only on the signal statistics, and are not limited to predefined frames. Adaptive segmentation can be conducted either via

parametric [15] or by nonparametric [102] methods. Energy operators are computationally efficient means of carrying out nonparametric adaptive segmentation [1].

2.1.1 Nonlinear energy operator

Teager's energy operator (TEO) was literally first presented by Kaiser [76], as a simple algorithm that enables calculation of the "energy" of a signal. TEO is defined as:

$$\Psi_{\mathrm{TEO}}\{x(n)\} = x(n)^2 - x(n+1)x(n-1). \tag{2.1}$$

Teager's energy operator is a particular case of a more generalized nonlinear annihilator [119]. In this context, "annihilator" means an operator that possesses an ideal annihilation property with respect to one signal while remaining ideally transparent to another; thus it becomes a powerful tool for the separation of short-duration superimposed signals with highly overlapping spectra. The generalized nonlinear annihilator can be presented as:

$$\Psi_{\mathrm{g}}\{x(n)\} = x(n-l)x(n-p) - x(n-q)x(n-s), \tag{2.2}$$

where index values are selected so that $l + p = q + s$, and $|l - q| = |p - s| \neq 0$. The index values can be selected, for example, to be $l = 1, p = 2, q = 0, s = 3$. With this selection, the variable known as the nonlinear energy operator (NLEO) is obtained:

$$\Psi_{\mathrm{NLEO}}\{x(n)\} = x(n-1)x(n-2) - x(n)x(n-3). \tag{2.3}$$

This variable was first used for EEG analysis by Agarwal et al. [1], who utilized it for nonparametric adaptive segmentation prior to classification in order to compress the information in long-term EEG recordings in ICUs. Because of its ability to capture both amplitude and frequency information of EEG signals, its low computational complexity, and the low susceptibility to noise, NLEO is a useful variable for low-level EEG signal processing tasks, such as EEG burst suppression detection. Also Teager's energy operator has been suggested for burst suppression detection [155].

During suppression, EEG amplitudes can fall to the preamplifier's electrical noise level. Therefore, signal processing techniques must tolerate the external noise if they are to detect EEG suppression periods reliably. Figure 2.1 illustrates with test

signals (sample frequency: 200 Hz) the behavior of the squaring operation, Teager's energy operator Ψ_{TEO}, and the nonlinear energy operator Ψ_{NLEO} for sinusoidal signal and also the summation of sinusoidal signal and white Gaussian noise signal. Figure 2.2 presents the periodograms of white Gaussian noise signal w (sample frequency: 200 Hz) and w subjected to the squaring operation $\{w\}^2$, Teager's energy operation $\Psi_{\mathrm{TEO}}\{w\}$, and nonlinear energy operation $\Psi_{\mathrm{NLEO}}\{w\}$. It can be seen that NLEO is less influenced by white noise in the low-frequency range than the squaring operator or TEO.

Figure 2.3 presents the periodograms of the sinusoidal test signal x, and x subjected to squaring operation $\{x\}^2$, Teager's energy operation $\Psi_{\mathrm{TEO}}\{x\}$, and nonlinear energy operation $\Psi_{\mathrm{NLEO}}\{x\}$. The total power of NLEO can be seen to be higher than the TEO total power; therefore, NLEO is favored over TEO for those applications where the aim is to eliminate the influence of noise and obtain a good dynamic range for the detection of signal itself.

2.1.2 Burst suppression detection (I, II)

Adaptive segmentation techniques can be applied for the detection of burst and suppression EEG patterns. This was first done by Lipping and colleagues [95], who divided EEG signal into burst, suppression, and artifact categories on the basis of the integrated absolute signal values in the predefined frequency bands. In this method, the adaptive segmentation (i.e., segment boundary setting) was done simultaneously with the EEG classification. The method was developed and tested with the EEG burst suppression signal from isoflurane and enflurane anesthesia. Review of the other methods used for burst suppression detection is given in Publication **I**.

The approach used by Lipping is developed further in Publication **I**. The publication describes a method utilizing absolute values for the nonlinear energy operator instead of absolute signal values, and it compares the performances of these methods with the EEG burst suppression data from propofol and thiopental anesthesia. Furthermore, the publication includes spectral analysis of burst patterns with both anesthetics. In deep propofol anesthesia, spindle oscillations of 14–16 Hz was observed. Those oscillations seemed to occur both during bursts and in suppressions. In the study, they were therefore treated as suppression, because spindles were recognized as an independent phenomenon and they are characterized by prolonged

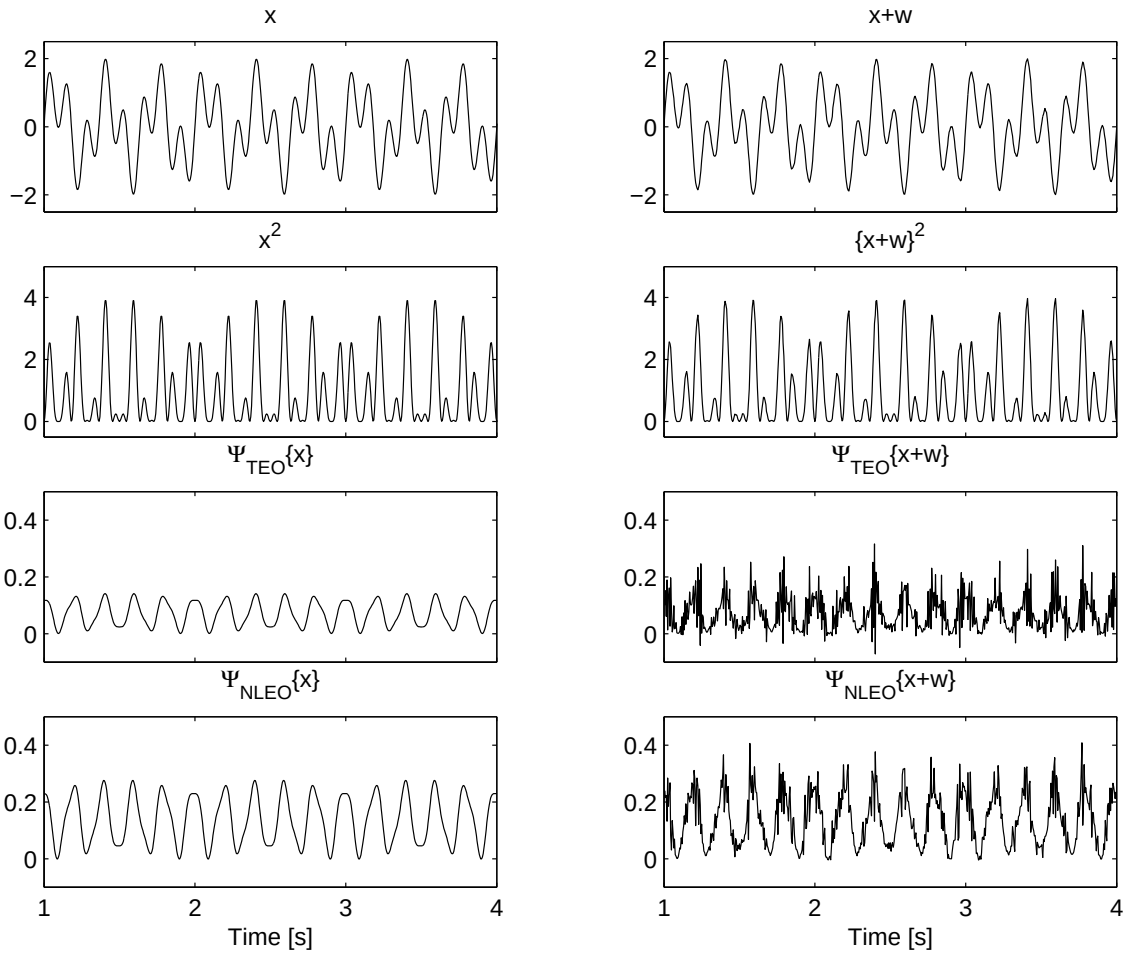

Figure 2.1: The left column presents a three-second epoch of signal x (sample frequency: 200 Hz), which is a summation of two sine frequencies (3 Hz and 8 Hz), and its corresponding instantaneous energy $\{x\}^2$, Teager's energy operator $\Psi_{\text{TEO}}\{x\}$, and nonlinear energy operator $\Psi_{\text{NLEO}}\{x\}$. The right-hand column presents the summation of signal x and white Gaussian noise w, and its corresponding instantaneous energy $\{x+w\}^2$, Teager's energy operator $\Psi_{\text{TEO}}\{x+w\}$, and nonlinear energy operator $\Psi_{\text{NLEO}}\{x\}$. In this example, the power of signal x is 2500 times higher than the power of white noise signal w.

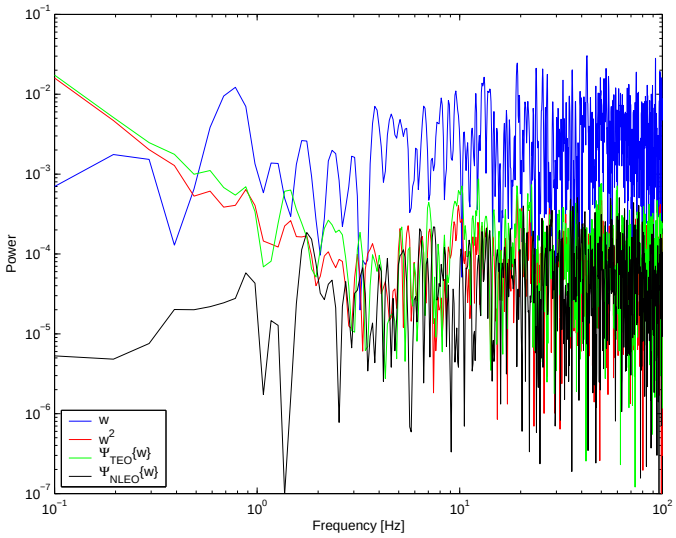

Figure 2.2: Periodogram of white noise signal w, w^2, $\Psi_{\text{TEO}}\{w\}$, and $\Psi_{\text{NLEO}}\{w\}$.

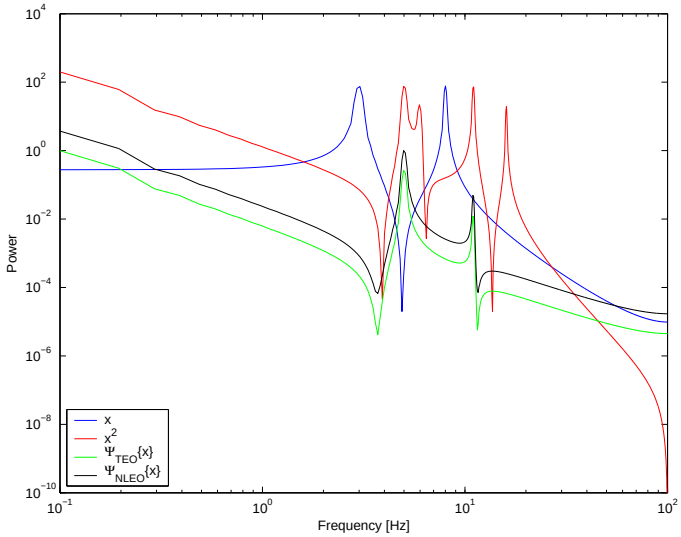

Figure 2.3: Periodogram of the sum signal x of two sinusoids (3 Hz and 8 Hz), x^2, $\Psi_{\text{TEO}}\{x\}$, and $\Psi_{\text{NLEO}}\{x\}$.

inhibitory postsynaptic potentials in thalamocortical cells, thus being related to the unconscious state of a subject [175].

Even though different methods exist for the compression of burst suppression information and some new ideas are presented in Publication **I**, burst suppression ratio (BSR), as first proposed by Rampil [128], remains the most common burst suppression derivative in anesthesia practice. The burst suppression ratio is the proportion of the suppression EEG in the analyzed epoch (usually one minute):

$$\mathrm{BSR}(\%) = \frac{total\ time\ of\ suppression}{epoch\ length} \cdot 100\%. \tag{2.4}$$

In deep anesthesia, BSR correlates with anesthetic gas end-tidal concentrations [20, 126]. The BSR value is an integral part of all commercially available depth-of-anesthesia monitors.

The method used in the study discussed in Publication **I** was refined further during the development of the Entropy monitor. The modifications implemented are described in Publication **II**; they included, for example, modification of the filters used. This was necessary because, in everyday anesthesia monitoring practice, the aim is to calculate BSR, and thus specific detection of suppressions is the most important feature. A major problem when one utilizes the technique described in Publication **I** is that low-voltage beta activity of the awake patient is easily classified as suppression. Therefore, the cutoff frequency of the low-pass filter used was increased from 8 Hz to 20 Hz. With that modification, the low-pass-filtered signal used in the NLEO calculation contains EEG beta activity also (see Table 2.1) and the method is no longer so prone to false positive suppression detections in awake patients. Figure 2.4 presents one minute of EEG signal in burst suppression anesthesia and the corresponding integrated absolute values of NLEO.

The performance evaluation for the method developed and for the Entropy monitor at the burst suppression level of anesthesia is reviewed in section 3.3.1.

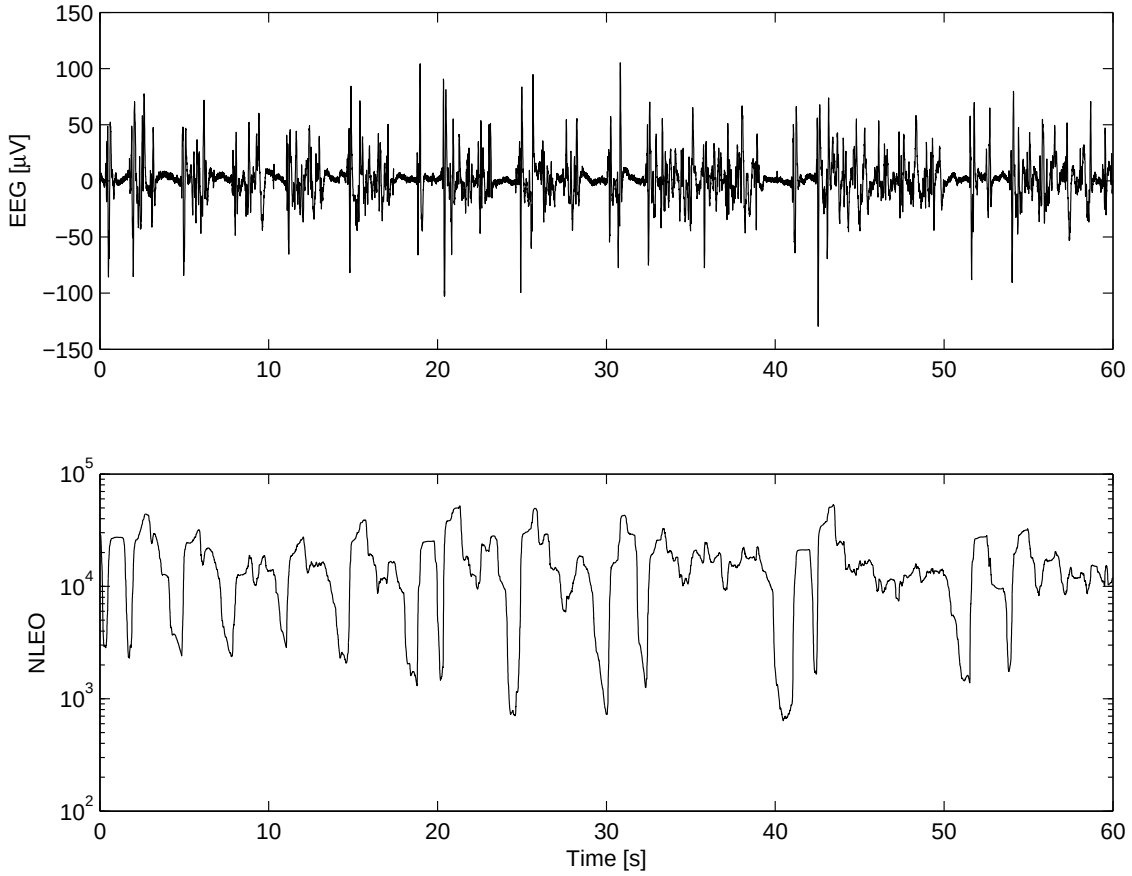

Figure 2.4: Illustration of the basic principle of burst suppression detection. The top panel illustrates one-minute EEG during burst suppression, and the bottom panel presents the decision function, absolute values of the Ψ_{NLEO} operation summarized in a sliding window of one second. Suppressions are detected when the decision function is below its threshold value. In this example, the BSR value is 36%.

2.2 Frequency-domain analysis

Similarly to time-domain analysis, frequency analysis can be performed either via nonparametric methods (e.g., a Fourier transform) or by parametric methods using signal modeling. Spectral analysis based on the discrete Fourier transform (DFT) is more computationally efficient and is used in commercial products like BIS [124] and Entropy.

2.2.1 Spectrum estimation

The Fourier transform of the infinite discrete signal $x(n)$ is:

$$X(e^{j\omega}) = \sum_{n=-\infty}^{\infty} x(n)e^{-jn\omega}, \tag{2.5}$$

where ω denotes digital frequency in radians per sample. In practice, signals of finite duration with N samples are used; in that case, the DFT is defined as:

$$\hat{X}(e^{j\omega}) = \sum_{n=0}^{N-1} x(n)e^{-jn\omega}. \tag{2.6}$$

An estimate of the power spectral density (PSD), as a periodogram, is obtained with the convolution theorem:

$$\hat{P}(e^{j\omega}) = \frac{1}{N}|X(e^{j\omega})|^2 = \frac{1}{N}X(e^{j\omega})X^*(e^{j\omega}), \tag{2.7}$$

where $*$ denotes complex conjugate. The cross-biperiodogram is the estimate of bispectral power in each frequency pair of the signal $x(n)$:

$$\hat{B}(e^{j\omega_1}, e^{j\omega_2}) = \frac{1}{N^2}X(e^{j\omega_1})X(e^{j\omega_2})X^*(e^{j(\omega_1+\omega_2)}). \tag{2.8}$$

The nonredundant region of the bispectral space for a continuous-time band-limited process, with a Nyquist frequency of 0.5, is the triangle with vertices (0, 0); (0.33, 0.33); and (0.5, 0) [167].

The Fourier transform assumes that the signal in the epoch being analyzed is repeated outside the epoch. If the signal value and phase at the beginning and at the end are not the same, there will be an abrupt change or discontinuity, which introduces additional small components in the spectrum that are not in the original signal. This is called spectral leakage. Instead of rectangular windows, tapering

windows can be used, to reduce spectral leakage. Such window forms include triangular (Bartlett), Blackmann, Hamming, and Hanning windows. With added window function w, Equation 2.6 takes the form:

$$\hat{X}(e^{j\omega}) = \sum_{n=0}^{N-1} x(n)w(n)e^{-jn\omega}. \tag{2.9}$$

The modified periodogram obtained with windowing is:

$$\hat{P}_M(e^{j\omega}) = \frac{1}{NU}|\sum_{n=0}^{N-1} x(n)w(n)e^{-jn\omega}|^2, \tag{2.10}$$

where U is:

$$U = \frac{1}{N}\sum_{n=0}^{N-1} |w(n)|^2. \tag{2.11}$$

A rectangular window has a narrow main lobe but relatively large side lobes when compared to the other windows. Therefore, the rectangular window produces the least spectral smoothing but may lead to masking of weak narrowband components.

The periodogram, modified periodogram, and cross-biperiodogram yield asymptotically unbiased estimates; however, the variance of the estimates does not converge to zero as N tends to infinity. Thus, the estimate is not consistent. To obtain a consistent estimate of the PSD, K successive and overlapping modified periodograms can be averaged to reduce the variation of PSD estimates. This is called Welch's method, and the periodogram obtained is:

$$\hat{P}_W(e^{j\omega}) = \frac{1}{K}\sum_{i=0}^{K-1} \hat{P}_M^{(i)}(e^{j\omega}). \tag{2.12}$$

The expected value of Welch's estimate (2.12) is the same as that of the modified periodogram (2.10):

$$E\{\hat{P}_W(e^{j\omega})\} = E\{\hat{P}_M(e^{j\omega})\} = \frac{1}{2\pi NU} P(e^{j\omega}) * |W(e^{j\omega})|^2, \tag{2.13}$$

where $W(e^{j\omega})$ is the Fourier transform of the N-point data window, $w(n)$, used in Equation 2.10. The variance of the periodogram estimated with Bartlett window without overlap is approximately proportional to $1/K$ times the square of the PSD [56]. In order to obtain a consistent estimate of the bispectrum, averaging and smoothing windows specifically developed for bispectrum estimation can be used [112, 167]. If cross-biperiodogram is estimated without averaging in the frequency

domain, the variance is approximately proportional to $1/K$ times the triple product of PSD [112]. Therefore, generally higher values of K are required to obtain consistent estimate of the bispectrum than with the PSD.

Alternatively, the periodogram and cross-biperiodogram can be derived using higher-order cumulants. The second-order cumulant of a zero-mean stationary process is an autocorrelation sequence. The periodogram, an estimate of second-order polyspectrum, is obtained by taking the Fourier transform of the autocorrelation sequence. Similarly, the cross-biperiodogram, an estimate of third-order polyspectrum, can be obtained with the Fourier transform of the third-order cumulant.

2.2.2 Classical spectral band powers

The spectral content of EEG signal is often analyzed by dividing the spectrum into predetermined frequency bands. The boundary frequencies of these bands may vary a little, depending on the definition applied. Table 2.1 illustrates the frequency bands with the boundary frequencies used in the studies described in publications **IV** and **V**. Activities in particular frequency ranges and within different regions of the cortex have been identified as reflecting particular neuronal activities originating in certain areas of the brain. For further information, see, for example, the work of John & Prichep [73].

Studies of the anesthetic effects on these classical EEG band powers were not successful and are infrequent nowadays. From the monitoring point of view, one reason is probably that different anesthetics produce different characteristic changes in these classical EEG variables, although a common effect with all agents acting via the $GABA_A$-receptor system is the slowing of EEG rhythms. However, use of spectral band power information in the monitoring of anesthetic depth is uncommon, and these variables might be more useful in the study of the physiological mechanisms of various drugs. On the other hand, band powers do carry important information for depth-of-anesthesia monitoring. Their main drawback is obviously that, for one to gain proper understanding of the anesthetic depth, several band power variables should be used simultaneously and information on the drugs given should be available. For example, relative delta-band power was one of the classical EEG variables compared against early versions of BIS [13, 79, 80, 151, 190].

Table 2.1: Classical EEG frequency band definitions.

Frequency band	**Frequency range [Hz]**
delta, δ	1–3.5
theta, θ	3.5–8
alpha, α	8–13
beta, β	13–30
gamma, γ	30–70

2.2.3 Spectral edge frequencies

Univariate descriptors of the EEG power spectrum, 95% or 90% spectral edge frequency (SEF) and median frequency (or 50% spectral edge frequency, MF), are traditional variables in anesthesia monitoring. Spectral edge frequency is a 95th or 90th percentile of PSD, and respectively MF is a 50th percentile of PSD.

Characteristically SEFs have large inter-individual variability, and after initial drop at induction the SEF may increase again to awake level [113]. Furthermore, the EEG spectrum in anesthesia is often bimodal; i.e., it exhibits two dominant frequency peaks. This has been demonstrated at least with halothane, enflurane and isoflurane [94], and propofol [170]. Obviously, this limits the applicability of MF.

During burst suppression, SEF and MF fail to monitor anesthetic depth [170] and tend to increase as BSR rises [20]. In order to compensate for this effect, burst-compensated spectral edge frequency (BcSEF) has been proposed [126]:

$$\mathrm{BcSEF} = \mathrm{SEF}(1 - \frac{\mathrm{BSR}(\%)}{100\%}). \tag{2.14}$$

Recent years have seen an increase in the reports of biphasic effects of anesthetics. This means that at induction there is an initial increase in alpha- and beta-frequency power, which is followed by the increase in delta and decrease in the alpha and beta range. This has been systematically demonstrated with propofol [84, 89, 90], thiopental, etomidate, and sevoflurane [90]. However, EEG in midazolam sedation does not follow a biphasic time course [90]. Although this effect has been known for a long time, since it appears in the classical definition of Stockard & Bickford, recent studies suggest that in propofol anesthesia the effect evolves systematically

in the induction phase [84]. Obviously, the biphasic effect of anesthetic is one of the strongest argument against the applicability of SEF and MF.

Sleigh and colleagues [157] introduced the median frequency of EEG signal (of sample frequency 256 Hz) first derivative. This variable proved to be superior to SEF, because it filtered out the fluctuating low-frequency artifact noise and emphasized the importance of gamma rhythms. The authors suggest that the biphasic effect can be attenuated or even eliminated by the inclusion of higher frequencies in the EEG signal analyzed.

Similar results were obtained in the recent study of Jordan et al. where a generalized form of spectral edge frequency, referred to as weighted spectral median frequency (WSMF), was introduced [74]. In the WSMF approach, new factors for the spectral edge frequency calculation are introduced. First, edge frequency is calculated not necessarily from PSD but from amplitude spectrum, which is raised to the power $p = [0.1 \dots 2.4]$; second, the cutoff frequencies of the original spectrum are well-defined; and, third, factor $r = [0.05 \dots 0.95]$ is used, the percentile of the spectrum (e.g., $r = 0.5$ for MF and $r = 0.95$ for SEF). With EEG data obtained from propofol+remifentanil and sevoflurane+remifentanil anesthesia, a high-pass cutoff frequency of 8 Hz and low-pass cutoff frequency of 30 Hz proved to be useful. Increasing the high-pass cutoff frequency eliminates the effect of eye movement artifacts and delta activity induced by opioids. Furthermore, $p = 0.4$ was found to be optimal, which can be explained by the reduced influence of sudden instances of high amplitudes in the signal, such as artifacts. With these settings for WSMF, the authors reported even better performance than that seen with BIS.

2.2.4 Canonical univariate parameter

In measurement of anesthetic drug effect, classical EEG band powers may contain redundant information [44]. Statistical methods can be used to find the best correlation between EEG frequency content and the modeled drug effect-site concentration. To avoid usage of redundant band power information, frequency bins with a width of 3 Hz [38, 44, 144, 145] or classical frequency bands [113] are optimally weighted to obtain the best possible correlation with the drugs' effect-site concentration as obtained from pharmacokinetic–pharmacodynamic (PK–PD) modeling. A variable derived from weighted frequency bins is called the canonical univariate parameter

(CUP). First used by Gregg et al. [44] for studying the drug effect of alfentanil, CUP is derived from the frequency range 0–30 Hz via summing logarithms of each 10 3-Hz normalized frequency bins p_k weighted by their individual weights γ_k.

$$\mathrm{CUP} = \sum_{k=1}^{10} \gamma_k \log p_k \tag{2.15}$$

Later the same method with the same weights was applied for other opioids (fentanyl, sufentanil, trefentanil, and remifentanil), obtaining better correlation with effect-site concentration than SEF yielded [38]. Specific weights have been derived for midazolam+flumazenil [144], for propofol [145], and for sevoflurane+remifentanil [113]. Generally CUP correlated better with the PK–PD model than variables like SEF did; in particular, it had less inter-individual variability [38, 44, 113]. With propofol, CUP displays the biphasic effect [145], which makes it impractical for monitoring purposes. With sevoflurane+remifentanil, CUP has better correlation with the PK–PD model than SEF but worse than BIS [113].

A related study with CUP was done by Dressler et al. [27], who studied the frontal-EEG power spectrum derived from the range 1–127 Hz, in order to find the frequency bins that best discriminate responsive and unresponsive patients in propofol+remifentanil and in sevoflurane+remifentanil anesthesia. The best performance was found in the frequency ranges <15 Hz and 35–127 Hz; however, the latter is probably dominated by facial EMG activity. The least discrimination capability was seen in the range 15–26 Hz.

When one considers all methods described in the three previous subsections, it must be emphasized that traditional spectral band power analysis and spectral edge frequencies may still have value in anesthesia monitoring. Several studies comparing the performance of classical EEG band powers, spectral edge frequencies, and modern depth-of-anesthesia monitors may be biased in favor of modern monitors, such as BIS and Entropy. These monitors have effective built-in artifact elimination algorithms, which is not necessarily the case with the traditional variables. For example, when SEF is calculated by the BIS monitor, an equivalent artifact elimination procedure to that of BIS is not applied [113]. However, in some comparison-based studies these values are directly compared without any visual analysis of EEG waveforms or additional artifact elimination [141, 142]. A recent study by Koskinen and colleagues suggests that, with careful artifact elimination and normalization of inter-

and intra-individual variations in EEG amplitude, information derived from a rather wide frequency bins (4-Hz) can be used even in forecasting the instant at which loss of response to verbal commands takes place [85].

2.2.5 Spectral entropy

Shannon entropy H [153] is the expected value of the self-information I of the random events $\overline{X} = \{x_i\}$, calculated as:

$$H(\overline{X}) = E\{I(\overline{X})\} = -\sum_{i}^{N} p(x_i) \log p(x_i), \tag{2.16}$$

where $p(x_i)$ denotes the probability of event x_i. Relative entropy is calculated by dividing Equation 2.16 by the maximum entropy, $\log N$:

$$H_{rel}(\overline{X}) = -\frac{\sum_{i}^{N} p(x_i) \log p(x_i)}{\log N}. \tag{2.17}$$

Spectral entropy was introduced in 1979 for studying the regularity of Hamiltonian systems [121]. Power spectral density resembles the probability density function: after the normalization of PSD for the total spectral power, each frequency bin p_k represents the probability of that frequency occurring in the signal. Spectral entropy (SpEn) is obtained by applying Equation 2.16 to the PSD:

$$\text{SpEn} = -\sum_{k}^{N} p_k \log p_k. \tag{2.18}$$

SpEn is also often presented in the form of relative entropy.

Spectral entropy was first used in EEG analysis by Inouye et al. in two studies, the first one concerning EEG desynchronization during mental arithmetic [66] and the second where the EEG background activity of epileptic patients was studied [67]. In both of these studies, SpEn proved to be a useful measure for EEG desynchronization, measuring irregularity of the EEG signal.

The concept of EEG synchronization refers to a phenomenon related to the behavior of neuronal populations. These populations display oscillatory behavior when they are synchronously active, with transient components of sensory evoked potentials and interictal epileptiform spikes being the exception. Whether these oscillations can be detected in scalp recordings depends on 1) the extent of the cortical area

where the synchronous activity is present, 2) the topology of this cortical area, and 3) the relationship of this area to the measurement sensors. The EEG signal sources can be modeled in macrocolumns; each contains 10^5 to 10^6 neurons. When 30 to 40 macrocolumns (corresponding to an area of 1 cm^2) are synchronously acting, a clear resonance peak in the EEG spectrum can be obtained, thus leading to decreasing SpEn values when compared to a spectrum without resonance peaks.[117]

Spectral entropy was first utilized for anesthesia EEG signals by Rezek & Roberts, in 1998 [131]. In anesthesia, EEG spectral entropy has been shown to exhibit similar characteristics to variables derived with complexity and fractal analysis [36, 131]. It has been claimed that spectral entropy only reflects EEG power concentration in the low-frequency band and CUP is its generalization [113]. Although SpEn is sensitive to EEG slowing, it also reflects neuronal synchronization: Inouye and colleagues concluded that spectral entropy over the rather narrow alpha band is actually a more sensitive measure of desynchronization than alpha-band power or alpha peak frequency [66].

2.2.6 Time-frequency balanced spectral entropy (II)

Publication **II** describes the algorithm used in the Entropy monitor, based on spectral entropy. The Entropy monitor utilizes different EEG frequencies in a novel way. Because the periodogram is an asymptotically unbiased estimate of PSD, higher frequencies can be estimated from shorter time windows than lower frequencies can. This allows fast response in the index value to the change occurring in the high-frequency range (for example, increased facial EMG activity). This concept is referred to as time-frequency balanced spectral entropy.

In the Entropy monitor, two spectral entropy variables are derived: state entropy (SE) from the frequency range 0.8–32 Hz and response entropy (RE) from the frequency range 0.8–47 Hz. Because of the time-frequency balanced concept and to emphasize response entropy's ability of fast response, RE is derived from a time window of 2–15 s and SE from a time window of 15–60 s. Thus, response entropy can be readily applied for the fast detection of possible impending arousals during anesthesia, often manifested as elevated facial EMG activity. By contrast, the use of state entropy is aimed at monitoring the cortical state of the patient, since this measure is less influenced by EMG activation due to the lower frequency range used.

In anesthesia, RE–SE difference is suggested for a surrogate measure of the balance between EEG and facial EMG activity [54, 99, 168, 194], although it should be remembered that gamma activity occurs in that particular frequency range.

The Entropy algorithm is based on the relative entropy of the PSD; however, normalization for both the SE and RE is done via $N_{0.8-47\text{Hz}}$, which represents the number of frequency bins for the range 0.8–47 Hz. SpEn values are scaled with the spline function $f(\text{SpEn})$ in order to improve resolution at light and surgical anesthesia levels. As a result, SE and RE values are in the range $[0 \ldots 91]$ and $[0 \ldots 100]$, respectively:

$$\text{SE} = f(\text{SpEn}) \frac{\text{SpEn}_{0.8-32\text{Hz}}}{\log N_{0.8-47\text{Hz}}}, \tag{2.19}$$

$$\text{RE} = f(\text{SpEn}) \frac{\text{SpEn}_{0.8-47\text{Hz}}}{\log N_{0.8-47\text{Hz}}}. \tag{2.20}$$

During burst suppression, there is substantial variation in the spectral contents of the EEG signal. To eliminate the effects of this variation, a 60-s time window is used for both RE and SE, and, instead of pure SpEn values, burst-compensated spectral entropy (BcSpEn) values are used. Burst-compensated spectral entropy is calculated as:

$$\text{BcSpEn} = \text{SpEn}(1 - \frac{\text{BSR}(\%)}{100\%}). \tag{2.21}$$

For example, in Figure 2.4, the BSR value is 36% and the median relative SpEn is 0.58; thus, the relative BcSpEn is 0.36.

Single-channel EEG/EMG signal measured from the forehead is used for the Entropy monitoring. Entropy has been validated in propofol, sevoflurane, and thiopental+desflurane anesthesia [179]. In Chapter 3, the performance and applicability of Entropy during burst suppression, with facial EMG activity, and with different drugs is reviewed.

2.2.7 Bispectral analysis

Bispectral analysis was first introduced by geophysicists in the early 1960s to study ocean wave motion, atmospheric pressure changes, seismic activity, and sunspots [156]. It was applied to EEG signal first by Barnett et al. [10] and Dumermuth et al. [29] in 1971. Polyspectrum of order higher than two has three advantages over power spectral analysis [112, 167]:

1. Gaussian processes have zero polyspectrum (and cumulant) of order higher than two. Due to this property, bispectral analysis has a high signal-to-noise ratio in applications where the additive noise is Gaussian and the signal is non-Gaussian.
2. A minimum-phase assumption, which is a necessity for the Gaussian process or second-order statistics, is not needed. In other words, phase information for the linear, mixed-phase, non-Gaussian process can be recovered from a polyspectrum of order higher than two.
3. It enables detection and characterization of the nonlinear properties of mechanisms that generate time series via phase relations of their harmonic components – for example, bicoherence (see Equation 2.22) is used to study quadratic phase coupling.

As stated above, the bicoherence index (Bic) can be used to determine the degree of phase coupling in cases where harmonically related peaks are identified in the power spectral domain [167]:

$$\mathrm{Bic}(e^{j\omega_1}, e^{j\omega_2}) = \frac{\hat{B}(e^{j\omega_1}, e^{j\omega_2})}{\sqrt{\hat{P}(e^{j\omega_1})\hat{P}(e^{j\omega_2})\hat{P}(e^{j(\omega_1+\omega_2)})}}. \tag{2.22}$$

Quadratic phase coupling implies interactions among regular stationary oscillators, and this limits the applicability of the bispectral analysis in practice. As described in section 2.2.1, the cross-biperiodogram requires longer time periods for its estimation than a simple periodogram and change in the signal stationarity can take place within the estimation window.

A Hinich test can be used to test for lack of skewness (loosely termed Gaussianness) and linearity in the process. The test has two steps: 1) if the bispectrum of the process is non-zero, the process is non-Gaussian and the test proceeds to the second

step. In 2) the second step, if the bicoherence is constant, the process is linear. Hinich tests have been applied to anesthesia EEG with isoflurane+alfentanil [149] and with propofol+alfentanil [69]. Eight-second epochs were used in the analysis, and a stationarity test was applied before bispectrum estimation. Both studies concluded that 90–95% of the anesthesia EEG can be considered to be a linear, Gaussian random process; i.e., the bispectrum and bicoherence were zero or a mere constant. As these two pieces of research bears out, most information in the EEG spectral content in anesthesia can be tracked with power spectral analysis.

However, non-zero bicoherence has been estimated reliably from anesthesia EEG signal. It has been illustrated that, in order to obtain somewhat consistent estimates, three minutes of EEG is required [49]. On the other hand, the long time window required might be a consequence of the dominance of linear and Gaussian EEG periods. Recent work by Rezek, Roberts & Conradt suggests an alternative method for bispectrum and trispectrum estimation; in this approach, spectra were estimated from the input noise process of an autoregressive model by a mixture of weighted Gaussian densities [130]. For bispectrum estimation with simulated test data, this approach leads to twelvefold savings in the quantity of data required when compared to a standard autoregressive approach. With this technique, the authors used only 2.5-second-long epochs to extract total spectral, bispectral, and trispectral powers in the frequency range 0.5–4 Hz. In the frequency range used in the study, bispectrum or trispectrum did not improve the informativeness of power spectrum in propofol anesthesia. However, slightly improved informativeness was obtained with desflurane and propofol+remifentanil.

Physiological explanation for the usefulness of bispectrum and bicoherence is obscure. Networks of neurons within the brain have nonlinear elements; namely, the membrane properties of the neurons display strong nonlinear properties [117]. It has been suggested that the degree of phase coupling is inversely proportional to the number of independent EEG pacemaker elements [124]. However, the lack of quadratic phase coupling does not guarantee independence of the components [156]. A plausible explanation has been offered by Hagihira and colleagues [55], who used bicoherence in examining whether the frequency shift observed in the power spectrum is caused by frequency modulation occurring in the same source or the change in the location of the source. In the first case, the same frequency shift should be found in the diagonal line of bicoherence space, whereas in the latter case a bico-

herence peak on the diagonal line would not be detected. Thus, bicoherence would be a useful tool to study possible reverberations.

Peaks in the diagonal line of the bicoherence at around 4 Hz have been shown to increase with increasing end-tidal isoflurane concentrations until a plateau is reached at 1.1% and with increasing end-tidal sevoflurane concentrations until a plateau is achieved at 1.4%. A similar increasing peak has been observed at around 10 Hz; however, that peak starts to vanish at 1.1% and at 1.4% with isoflurane and sevoflurane, respectively.[50, 106] Interestingly, these peaks have been shown to decrease consistently after skin incision, without simultaneous consistent change in SEF or BIS values [51].

2.2.8 Bispectral Index

Bispectral Index is a result of a multivariate model from a prospectively collected database of EEG recordings matched to observed anesthetic depth and drug level. Bispectral Index is widely used in clinical practice and there are over 550 peer-reviewed publications on BIS.[71] Since 1992, several different versions of the BIS algorithm have been published; see Table 2.2.

The best description of the BIS algorithm can be found in the article by Rampil [124]. The article probably describes version 3.2 or 3.3 (see Table 2.2). This version involves a weighted sum of four variables derived from the time domain, spectral domain, and bispectral domain. The time-domain variables are BSR and QUAZI suppression, the latter detects slow wave (<1.0 Hz) activity occurring during burst suppression, which would otherwise interfere with the original burst suppression detection algorithm. In the frequency domain, the variable called BetaRatio is derived as:

$$\text{BetaRatio} = \log \frac{\hat{P}_{30-47\text{Hz}}}{\hat{P}_{11-20\text{Hz}}}. \tag{2.23}$$

In the bispectral domain, the variable SynchFastSlow is derived thus:

$$\text{SynchFastSlow} = \log \frac{\hat{B}_{40-47\text{Hz}}}{\hat{B}_{0.5-47\text{Hz}}}. \tag{2.24}$$

Before calculation of BetaRatio and SynchFastSlow, the spectrum and bispectrum, derived from two-second epochs, are smoothed using a running average against those calculated in the previous minute.[124]

Suppression is detected by calculating the logarithmic power of overlapping one-second epochs with offsets of 0.5 seconds in the frequency bands 2–30 Hz and 31–40 Hz. For the preliminary classification, the weighted sum of these powers is compared to the adaptive threshold. Suppression is detected separately for each 0.5-second epoch if either of the two overlapping one-second epochs is identified as suppressed in the preliminary classification. The BSR is the percentage of suppressed 0.5-second epochs in the past 63 seconds.[182]

The BIS algorithm emphasizes BetaRatio most strongly when the EEG has the characteristics of light sedation. SynchFastSlow predominates at surgical levels of hypnosis, and the BSR and QUAZI combination detects deep anesthesia. The weighting factors are proprietary. The final BIS value on the monitor screen is an average value for the previous 60 seconds.[124]

Some reverse engineering has been conducted to study characteristics of different variables for BIS. Sleigh et al. [157] derived BetaRatio, SynchFastSlow, and bispectral power in the frequency bands 0.5–47 Hz and 40–47 Hz. They illustrated that during induction SynchFastSlow is influenced by the progressive decrease of bispectral power in the band 40–47 Hz and mildly increased bispectral power in the band 0.5–47 Hz at loss of consciousness. Later, the group [103] utilized a subset of the same data set to compare SynchFastSlow against PowerFastSlow, which was derived from the same frequency bands as SynchFastSlow but using power spectrum. The researchers found a significant correlation between these variables. Additionally, they derived a variable called SFSbicoh, the bicoherence from the corresponding frequency ranges for SynchFastSlow, to eliminate the influence of changes in signal amplitude. This variable has not proven to be useful. In the area under receiver operating characteristics (ROC) curve analysis, SynchFastSlow and PowerFastSlow displayed roughly similar performance in identifying EEG epochs from awake and anesthetized states.

As a weakness of these studies it should be noted that the authors utilized only eight-second-long time windows in the bispectrum estimation, without any averaging. Although they illustrated the ability of their method to detect quadratic phase coupling with artificial and stationary test signals, previous studies suggested that a three-minute window is required if one is to obtain a consistent estimate of the bicoherence with stochastic EEG signal measured in anesthesia [49], and even BIS

Table 2.2: An overview of Bispectral Index development, adapted from several sources [41, 71, 72, 81].

BIS version	**Release**	**Comment**
1.0	1992	Agent-specificity, modified for analgesic dose, clinical endpoint: response to skin incision and hemodynamic response to laryngoscopy
2.0	1994	Reformulation of index, agent-independence, clinical endpoint: hypnosis and awareness
2.5	1995	Awake-EEG recognition
3.0	1995	Sedation performance enhanced by incorporating high-frequency band
3.1	1996	Enhanced burst suppression detection
3.2	1997	EMG and near-suppression handling improved
3.3	1998	Improved EMG detection
3.4	1999	15-second smoothing, less susceptible to arousal delta EEG on emergence
4.0	2001	XP-level, dual-channel sensor for the elimination of EMG contamination and eye movement artifacts, enhanced near-suppression detection, and electrocautery artifact filtering
4.1	2004	Improved performance in sedation range

is derived from one-minute windows [124]. Additionally, EEG signal obtained over a non-standard inter-hemispheric montage was used, and signal analysis covered only the induction period of anesthesia – the period when BetaRatio probably has greater influence than SynchFastSlow on the BIS.

Because results from the BIS development database are not made public, it is difficult to conclude anything about the advantages of bispectral analysis over power spectrum analysis. As mentioned above, bispectral analysis is affected by several factors contributing to variance in estimation. It is questionable whether these factors are always fully taken into account in comparison of bispectral values to power spectral values. Excluding Aspect Medical Systems, the Japanese group including Hagihira and Morimoto is probably the most experienced in bispectrum estimation for anesthesia EEG. Even they have reported that at BIS levels of 30 to 80, SEF correlated significantly better with BIS than the SynchFastSlow variable derived by the authors themselves [105].

Additionally, BIS has been criticized because the basis of the algorithm is not freely available and it is difficult to interpret the changes in terms of known neurophysiological processes. Additionally, the exact point at which individual patients lose consciousness occurs over a wide range of BIS values, it exhibits a significant time lag, and it does not reliably warn of impending arousal [157]. Time delays have been studied with artificial test signals; in that study, the delay from the "awake" BIS value of 98 to the "general anesthesia" BIS value of 52 was 14 s, and, vice versa, from "general anesthesia" to "awake" was 30 s [118], demonstrating the nonlinear behavior of the BIS algorithm. Although the delay seems long, it should be remembered that EEG signals in anesthesia seldom change instantly, instead exhibiting gradual change.

Index values from two BIS-XP monitors for the same patients have been compared with each other [111]. In this setup, another sensor needs to be attached, just above the eyebrows, contrary to recommendations. With that positioning, the EMG signal is typically more dominant than with electrodes higher on the forehead [42], and EEG signal amplitudes may be smaller, because of the attenuation effect of the frontal sinuses. Although the results were not biased, they indicate that both effects influenced the results. With one patient there was a particularly large difference between monitors in the burst suppression period. Similar discrepancy can

be observed with high BIS values, when the EMG certainly influences the final BIS values. A recent report on a study [60] with three-electrode configuration for BIS stated that during induction the BIS value originating from a sensor in the recommended position decreased earlier than the BIS value originating from a sensor located lower on the forehead. During emergence, the order was reversed. These observations suggest that facial EMG is a dominant factor in BIS calculation and, thus, correct electrode placement is a critical factor.

Limitations of the BIS monitor with certain drugs, types of electrical interference, clinical conditions, and abnormal EEG patterns are discussed in the works of Dahaba and Kelley [24, 81]. Publication **III** describes the effect of epileptiform EEG on BIS.

2.3 Wavelet analysis

An important aspect of wavelet analysis is the desire to achieve good localization in both time and frequency. With two new degrees of freedom of the basis functions, scaling and translation, it is possible to analyze and resolve the joint presence of global waveforms as well as fine structures in signals by using wavelet analysis. The fundamental basis of analyzing signals at different scales, with an increasing level of detail resolution, is referred to as multiresolution analysis. In the following sections, wavelet analysis is described in the extent necessary for understanding the basis of wavelet subband entropy.

2.3.1 Definition of a wavelet

A family of wavelets $\psi_{s,\tau}(t)$ is defined by scaling and translating the mother wavelet $\psi(t)$ by means of the continuous-valued parameters: scale $s(>0)$ and translation τ:

$$\psi_{s,\tau}(t) = \frac{1}{\sqrt{s}}\psi(\frac{t-\tau}{s}), \tag{2.25}$$

where s and τ are real numbers. The factor $1/\sqrt{s}$ assures that all scaled functions have equal energy. Thus, the wavelet is compressed for $0 < s < 1$, whereas it is expanded for $s > 1$. The compression of the wavelet to a smaller scale makes it more localized in time, while the corresponding frequency response is shifted to higher frequencies and the bandwidth is increased to become less localized in frequency; the reverse behavior is obtained when the wavelet is expanded in time.

The continuous wavelet transform (CWT) of a continuous-time signal $x(t)$ is defined by the correlation between $x(t)$ and a scaled and translated version of $\psi(t)$:

$$W(s,\tau) = \int_{-\infty}^{\infty} x(t)\frac{1}{\sqrt{s}}\psi(\frac{t-\tau}{s})dt, \tag{2.26}$$

thus constituting two-dimensional mapping to the time-scale domain. The signal $x(t)$ can be exactly recovered from Equation 2.26 by using the reconstruction equation:

$$x(t) = \frac{1}{C_\psi}\int_{-\infty}^{\infty}\int_{0}^{\infty} W(s,\tau)\frac{1}{\sqrt{s}}\psi(\frac{t-\tau}{s})\frac{d\tau ds}{s^2}, \tag{2.27}$$

where

$$C_\psi = \int_0^\infty \frac{|\Psi(\omega)|}{|\omega|}d\omega < \infty \tag{2.28}$$

and $\Psi(\omega)$ refers to the Fourier transform of $\psi(t)$. For the integral in Equation 2.28 to exist, $\Psi(0)$ must equal zero; i.e., the DC gain must be zero:

$$\Psi(0) = \int_{-\infty}^{\infty}\psi(t)dt = 0 \tag{2.29}$$

and

$$\lim_{|\omega|\to\infty}|\Psi(\omega)| = 0. \tag{2.30}$$

Equations 2.29 and 2.30 imply that the wavelet function $\psi(t)$ must have bandpass characteristics.

2.3.2 Discrete wavelet transform

The CWT is a two-dimensional function $W(s,\tau)$ that is highly redundant. It is, therefore, necessary to discretize the scaling and translation parameters s and τ according to a suitably chosen sampling grid. The most popular approach is to use dyadic sampling of the two parameters:

$$s = 2^{-j}, \tau = k2^{-j}, \tag{2.31}$$

where j and k are integers. Accordingly, the discretized wavelet function is defined by:

$$\psi_{j,k}(t) = 2^{j/2}\psi(2^j t - k). \tag{2.32}$$

Inserting Equation 2.32 into CWT in Equation 2.26, we obtain the discrete wavelet transform (DWT):

$$W_{j,k} = \int_{-\infty}^{\infty} x(t)\psi_{j,k}(t)dt. \tag{2.33}$$

It can be shown that with dyadic sampling it is still possible to exactly reconstruct $x(t)$ from the coefficients $W_{j,k}$ resulting from discretization of the CWT; a coarser sampling grid is retrieved via the inverse DWT, or the wavelet series expansion:

$$x(t) = \sum_{j=-\infty}^{\infty} \sum_{k=-\infty}^{\infty} W_{j,k}\psi_{j,k}(t), \tag{2.34}$$

where $\psi_{j,k}(t)$ is a set of orthonormal basis functions.

2.3.3 Multiresolution analysis

A signal can be viewed as the sum of a smooth part and a detailed part; the smooth part reflects the main features of the signal (and therefore is called an approximation signal), whereas the faster fluctuations represent the details of the signal. The separation of a signal into two parts is determined by the resolution with which the signal is analyzed. A progressively better approximation of the signal is obtained by increasing the resolution so that finer and finer details are included in the smooth part. The approximation of a signal $x(t)$ at scale j is defined as $x_j(t)$. At the next scale, $j+1$, the approximation signal $x_{j+1}(t)$ is composed of $x_j(t)$ and the details $y_j(t)$. By adding more and more detail to $x_j(t)$, we arrive, as the resolution approaches infinity, at a dyadic multiresolution representation of the original signal $x(t)$:

$$x(t) = x_j(t) + \sum_{l=j}^{\infty} y_l(t). \tag{2.35}$$

The scaling function $\varphi(t)$ is introduced for the purpose of efficiently representing the approximation signal $x_j(t)$ at different resolution. The approximation coefficients a_j of the series expansion result from computing the inner product:

$$a_j(k) = \int_{-\infty}^{\infty} x(t)\varphi_{j,k}(t)dt. \tag{2.36}$$

Analogously to dyadic sampling of the wavelet function $\psi(t)$ in Equation 2.32, the scaling function can be generalized through dyadic sampling to generate a set of orthonormal scaling functions for approximations at different resolutions:

$$\varphi_{j,k}(t) = 2^{j/2}\varphi(2^j t - k). \tag{2.37}$$

Scaling functions with different translation indices k for a fixed scale j are orthonormal to each other. However, scaling functions are not required to be orthonormal

between different scales. An important relation is the **refinement equation** that relates $\varphi(t)$ (spanning the subspace ν_0) to $\varphi(2t)$ (spanning the subspace ν_1), where these subspaces are such that $\nu_0 \subset \nu_1$:

$$\varphi(t) = \sum_{n=-\infty}^{\infty} h_\varphi(n)\varphi_{1,n}(t) = \sqrt{2} \sum_{n=-\infty}^{\infty} h_\varphi(n)\varphi(2t-n), \tag{2.38}$$

where $h_\varphi(n)$ is a sequence of scaling coefficients.

The wavelet function $\psi(t)$ complements the scaling function by accounting for the details of a signal, rather than approximations. Wavelet functions (see Equation 2.32) at scale j are orthonormal to the scaling functions at scale j. Detail coefficients $d_j(k)$ can be calculated as the inner product of the signal $x(t)$ and the wavelet function $\psi_{j,k}(t)$:

$$d_j(k) = \int_{-\infty}^{\infty} x(t)\psi_{j,k}(t)dt. \tag{2.39}$$

The coefficients $d_j(k)$ are the same as $W_{j,k}$ in Equation 2.33. Similarly to the refinement equation of the scaling function, the wavelet function can be expressed by the **wavelet equation**:

$$\psi(t) = \sum_{n=-\infty}^{\infty} h_\psi(n)\sqrt{2}\varphi(2t-n). \tag{2.40}$$

The coefficients $h_\psi(n)$ constitute a sequence of wavelet filter coefficients. These coefficients can be determined from the scaling coefficients $h_\varphi(n)$ such that, when the number of scaling coefficients N_φ is finite and even:

$$h_\psi(n) = (-1)^n h_\varphi(N_\varphi - 1 - n) \quad n = 0, ..., N_\varphi - 1. \tag{2.41}$$

The two types of coefficients are thus the same except that the coefficients alternate in sign.

2.3.4 Mother wavelets

Since the requirements presented in section 2.3.1 for the mother wavelet are relatively modest, the wavelets are highly adjustable functions that can be designed to suit various signal processing applications. The simplest wavelet example is the Haar wavelet, which is defined as:

$$\psi(t) = \begin{cases} 1, & 0 \leq t < \frac{1}{2} \\ -1, & \frac{1}{2} \leq t < 1 \\ 0, & otherwise. \end{cases} \tag{2.42}$$

The corresponding scaling function is:

$$\varphi(t) = \begin{cases} 1, & 0 \leq t < 1 \\ 0, & otherwise. \end{cases} \tag{2.43}$$

The Haar wavelet belongs to the Daubechies wavelet family, as the Daubechies wavelet of order $N = 1$. In this wavelet family, the number of wavelet filter and scaling coefficients is equivalent to $2N$. Figure 2.5 presents Daubechies scaling and wavelet functions of orders $N = 1, 2, 3$.

2.3.5 The Mallat algorithm

An important reason for the popularity of multiresolution analysis is the efficient calculation of DWTs with filter-bank implementation by means of the Mallat algorithm, sometimes called a fast wavelet transform (FWT). In this technique, the wavelet transform is obtained by cascade implementation of a filter bank of two filters: a high-pass and low-pass filter. Approximation coefficients a_j are obtained by the convolution of time-reversed scaling coefficients $h_\varphi(-n)$ and the approximation coefficients $a_{j+1}(n)$ on the finer scale, followed by subsequent downsampling by a factor of two:

$$a_j(k) = \sum_{n=-\infty}^{\infty} h_\varphi(n-2k)a_{j+1}(n) = h_\varphi(-n) * a_{j+1}(n)|_{n=2k}. \tag{2.44}$$

In an analogous manner, the wavelet coefficients $d_j(k)$ can be calculated by convolving the time-reversed wavelet filter coefficients $h_\psi(-n)$ with $a_{j+1}(n)$ and subsequent downsampling of the filtered output by a factor of two:

$$d_j(k) = \sum_{n=-\infty}^{\infty} h_\psi(n-2k)a_{j+1}(n) = h_\psi(-n) * a_{j+1}(n)|_{n=2k}. \tag{2.45}$$

Figure 2.6 illustrates the implementation of the Mallat algorithm. For the initialization it is often decided that the signal itself serves to provide the approximation coefficients a_j in the first stage (a_5 in Figure 2.6). It is important to realize that the scaling and wavelet functions do not explicitly appear in calculation of the DWT by means of the Mallat algorithm; only the scaling filter coefficients and wavelet filter coefficients are required. The frequency-domain interpretation comes from the filter parts of equations 2.44 and 2.45. An example of the frequency responses of a five-level filter bank with mother wavelets Daubechies 1, 2, and 3 is presented in

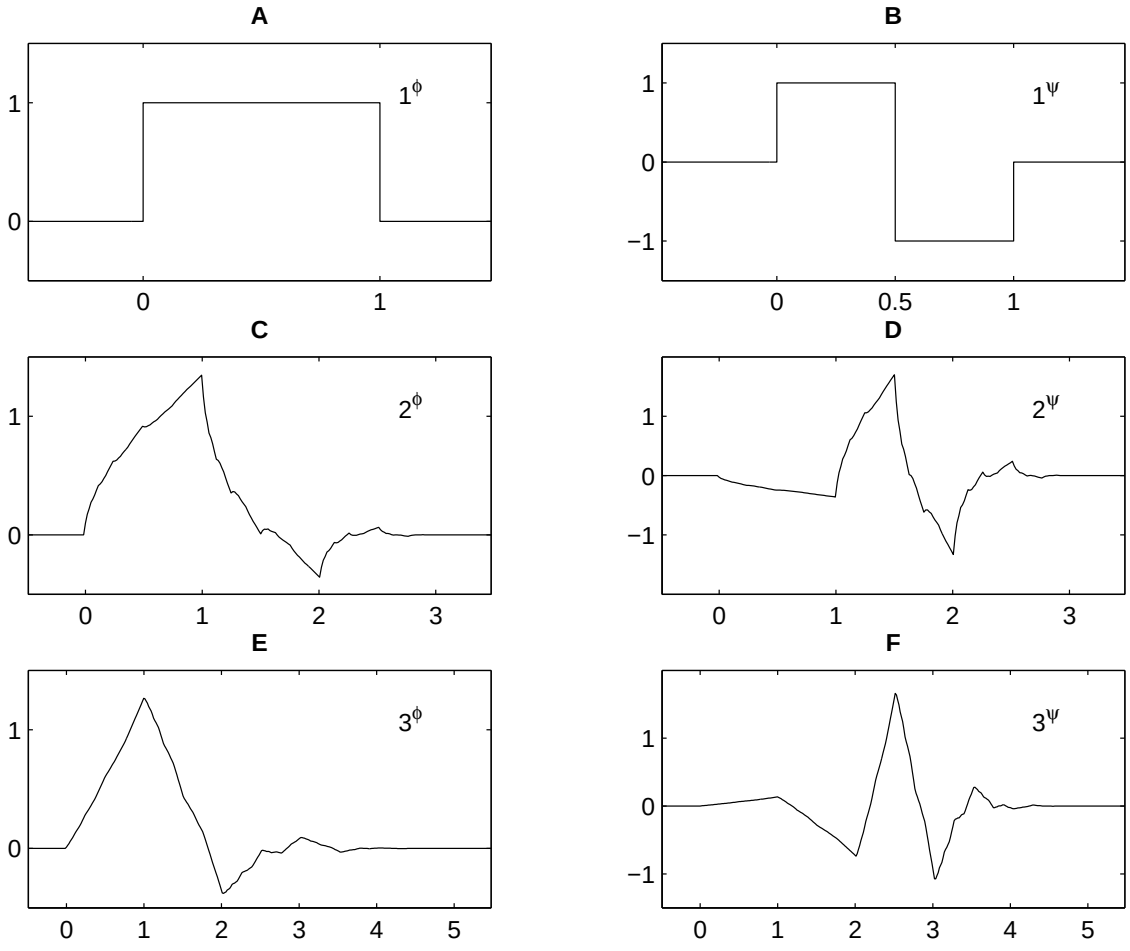

Figure 2.5: Scaling functions of Daubechies 1 (panel A), 2 (panel C), and 3 (panel E) in the left column, with the corresponding mother wavelet functions in the right column.

Figure 2.7. As illustrated, increasing the order of the Daubechies mother wavelet enhances the separation of frequencies.

2.3.6 Wavelet entropy

Wavelet entropy (WE) is proposed for the analysis of short-duration epochs of EEG activity, such as event-related potentials [122, 135]. To obtain WE, wavelet energy $E_j^{(N_j)}$ at each fixed scale j is first derived from running windows of length N_j:

$$E_j^{(N_j)} = \sum_{k=m_j}^{m_j+N_j-1} d_j(k)^2, \tag{2.46}$$

where m_j is running index within each level j. E_j can also be normalized with N_j of each resolution level in order to calculate the mean energy of coefficients at each level and within each epoch [135]. Total energy E_{tot} over all scales used is calculated:

$$E_{tot} = \sum_j E_j^{(N_j)} = \sum_j \sum_{k=m_j}^{m_j+N_j-1} d_j(k)^2. \tag{2.47}$$

To obtain relative wavelet energy (RWE) at each scale and within each epoch, wavelet energy at each scale is divided by the total energy over all scales:

$$p_j^{(N_j)} = \frac{E_j^{(N_j)}}{E_{tot}} = \frac{E_j^{(N_j)}}{\sum_j E_j^{(N_j)}} = \frac{\sum_{k=m_j}^{m_j+N_j-1} d_j(k)^2}{\sum_j \sum_{k=m_j}^{m_j+N_j-1} d_j(k)^2}. \tag{2.48}$$

In calculation of RWE, the aim is to use relatively short windows; i.e., N_j is small. It must be remembered that different scales have different numbers of coefficients, and therefore the shortest epoch must contain at least one sample from the smallest j used. The wavelet entropy is calculated from RWE distributions between scales:

$$\mathrm{WE} = -\sum_j p_j^{(N_j)} \log p_j^{(N_j)}. \tag{2.49}$$

Although this method might be useful in analysis of short-duration signals, where, in addition, wavelet analysis is most beneficial in comparison to Fourier analysis, it is questionable whether it adds something relevant to SpEn when one is analyzing a continuous EEG signal in epochs of a few seconds. When WE was applied for epileptiform EEG activity, 2.5-second-long epochs were used and WE clearly reflected the changes in the corresponding RWE values [134]. In Figure 2.8, relative forms of WE and SpEn are calculated from five-second epochs sliding one second at a time. As we have seen, the two variables behave quite similarly on this occasion, but neither is a specific indicator of epileptiform activity in anesthesia.

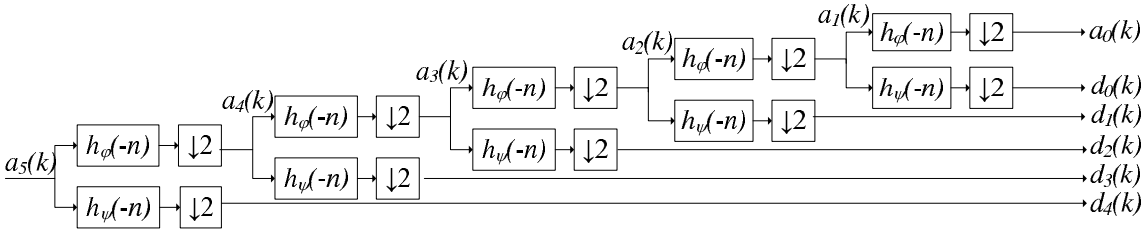

Figure 2.6: Schematic illustration of the Mallat algorithm. The original signal is $a_5(k)$.

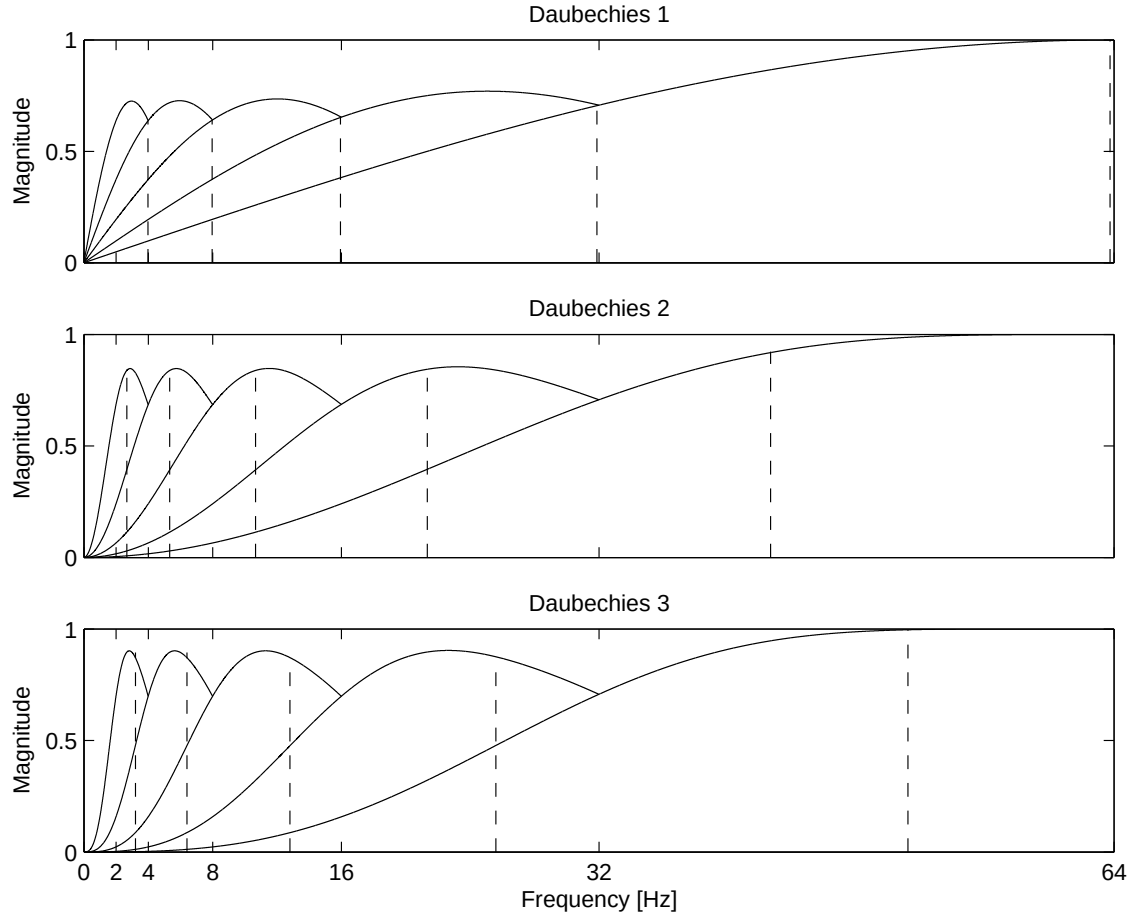

Figure 2.7: Frequency responses of the Mallat algorithm filter-bank implementation with Daubechies 1, 2, and 3. The original signal is sampled at 128 Hz. Vertical dashed lines represent the center frequencies of each wavelet basis function.

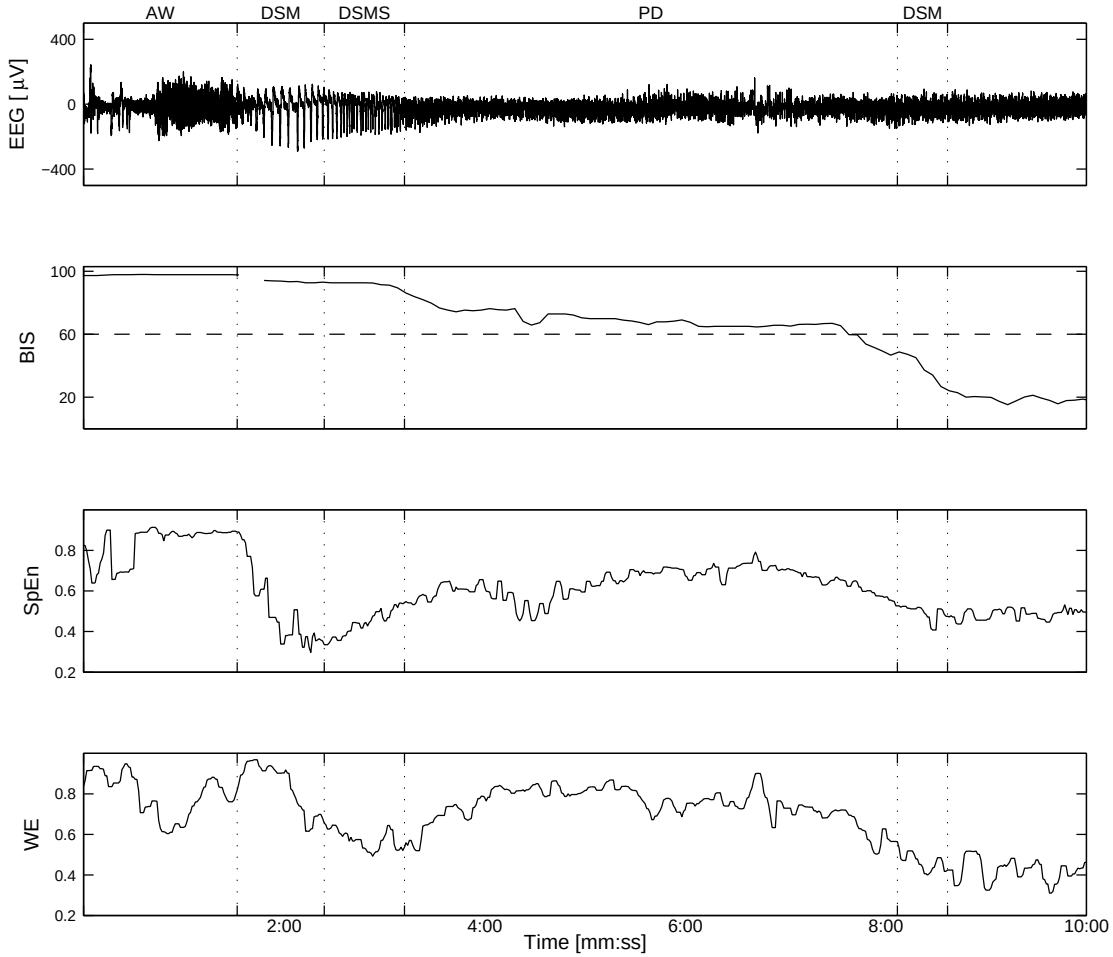

Figure 2.8: Electroencephalogram (EEG), Bispectral Index Scale (BIS), spectral entropy (SpEn), and wavelet entropy (WE) during sevoflurane mask induction. Abbreviations are "AW" for awake activity, "DSM" for slow-delta monophasic activity, "DSMS" for slow-delta monophasic activity with spikes, and "PD" for periodic discharges. The BIS value remains over 60 in deep anesthesia with epileptiform activity, thus indicating moderate sedation [81]. Spectral entropy is calculated over the frequency range 1–47 Hz. SpEn decreases at the onset of DSM activity but starts to increase with emerging spike activity, to reach almost the awake level during the PD period. Wavelet entropy is calculated over the five-level Daubechies 3 wavelet decomposition, therefore including frequencies 2–64 Hz. Because the original EEG contains only frequencies up to 47 Hz, wavelet entropy makes effective use of the same frequency range as spectral entropy 1–47 Hz. As can be seen, wavelet entropy behaves quite similarly to spectral entropy. In this example, there are some differences during awake and DSM periods. As this example illustrates, BIS, SpEn, and WE are sensitive indicators of epileptiform activity but not specific to epileptiform activity only, since the same index values may be obtained as a result of non-epileptiform EEG activity occurring in anesthesia; therefore, their applicability for patient monitoring purposes is limited. The data set used is the same as in Figure 6D in Publication **III**.

2.3.7 Wavelet subband entropy (III)

Publication **III** presents a novel variable, wavelet subband entropy (WSE), derived over the obtained wavelet coefficients only within each scale. To calculate the WSE value, detail coefficients d_j are squared to obtain coefficient energy $E_j^{(1)}$, which is the same operation as that in Equation 2.46 but with window length N_j=1.

$$E_j^{(1)}(k) = d_j(k)^2 \tag{2.50}$$

Relative coefficient energy $\tilde{p}_j$ within each scale j and each epoch of length N_j is calculated by dividing $E_j^{(1)}$ by the signal energy $E_j^{(N_j)}$ (see Equation 2.46) within each scale and given epoch of length N_j:

$$\tilde{p}_j = \frac{E_j^{(1)}}{E_j^{(N_j)}} = \frac{d_j(k)^2}{\sum_{k=m_j}^{m_j+N_j-1} d_j(k)^2}. \tag{2.51}$$

Relative coefficient energies within each scale j and epoch are used in the calculation of WSE:

$$\mathrm{WSE_j} = -\sum_{n=1}^{N_j} \tilde{p}_j(n) \log \tilde{p}_j(n). \tag{2.52}$$

It is advantageous to use the relative form of Shannon entropy, because it facilitates comparison between WSE values obtained from different scales with different N_j. Wavelet subband entropy can be interpreted to describe how concentrated energy is over a given time. Additionally, by using different mother wavelets, WSE can be used as an indicator of the correlation between the wavelet of the scale under consideration and the signal being observed, as is demonstrated in Publication **III**.

In the preliminary study [34] conducted with the same data as Publication **III**, WSE values derived with the mother wavelet Daubechies 3 were used in combination with 43 other variables derived from the single-channel EEG signal in order to develop a classification algorithm for different epileptiform waveforms. The other variables included time-domain measures for EEG signal (mean, median, root-mean-square, and peak-to-peak amplitudes), measures derived from wavelet coefficients of each scale (standard deviation, skewness, and kurtosis), and spectral domain measures (peak power, peak frequency, spectral edge frequency, median frequency, entropies, relative powers, and absolute powers in different frequency bands). In this study, WSE variables turned out to have the best classification capability and were therefore selected for further development.

In Publication **III**, WSE values were calculated for both the approximation and detail coefficients, with five different scales and with three mother wavelets: Daubechies 1, 2, and 3. The WSE of approximation coefficients did not prove to be useful, probably because of the wider pass-band characteristics of the low-pass stage of the filter bank in the Mallat algorithm. Figure 2.7 presents the frequency responses of the Mallat algorithm when applied to EEG signal in Publication **III** with sample frequency 128 Hz. In the study, two different morphologies of epileptiform activity were considered relevant for monitoring purposes: a slow monophasic pattern in the delta-activity frequency range and epileptiform spike activity. It was observed that spike activity was best captured with Daubechies 3 of scale $j = 3$ – i.e., roughly corresponding to frequency band 16–32 Hz (see Figure 2.7). The monophasic pattern was best detected with Daubechies 1 of scales $j = 1$ and $j = 2$ (roughly corresponding to frequency bands 4–8 Hz and 8–16 Hz, respectively). The WSE variables from these two scales were combined into a single variable, combined wavelet subband entropy (cWSE), using weights obtained from linear regression analysis:

$$\mathrm{cWSE}_{4-16\mathrm{Hz}} = 0.4391 \cdot \mathrm{WSE}_{4-8\mathrm{Hz}} + 0.5609 \cdot \mathrm{WSE}_{8-16\mathrm{Hz}}. \tag{2.53}$$

Although numerous and varied techniques have been proposed for the monitoring of epileptiform activity in different contexts, none of the methods have been applied in anesthesia monitoring practices for that purpose – actually, some of the methods are in use for depth-of-anesthesia monitoring (for example, spectral entropy [67]). It must be remembered that anesthesia is a challenging condition, in which the EEG exhibits a wide range of activity types, starting with the awake-state EEG when the patient is admitted to the operating room and ending in the delta, or burst suppression, activity of the anesthetized patient. As is obvious, development of a specific indicator of epileptiform activity for these purposes is challenging, and it is probable that those signal processing techniques that utilize the whole spectrum of the EEG signal (such as 1–47 Hz) are not specific enough, even though they may be sensitive as is illustrated in Figure 2.8 with spectral entropy and wavelet entropy present.

Some attempts to develop a subband-specific EEG indicator utilizing wavelet and entropy analyses have been made at Johns Hopkins University [4, 5, 114]. In two of these studies [4, 5], the equation for wavelet entropy (2.49) is presented. However these studies present wavelet entropy results from different subbands, indicating

that the authors derive their WE variable differently than described.

Because descriptions in these studies could be misunderstood as comparable to the WSE variable presented in Publication **III** and in Equation 2.52, this topic is discussed further. In the material presented below it is assumed that the variables derived in the studies are calculated as presented by Paul and colleagues [114]. The coefficient energy $E_j^{(1)}$ is first derived as in Equation 2.50. After that, RWE is calculated for each coefficient separately (note the difference for Equation 2.48):

$$p_j^{(1)} = \frac{E_j^{(1)}}{E_{tot}} = \frac{E_j^{(1)}(k)}{\sum_j \sum_{k=m_j}^{m_j+N_j+1} E_j^{(1)}(k)} = \frac{d_j(k)^2}{\sum_j \sum_{k=m_j}^{m_j+N_j+1} d_j(k)^2}. \tag{2.54}$$

Entropy for each subband is obtained thus:

$$\mathrm{WE_j} = -\sum_{n=1}^{N_j} p_j^{(1)}(n) \log p_j^{(1)}(n). \tag{2.55}$$

The authors call the variable **subband wavelet entropy**. However, it should be noted that this variable is not a pure measure of each subband's activity, since Equation 2.54 takes into account the energy of the whole signal, E_{tot}, as well. For clarification, in this thesis Equation 2.55 is referred to as that for **wavelet entropy of scale j** ($\mathrm{WE_j}$). As Figure 2.9 illustrates, $\mathrm{WE_j}$ follows the relative wavelet energies $p_j^{(N_j)}$ of the corresponding subband and there is considerable doubt as to whether utilization of the Shannon entropy equation offers any extra information in this application. The same figure illustrates WSE as calculated from identical scales to $\mathrm{WE_j}$. As can be observed readily, WSE can capture subband-specific entropy information independently from relative wavelet energies. Furthermore, based on the results from the extensive data set used in Publication **III** WSE is specific to epileptiform activity only (excluding eye movement artifacts at the beginning of the record and burst suppression) and does not react to any other EEG changes during anesthesia.

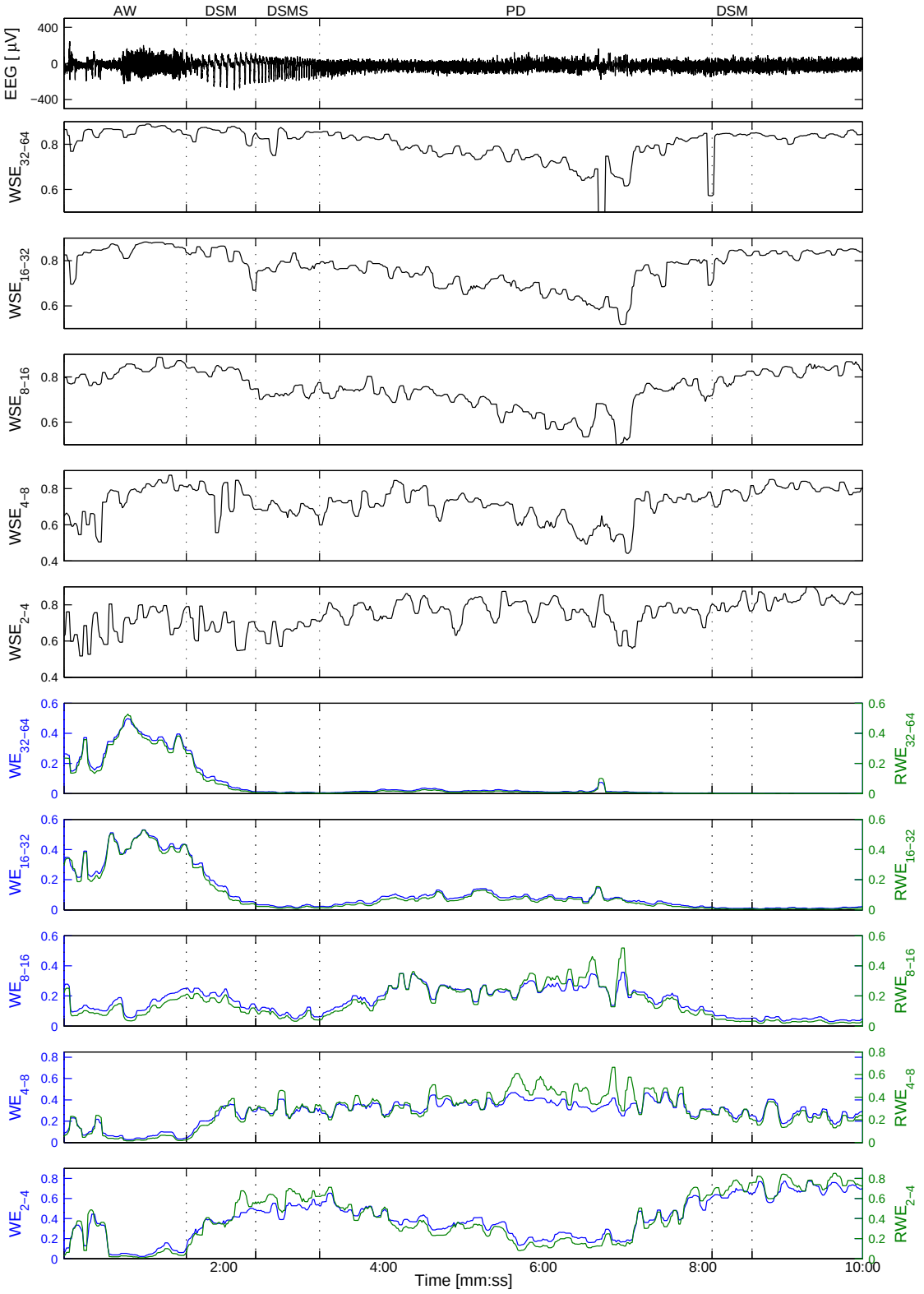

Figure 2.9: Electroencephalogram (EEG) and processed wavelet variables WSE_j, WE_j (blue), and RWE_j (green) from different subbands during sevoflurane mask induction. Daubechies 3 is used as the mother wavelet. The data set used is the same as for Figure 6D in Publication **III**.

3 Evaluation of the methods developed

This chapter presents an overview of the evaluation of the methods developed in the thesis project. First, integration of burst suppression quantification into the depth-of-anesthesia indices SEF, BIS, and Entropy is discussed. Second, the effect of facial electromyographic activity on depth-of-anesthesia monitors and the Entropy monitor's ability to make use of both EEG and EMG signal information are discussed. Third, the discussion addresses the performance of wavelet subband entropy for monitoring epileptiform EEG waveforms and to detect misleading depth-of-anesthesia monitor readings.

Methods used in evaluating the performance of depth-of-anesthesia monitors are reviewed, as are studies with a relationship to the Entropy and Bispectral Index tools in anesthesia monitoring with different drugs. Publication **IV** presents results and explanation for the limited applicability of Entropy on the basis of quantitative EEG analysis from single-agent S-ketamine anesthesia. Publication **V** is one of the first two studies to describe the effects on the human EEG of the recently introduced sedative drug dexmedetomidine.

3.1 Definitions of anesthetic depth

3.1.1 Observed depth of anesthesia

In the past, responses such as movement [79] and increased heart rate or blood pressure [80] to noxious stimuli were used as control metrics in development of EEG indicators of anesthetic depth. However, response to noxious stimuli does not necessarily reflect cortical processing; it can be merely subcortical reflex [9, 123, 127]. Accordingly, responses to these stimuli are less suitable for use in studying EEG-based variables. Comprehension of that fact began a new era in EEG-based depth-of-anesthesia monitoring.

The observer's assessment of alertness/sedation scale, or OAAS, was introduced by Chernik and colleagues in 1990 [22]. Glass and colleagues used a modified form of it (shown in Table 3.1) for the validation of BIS [41] in 1997. Because the OAAS requires intermittent interventions affecting the patient, in many studies only a loss

Table 3.1: The modified observer's assessment of alertness/sedation scale (OAAS) as proposed by Glass et al. [41].

Score	Responsiveness
5	Responds readily to name spoken in normal tone
4	Lethargic response to name spoken in normal tone
3	Responds only after name is called loudly and/or repeatedly
2	Responds only after mild prodding or shaking
1	Does not respond to mild prodding or shaking
0	Does not respond to noxious stimulus

of response to verbal commands (defined as a loss of consciousness, LOC) is used in the assessment. LOC is identical to the transition OAAS<3. Alternatively, loss of eyelash reflex is also used. In propofol induction, loss of this reflex occurs, on average, between OAAS=4 and OAAS=3 [70].

Because the OAAS scale is based on the patient's responses, comparison between the OAAS score and EEG-derived indicator is subject to systematic errors when muscle relaxants or opioids are in use. It has been shown that when remifentanil is given before the start of propofol induction the patient does not respond to noxious stimuli even at the level OAAS=4 [70, 165]. Therefore, the dependency relationship between the EEG and the modified OAAS score (see Table 3.1) is more reliable at levels 3 to 5, where it measures responses to verbal commands (i.e., merely cortical processing), whereas levels 2 down to 0 reflect responses to tactile or noxious stimuli, related to the subject's subcortical state.

3.1.2 Anesthetic drug concentration

Pharmacokinetic–pharmacodynamic (PK–PD) modeling separates the relationship between drug dose and effect into two successive physiological processes. The pharmacokinetic side of the model describes how the concentration of the drug varies with time and site, while the pharmacodynamic side describes the relationship between the concentration of the drug at its effect site and its measured effect.

Effect-site concentration C_e is estimated from the end-tidal (with inhalational drugs)

or plasma (with intravenous drugs) concentrations C_p via pharmacokinetic modeling:

$$\frac{dC_e}{dt} = (C_p - C_e) \cdot k_{e0}, \tag{3.1}$$

where k_{e0} is the rate constant determining the efflux from the effect site. The relation between anesthetic drug effect-site concentration and the EEG-derived variables is often modeled with the pharmacodynamic sigmoid E_{max} model [32, 100, 182]:

$$Effect = E_0 - (E_0 - E_{max}) \cdot \frac{C_e^{\gamma}}{EC_{50}^{\gamma} + C_e^{\gamma}}, \tag{3.2}$$

where *Effect* is the predicted electroencephalographic effect, E_0 is the baseline measure of the EEG-derived variable and E_{max} is the EEG-derived variable at maximum possible drug effect, C_e is the calculated effect-site concentration, EC_{50} is the effect-site concentration associated with 50% of maximal drug effect, and γ is the steepness of the concentration-versus-response relation. With isoflurane and with propofol, in the case where the EEG signal contains burst suppression, the model including two sigmoid functions has been applied [33, 87].

Although the models used correspond surprisingly well to the measured BIS and Entropy values, it should be remembered that comparison studies are usually conducted without surgical stimulus. If surgical stimulus is applied, the concentration v. effect curve is shifted towards higher concentrations; with volatile anesthetics, approximately 2 to 3 times higher concentrations are required to maintain the desired level of cortical suppression [133]. Nociceptive stimulus may influence the level of consciousness or at least the level of electrical activity in the brain. In addition, the models are based on population mean and therefore they do not take interindividual variation into account.

3.2 Methods of performance estimation

3.2.1 Receiver operating characteristics

A receiver operating characteristics curve is a technique for visualizing, organizing, and selecting classifiers on the basis of their performance. ROC curves have long been used in signal detection theory to depict the tradeoff between hit rates and false alarm rates of classifiers. The method was developed for radar signal processing [116], where its name originates. Today ROC curves are widely used in the medical sciences.

An ROC analysis is based on the two-by-two confusion matrix, also called a contingency table. The confusion matrix presents the number of true and false classifications made by the classifier. Table 3.2 presents the confusion matrix applied to depth-of-anesthesia monitoring. In this application, a positive classification means consciousness and a negative one unconsciousness. From the confusion matrix several different performance measures can be derived. Equations 3.3 through 3.7 present some of the most widely used.

$$\text{Sensitivity} = \frac{\text{TP}}{\text{TP} + \text{FN}} \tag{3.3}$$

$$\text{Specificity} = \frac{\text{TN}}{\text{TN} + \text{FP}} \tag{3.4}$$

$$\text{PPV} = \frac{\text{TP}}{\text{TP} + \text{FP}} \tag{3.5}$$

$$\text{NPV} = \frac{\text{TN}}{\text{TN} + \text{FN}} \tag{3.6}$$

$$\text{Accuracy} = \frac{\text{TP} + \text{TN}}{\text{TP} + \text{TN} + \text{FP} + \text{FN}} \tag{3.7}$$

An ROC curve depicts relative tradeoffs between benefits (true positives/negatives) and costs (false positives/negatives). The curve displays sensitivity as a function of 1-specificity. The lower left point in the ROC space (0,0) represents the strategy of never issuing a positive classification; such a classifier yields no false positive errors but also identifies no true positives. The opposite classifier is represented by the upper right point (1,1), and the point (0,1) represents perfect classification. The diagonal line represents the strategy of randomly guessing a class. A discrete classifier produces a single point in the ROC space, but an ROC curve can be

Table 3.2: Confusion matrix applied in evaluation of the accuracy of depth-of-anesthesia monitors.

Monitor's assessment	**Clinical assessment**	
	Conscious	Unconscious
Conscious	True positives (TP)	False positives (FP)
Unconscious	False negatives (FN)	True negatives (TN)

drawn by varying the threshold from $-\infty$ to ∞. In contrast to positive predictive value (PPV) and negative predictive value (NPV), ROC curves are insensitive to changes in class distribution. The area under the ROC curve is equivalent to the probability that the classifier will rank a randomly chosen positive instance higher than a randomly chosen negative instance.[35]

The anesthetic depth monitors do not have numeric thresholds for loss and/or return of consciousness. In the performance studies, threshold values have been derived from the available data; however, those values have not been validated with a large patient population. Additionally, for each individual patient the loss and return of consciousness are associated with different BIS values [143]. Furthermore, the performance studies are usually carried out with relatively healthy adult patients without neurologic diseases, medications affecting the central nervous system, or alcohol/drug abuse. In practice, monitors like BIS and Entropy are more useful for providing trend information for individual patients [28] and measures requiring threshold values are less suitable for the analysis of their performance.

Avoidance of false negatives has been stated to be clinically more important in an anesthetic depth monitor than prevention of false positives [28]. It is justified for clinicians to seek a specific numeric threshold that can be interpreted as meaning "not aware." Practically, awareness during anesthesia is a rare event, and therefore a monitor with no false negatives might cause false positive events in greater numbers than the false negatives it prevents. Often the specified thresholds are equally balanced between false negatives and false positives by maximizing the sum of sensitivity and specificity.

3.2.2 Prediction probability

Prediction probability P_K has become a standard measure in the evaluation of depth-of-anesthesia monitors against clinical endpoints. Both the anesthetic depth indicator value and the observed anesthetic depth are ordinal variables. Therefore, ideal indicator performance is achieved when observed anesthetic depth is mathematically a monotonically nondecreasing function of the indicator's value. P_K is used to assess this monotonicity:

$$P_K = \frac{P_c + 0.5P_{tx}}{P_c + P_d + P_{tx}}, \tag{3.8}$$

where P_c is the probability of concordance, P_d is the probability of discordance, and P_{tx} is the probability of indicator-only tie. As a result, P_K rewards concordances, penalizes discordances and indicator-only ties, and ignores ties in the observer anesthetic depth. Prediction probability's advantage over Spearman rank-order correlation coefficient is that the latter assumes no ties in the indicator value or in the observed anesthetic depth. Although ties can be corrected, Spearman correlation coefficient still lacks an intrinsic meaning, in contrast to the interpretation of P_K as a probability.[160]

Prediction probability belongs to the class of measures of association, as a rescaled variant of Kim's measure of association. Where prediction probability has the advantage over Kim's measure of association that P_K directly relates to the probability of indicator value predicting observed anesthetic depth. For example, a P_K value of 0.5 means that the indicator predicts the observed anesthetic depth only 50% of the time.[160]

Prediction probability is typically estimated using the jackknife method. For a sample of N data points, the method requires computation of $N+1$ estimates of P_K: one from all data of N points and N estimates calculated from subsets obtained by deleting a different data point per estimation. The jackknife estimate is the mean of the subset estimates, and the standard error of the mean σ_{mean} is calculated as:

$$\sigma_{mean} = \sqrt{\frac{(N-1)\sum_{i=1}^{N}(x_i - \bar{x})^2}{N}}, \tag{3.9}$$

where the x_i values are subset means and $\bar{x}$ is the mean over all samples. The jackknife method is recommended by the developers [160] because sampling variability can be approximated by the Student's t distribution, thus taking into account sample size. In addition, the method make possible of paired-data and grouped-data

statistical comparisons of P_K values and reduces bias in the estimation. Another possibility to estimate P_K is to apply Equation 3.8 separately to all individuals by replacing the probabilities with sample estimates and calculating an average of these P_K values [93]. With this method obtained P_K estimate is higher than with the jackknife method using pooled data over all subjects [93].

Prediction probability offers several advantages over the performance measures described in the previous section. First, using sensitivity, specificity, NPV, and PPV takes into account only one of the two possible types of classification errors. All of the measures described, including accuracy, depend on the choice of threshold value. Furthermore, they cannot be used beyond dichotomous patient state [160]. Prediction probability has a close connection to the area under the ROC curve. P_K equals the value of the nonparametric area under the ROC curve for dichotomous patient state, and standard errors estimated with the jackknife method are the same. For a polytomous patient state, P_K is a weighted average of the area under the curves of all pairs of distinct states.[159]

P_K was introduced by Smith, Dutton, & Smith in the January 1996 issue of *Anesthesiology*, and in the same issue it was used to study performance of propofol effect-site concentration, BIS, SEF, pupillary reflex amplitude, and systolic blood pressure in predicting movement after painful stimuli in propofol + nitrous oxide anesthesia [93]. Katoh et al. [78] used P_K to study BIS, SEF, MF, and sevoflurane end-tidal concentration against a polytomous scale (OAAS) in 1998. Also P_K has been used to study the relationship between an anesthetic depth monitor and drug effect-site concentrations, although it is usually supported with correlation analysis [32, 33, 182].

3.3 Principal features of the methods developed

3.3.1 Integration of burst suppression quantification

Because of its nonstationary nature, burst suppression is not suitable for spectral analysis conducted from arbitrarily located time windows. The detrimental effects of improper spectral analysis of burst suppression were demonstrated as early as in 1984 [94].

Increases of the SEF and MF values during burst suppression have been misinterpreted as associated with the occurrence of "high-frequency" waves during burst suppression [20]. Evidently, this trend only indicates spectral analysis conducted with the flat EEG signal since the same study illustrates values of SEF $>$ 20 Hz and MF $\approx$ 5 Hz when BSR = 100%. Publication **I** describes the spectral content of a human burst suppression EEG with propofol and thiopental. As the results indicate, the power of bursts – especially with thiopental – is concentrated in the frequencies below 10 Hz. Similar results have been obtained in the other study with neurosurgical patients sedated with propofol, thiopental, and etomidate [197]. How the spectral content of bursts changes with increasing BSR remains an unstudied question.

Thus, in order to make a univariate EEG descriptor capable of giving a reliable estimate of anesthetic depth, suppression detection must be sensitive in the important phase in which the first suppression periods emerge in the EEG. Otherwise, there is risk of an increase in the univariate descriptor value.

Early versions of BIS had serious problems in the emerging phase of burst suppression. Detsch and colleagues demonstrated that when isoflurane end-tidal concentration was increased from 0.8% to 1.6% the BIS value (in version 3.12) increased in 40% of patients and was unchanged in 33% [26]. The authors confirmed that BSR increased in all patients with burst suppression, therefore the problem was probably not related to burst suppression detection itself but rather to integration of burst suppression quantification. Additionally, burst-compensated SEF did not increase in the patients with increasing BIS values. A later study by Morimoto and colleagues reported similar results with BIS version 3.4 [105]. They found that when burst suppression emerged from isoflurane end-tidal concentration of 1.2% to 1.6% BIS increased, whereas BcSEF decreased. Additionally, linear correlation (R = 0.78)

between BcSEF and BIS < 80 was found.

In propofol anesthesia, it has been shown that BIS (version 3.22) can be estimated with the equation $\mathrm{BIS} = 50 - \mathrm{BSR}/2$, when the BSR is over 40% [17]. The experiment was later reproduced with an XP-level BIS monitor, where a linear relationship at BSR levels of over 40% was observed [182, 189]. However, whereas in the old BIS version BIS = 30 corresponds to BSR = 40%, in the XP version BIS = 25 corresponds to BSR = 40%. Vereecke and colleagues [189] included all BIS (version 4.0) values from the burst suppression period and obtained nonlinear correlation ($R^2 = 0.93$):

$$\mathrm{BIS} \approx 22 + 0.52 \cdot \mathrm{BSR} - 0.014 \cdot \mathrm{BSR}^2 + 0.0001 \cdot \mathrm{BSR}^3,\ \mathrm{BSR} = [0 \ldots 100\%]. \quad (3.10)$$

Entropy variables fit quadratic polygonal curves; therefore, and unlike BIS values, they decrease monotonically with increasing BSR ($R^2 = 0.71$ for RE and $R^2 = 0.72$ for SE) [182].

$$\mathrm{RE} \approx 37.29 - 0.6553 \cdot \mathrm{BSR} + 0.002887 \cdot \mathrm{BSR}^2,\ \mathrm{BSR} = [0 \ldots 100\%] \quad (3.11)$$

$$\mathrm{SE} \approx 35.37 - 0.6379 \cdot \mathrm{BSR} + 0.002928 \cdot \mathrm{BSR}^2,\ \mathrm{BSR} = [0 \ldots 100\%] \quad (3.12)$$

In sevoflurane anesthesia and with XP-level BIS, linear correlation between BIS and BSR $> 40\%$ has also been reported ($R^2 = 0.99 \pm 0.01$) [32]:

$$\mathrm{BIS} \approx (44.1 \pm 2.0) - \frac{\mathrm{BSR}}{(2.25 \pm 0.13)},\ \mathrm{BSR} > 40\%. \quad (3.13)$$

However, for Entropy variables linear correlation was found over the entire BSR range ($R^2 = 0.88$):

$$\mathrm{RE} \approx \mathrm{SE} \approx 29 - \frac{\mathrm{BSR}}{3.25},\ \mathrm{BSR} = [0 \ldots 100\%]. \quad (3.14)$$

Similar results have been reported with other inhalational agents. With isoflurane, correspondence between BIS (XP-level) and BSR $> 40\%$ is $\mathrm{BIS} \approx 42 - 0.42 \cdot \mathrm{BSR}$ [87]. Vakkuri et al. [179] combined the data from propofol + nitrous oxide and thiopental + desflurane + nitrous oxide anesthesia. For BIS and BSR values higher than 50% they obtained the same linear correlation: $\mathrm{BIS} \approx 42 - 0.42 \cdot \mathrm{BSR}$. For Entropy variables, linear correlation was not found. Furthermore, Vakkuri and colleagues observed biphasic dependence between BIS and BSR. At low levels of burst

suppression (BSR $< 20\%$), BIS and BSR increased similarly, as reported by Vereecke and colleagues with propofol [189]. However, with the same patient population, the dependence relationship between RE and BSR was monotonic throughout the range BSR $= [0 \ldots 100\%]$ [179].

The performance of the burst suppression detector of Entropy has been studied with brain-dead organ donor patients as well [193]. The study compared BIS, SE, and RE values that were measured simultaneously and analyzed their difference from zero. When cases with possible residual activity were excluded, SE and RE differed from zero significantly less than BIS in terms of total time (17%, 18%, and 62%, correspondingly). This suggests that the NLEO method used in the Entropy monitor is able to eliminate the influence of noise more effectively than the simple band-power-based algorithm used by BIS. Entropy is also more resistant to electrocautery artifacts [196], which may go some way toward explaining the results obtained.

In summary, BIS has had serious problems in the emerging phase of burst suppression, forming one reason for several new revisions of the algorithm (see Table 2.2). Entropy performs better than the recent XP-level BIS (version 4.0) during that important phase [32, 182]. Additionally, Entropy is more resistant to noise [193, 196], which is an important property in suppression detection.

3.3.2 Simultaneous monitoring of electroencephalographic and facial electromyographic activity

Muscle relaxants are generally believed to have no, or minimal, effect on the EEG [158]. However, some evidence exists of muscle relaxants affecting EEG signals [92, 146]. This phenomenon is explained as occurring because stretching or contracting muscle fibers provide stimulation to arousal centers in the brain, in what is called muscle afferent activity. Nondepolarizing neuromuscular blocking agents are believed to reduce muscle afferent activity while depolarizing neuromuscular blocking agents should increase it. Anticholinesterase agents, such as neostigmine, can be used to reverse the effects of nondepolarizing neuromuscular blocking agents.

It has been shown that the nondepolarizing neuromuscular blocking agent pancuronium produces a dose-correlated increase in BSR in dogs anesthetized with iso-

flurane, and the effect was reversed with neostigmine [146]. The depolarizing neuromuscular blocking agent succinylcholine causes fasciculations followed with EEG arousal in dogs anesthetized with halothane [92]. Therefore, it could be hypothesized that administration of a nondepolarizing neuromuscular block would decrease Entropy and BIS values, whereas depolarizing would increase these values. Experiments have shown that in anesthetized patients BIS is not affected by the nondepolarizing agent [45, 183]. However, administration of neostigmine for neuromuscular block reversal has been shown to increase BIS values [183].

It is well known that the BIS and Entropy variables are affected by EMG activation. This is not a problem when the patients are fully paralyzed but should be taken into consideration when the monitors are used in the absence of muscle relaxants [18]. On the other hand, it has been demonstrated that BIS (version 3.31) can fall even to value 9 when succinylcholine is administered to a fully awake subject who is able to communicate because circulation to the forearm was occluded (this is known as isolated forearm technique) [101]. This particular drop is probably caused by the false positive suppression detection; the figure obtained in the study supports this assumption. However, the same study also illustrates BIS values of 64 and 57 in the experiment where a neuromuscular block was not fully achieved. In that range, BIS utilizes BetaRatio and SynchFastSlow calculations, therefore clearly demonstrating that these variables are affected by the EMG activation.

Schneider and colleagues [143] created a study setup wherein patients were inducted to anesthesia, then after loss of consciousness the isolated forearm technique was applied. Succinylcholine was administered and the patient was then allowed to awaken. After that, a second anesthesia induction was started. The mean (SD) BIS at the first LOC was 62 (19) and at the second LOC 70 (16). The results demonstrate that inter-individual variation in BIS is high but does not seem to be caused by EMG.

In routine anesthesia, neuromuscular blockades are often used in combination with anesthetic agents, facilitating the interpretation of depth-of-anesthesia monitors. However, the possible influence of EMG should be taken into account if depth-of-anesthesia monitors are used in other settings, such as intensive care units. In ICU application, instantaneous Entropy or BIS values do not necessarily provide useful information, since the values may be overestimated because of the concomitant EMG

activity [171, 192].

It has been claimed that BIS-XP is less sensitive to EMG activity than the previous versions of BIS [81]. In the study conducted in remifentanil+propofol anesthesia it was observed that BIS 3.4 and BIS-XP diverged following administration of the nondepolarizing neuromuscular blocker (mivacurium). The mean (SD) BIS-XP values decreased from 41 (3) to 35 (3) and BIS 3.4 values increased correspondingly from 43 (4) to 49 (7) [25]. Simultaneous SEF values of neither monitor changed in this experiment. The XP-level monitor calculates BIS values from two different electrode locations on the forehead, both referred to the temporal electrode. The authors noticed that the BIS value derived from the fourth electrode of the XP sensor (located closer to the temple) was nearly identical to the BIS 3.4 value derived from the conventional three-electrode sensor strip. One might conclude that the BIS-XP drop is caused by reduced muscle afferent activity; however, the divergence between electrodes is surprising and suggests that only artificial correction is done when peculiar changes occur in the signal.

High-dose opioid induction is frequently associated with chest-wall rigidity and elevated facial EMG power [129]. In comparing groups given high-dose fentanyl to those given low-dose fentanyl and etomidate, it was shown that the correlation between facial EMG power and BIS (version 3.4) is much stronger than that between the OAAS score and BIS [129]. However, the authors did not discuss the effect of fentanyl administration on the OAAS score and its possible influence on the results.

In sevoflurane anesthesia without neuromuscular blockade, the RE, RE–SE difference, and facial EMG power discriminate movers and non-movers after skin incision, unlike SE [152]. This clearly indicates that RE and RE–SE difference can be used to monitor facial EMG responses after nociceptive stimulation. The results are confirmed in the other study [168] where RE–SE difference increased with increasing electrical stimulation currents, and there was no significant change in RE–SE difference with increasing sevoflurane concentrations. Other variables studied; BIS, RE, and SE also increased with increasing stimulation, but this increase tended to suppress with increasing sevoflurane concentrations. In paralyzed patients RE–SE difference has been found to increase after noxious stimulation [194].

Two studies compared the effects of muscle relaxants on BIS and Entropy variables. First, Liu and colleagues [96] demonstrated that atracurium administration two

minutes after loss of consciousness decreases BIS and RE but not SE. The experiment was later repeated with rocuronium in deep steady-state anesthesia by Vereecke and colleagues [188]. Again, both BIS and RE decreased after muscle relaxant administration, but not SE.

The agreement between SE and BIS in propofol anesthesia has been analyzed with a Bland–Altman plot [16]. The narrowest limits of agreement were obtained in the baseline before anesthetic induction, and, if rocuronium was administered, in steady-state anesthesia and immediately after laryngoscopy. The widest limits of agreement between BIS and SE were observed at the loss of eyelash reflex and immediately after laryngoscopy if rocuronium was replaced with saline. This suggests that EMG activation contributes to the measurements, and that the BIS and SE process elevated EMG activity differently or with different time delays.

When responses to laryngoscopy were analyzed, it was observed that BIS, RE, and SE increased in both groups (rocuronium and saline) when compared to the baseline [54]. However, only with RE was the increase significantly higher in the saline group than in the rocuronium group. With SE and BIS there were no differences between the groups. With an RE–SE gradient, even more pronounced results were observed: the RE–SE gradient discriminated between groups already two minutes after rocuronium or saline administration prior to laryngoscopy. These results clearly indicate that RE is more reactive to elevated EMG than is either BIS or SE.

Also, RE–SE difference has been demonstrated to have trend-like behavior in paralyzed patients during neurosurgical anesthesia that is similar to that of mean arterial pressure and heart rate [98, 194]. The RE–SE difference has been used successfully for the administration of remifentanil in propofol anesthesia [99].

To conclude, BIS has had problems in the discrimination of EEG and EMG activity, whereas the Entropy algorithm produces two variables. SE is aimed for EEG monitoring, and RE is intended for the identification of impending arousals manifested as elevated EMG activity. SE is not affected by neuromuscular blockers, while BIS and RE are [96, 188]. Without muscle relaxation, RE is more reactive to nociceptive stimulation than BIS or SE [54], therefore presumably reacting more rapidly to impending arousal during surgery than BIS.

3.3.3 Monitoring of epileptiform activity

In Publication **III**, the performance of the method developed, wavelet subband entropy, was evaluated with test data collected from 30 patients during sevoflurane mask induction. Epileptiform activity during sevoflurane anesthesia is characterized by an evolutionary pattern [68, 75, 176, 178, 200] starting with gradual slowing of the EEG, which leads to appearance of the monophasic pattern. Later, spike activity starts with a gradual increase in amplitude and, when evolving further, becomes rhythmic and periodic. During that evolution, the EEG classes that appear are, in chronological order, delta activity (D), slow delta activity (DS), slow-delta monophasic activity (DSM), slow-delta monophasic activity with spikes (DSMS), and periodic discharges (PD). The D and DS activity are not considered epileptiform, and they are typical observations in anesthesia. By contrast, DSM activity is epileptiform activity with mild severity, because it typically precedes spike activity. Epileptiform activity with moderate severity, DSMS activity includes some amount of spike activity superimposed on the monophasic pattern. Finally, PD is severe epileptiform activity. It has been observed to precede seizures in sevoflurane anesthesia [68, 198] and is a typical EEG pattern in status epilepticus, where it also indicates severe risk of irreversible brain damage [14, 172, 173].

Figure 3.1 presents median and interquartile ranges of BIS, $\mathrm{cWSE}_{4-16\mathrm{Hz}}$, and $\mathrm{WSE}_{16-32\mathrm{Hz}}$ during evolutionarily successive EEG waveforms in sevoflurane mask induction. The method developed produced consistently decreasing values following the evolutionary pattern of increasing severity of epileptiform activity. In the range 4 to 16 Hz, $\mathrm{cWSE}_{4-16\mathrm{Hz}}$ was shown to decrease consistently with increasing severity of epileptiform activity, with the P_K value being 0.81. The same applied for the range 16 to 32 Hz, with the P_K value reaching 0.80. The figure shows that BIS increased demonstrably during epileptiform activity. The WSE variables detected BIS values higher than 60 in deep anesthesia with event-sensitivity of 97.1%.

The monophasic patterns resemble the K complex seen in EEG activity during natural sleep [200]. It has been shown that the K complex is a rhythmic waveform resulting from oscillations of excitation and inhibition; maximal cellular activity coincided with the sharp peaks in this waveform [7]. Epileptiform spikes in the data set of Publication **III** coincided with the monophasic pattern. Therefore, monophasic patterns and spikes in this study may share a common mechanism at the cellular

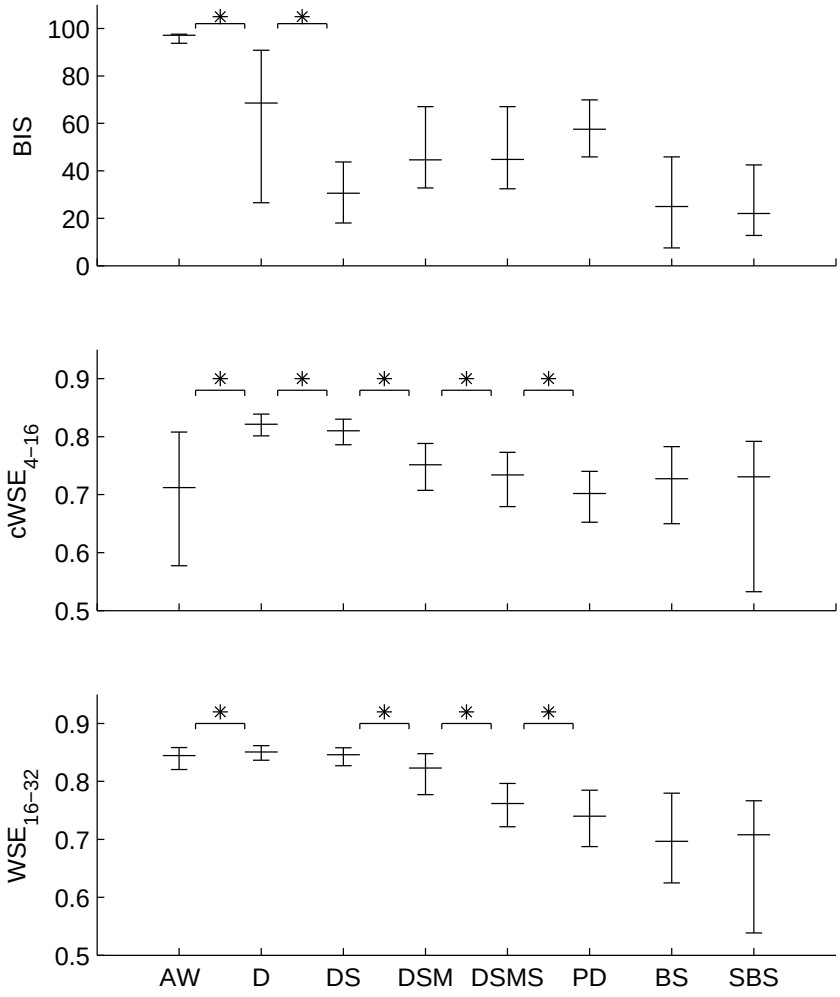

Figure 3.1: Median and interquartile ranges of Bispectral Index Scale (BIS), combined wavelet subband entropy for 4–16 Hz ($cWSE_{4-16Hz}$), and wavelet subband entropy for 16–32 Hz ($WSE_{16-32Hz}$) in evolutionarily successive EEG classes during sevoflurane mask induction. BIS tended to increase during epileptiform waveforms: slow-delta monophasic activity (DSM), slow-delta monophasic activity with spikes (DSMS), and periodic discharges (PD). The most prominent decrease in $cWSE_{4-16Hz}$ was observed when a monophasic pattern emerged in the EEG between evolutionarily successive classes slow delta activity (DS) and DSM. Similarly, the most pronounced decrease in $WSE_{16-32Hz}$ was observed when spike activity emerged in the EEG between evolutionarily successive classes DSM and DSMS. Low values of $cWSE_{4-16Hz}$ in awake (AW) periods are caused by eye movements. The delta (D) and DS classes are considered non-epileptiform activity; DSM, DSMS, and PD are considered epileptiform activity. During burst suppression (BS) and burst suppression with spikes (SBS), the interquartile ranges of WSE variables increased, because flat EEG periods produce high WSE values. The "$*$" sign indicates statistical significance ($p<0.05$) between evolutionarily successive EEG classes.

level, and the decreased inhibition may produce the epileptiform spikes, particularly when cellular activity is maximal during the monophasic patterns. It has been discussed already that the data set with monophasic pattern and spikes demonstrates an imbalance between inhibitory and excitatory mechanisms [200]. With some limitations, two WSE variables succeeded in monitoring the evolution of this imbalance.

In summary, WSE variables consistently decreased with increasing severity of epileptiform activity and detected the misleading readings of the BIS monitor with a high level of sensitivity. Further development is required in considering the burst suppression level. In the future, the method developed may prove to be useful in anesthesia and intensive care by helping to avoid epileptiform discharges.

3.4 Performance during intravenous anesthesia and sedation

3.4.1 Propofol

Quantitative EEG (qEEG) changes associated with loss and return of consciousness with propofol and sevoflurane have been studied by Gugino et al. [46], whose work utilized artifact-free whole-head EEG data. The results showed biphasic behavior: light sedation was accompanied by an increase in frontal/central beta and total power, and deeper sedation (until OAAS=0) resulted in further increases in frontal/central beta and delta activity, beginning in the frontal regions and propagating to posterior regions. The pattern of qEEG changes observed during emergence was a reversal of that observed during induction. In deeper levels of anesthesia, the propofol EEG follows the classical definition of Stockard & Bickford.

The performance of Entropy in predicting loss of consciousness has been compared to that of BIS in several studies. An overview of the results is presented in Table 3.3. Entropy and BIS perform equally well in propofol anesthesia; statistically significant differences between these variables have not been reported.

The results of the studies comparing the performance of BIS and Entropy against estimated propofol effect-site concentrations are controversial (Table 3.4), and no comparison studies have been carried out in the presence of surgical stimulus. Additionally, it should be remembered that BIS is developed using drug level information

[71], presumably referring to PK–PD models, whereas models have not been utilized in Entropy's development. Therefore, comparison may favor BIS if the model used therein is the same as that used in the BIS development.

3.4.2 Ketamine (IV)

The effects of anesthetic ketamine on the human EEG have been reported since 1974, when frontally dominant fast activity at 30–40 Hz was reported as the most characteristic feature of ketamine-induced EEG activity [147]. Also rhythmic theta and episodic delta activity were reported. In single-agent ketamine anesthesia with bolus of 1.5 mg/kg, an increase in the relative theta power and decreases in the relative alpha and relative slow-beta (13–20 Hz) powers were reported by Plourde and colleagues [120]. Effects of racemic and S-ketamine have been compared after midazolam induction by Hering et al. [57], in whose study the EEG effects of racemic ketamine 2 mg/kg and S-ketamine 1 mg/kg boluses did not differ. The authors of the report also reported persistent theta activity and intermittent high-amplitude delta activity superimposed with fast beta (20–40 Hz) activity. Similarly to Plourde and colleagues, these authors reported decreases in the relative alpha and slow-beta powers and interpreted this as a loss of alpha rhythm.

Low doses (0.25 mg/kg and 0.5 mg/kg) of ketamine produce a dose-dependent decrease in absolute alpha power and an increase in absolute theta power. Additionally, the duration of theta activity correlated with the duration of patient unresponsiveness and may therefore be related to the hypnotic property of ketamine [82].

Recent studies investigated the effects of ketamine on propofol-induced spindle oscillations. It is known that propofol induces spindle oscillations in the alpha frequency range. Administration of a ketamine bolus (0.5 mg/kg) caused an increase of spindle frequency from 10 Hz to 15 Hz [175]. The follow-up study found a similar shift in the diagonal line of bispectrum [55]. The ketamine bolus caused a decrease in the relative alpha-band power and an increase in relative slow-beta-, relative fast-beta-, and relative gamma-band powers. The authors suggest that increases in the beta-band powers may be caused by these spindle oscillations. They suggest that the observation of the spindle frequency shift phenomenon in bispectrum indicates that the same source is generating spindle oscillations after the ketamine bolus as with propofol (i.e., thalamic reticular neurons and thalamocortical relay neurons).

Table 3.3: Performance of BIS, RE, and SE against the OAAS with hypnotic drugs. P_K and the corresponding standard errors are presented, except in White et al. [196], where the area under the ROC curve was used. In the latter study and in the propofol and thiopental data sets of Vakkuri et al. [179], the data included both the periods of loss and return of consciousness. In these two studies, P_K was assessed against conscious and unconscious states. In Schmidt et al. [140], P_K was calculated against the whole OAAS range. In the other studies, P_K was assessed only against loss of consciousness (i.e., OAAS<3). P_K was estimated with the jackknife method in Schmidt, Vanluchene et al. [181], Laitio et al. [91], Publication **IV**, and **V**. Presented P_K values of Vakkuri are medians of individual values. In Iannuzzi et al. [64] and Takamatsu et al. [168] estimation method is not described. In Schmidt, Vanluchene, and Laitio only one data point per subject from each OAAS level was used in the estimation. In Vakkuri and Publication **IV** P_K was estimated using the data from 40-minute-long windows. In Publication **V** time window was 20 minutes. Long time windows (and median of individual values presented in Vakkuri) explain the higher P_K values obtained. The number of subjects is represented by N.

Study	**OAAS**	**N**	**BIS**	**RE**	**SE**
Propofol					
Vakkuri [179]	<3	28	0.998	0.998	0.998
Schmidt [140]	5–0	20	0.87 (0.01)	0.88 (0.01)	0.89 (0.01)
Vanluchene [181]	<3	20	0.91 (0.01)	0.88 (0.02)	0.86 (0.02)
Iannuzzi [64]	<3	20	0.90 (0.02)	—	0.95 (0.04)
Propofol+desflurane					
White [196]	<3	30	0.97 (0.04)	0.98 (0.04)	0.93 (0.04)
Thiopental					
Vakkuri [179]	<3	18	0.995	0.996	0.990
S-ketamine					
Maksimow [**IV**]	<3	8	—	0.89 (0.01)	0.93 (0.01)
Dexmedetomidine					
Maksimow [**V**]	<3	11	—	0.98 (0.00)	0.98 (0.00)
Sevoflurane					
Vakkuri [179]	<3	18	1.000	0.996	0.998
Takamatsu [168]	<3	40	0.84 (0.03)	0.84 (0.02)	0.83 (0.03)
Xenon					
Laitio [91]	<3	17	0.46 (0.09)	0.62 (0.10)	0.66 (0.09)

Table 3.4: Performance of BIS, RE, and SE against estimated drug effect-site concentrations. The measures presented are Spearman rank correlation in the study of Vanluchene et al. [182] and coefficient of determination in the studies of Iannuzzi et al. [64] and Ellerkmann et al. [32, 33]. The mean values are presented (SD). The endpoint indicates the deepest level of anesthesia reached in the study, and N is the number of subjects.

Study	**Endpoint**	**N**	**BIS**	**RE**	**SE**
Propofol					
Vanluchene [182]	BSR≥80/MAP<50	10	0.89 (0.01)	0.86 (0.01)	0.84 (0.01)
Ellerkmann [33]	BSR≥50/MAP<60	20	0.92 (0.06)	0.89 (0.07)	0.88 (0.08)
Iannuzzi [64]	OAAS=0	20	0.77	—	0.84
Sevoflurane					
Ellerkmann [32]	$C_{et} = 5\%_{vol}$	16	0.85 (0.12)	0.86 (0.10)	0.87 (0.09)

The EEG effects of ketamine are contradictory. Theta activity is reported to be intermittent, and therefore it may remain undetected in spectral analysis. A decrease in the relative alpha-band power [57, 120, 175] or absolute alpha power [82] is reported consistently. Interestingly, Publication **IV** reported an increase of absolute alpha power for S-ketamine at anesthetic level as compared to subanesthetic level. However no dominant frequency peaks were observed in the spectrum in the alpha band for the anesthetic level and relative alpha-band power did not change. Decreases in the relative slow-beta-band powers have been reported in single-agent anesthesia and with midazolam [57, 120]; however, with propofol ketamine causes an increase in relative slow-beta power [175]. Contrary to earlier reports, we reported an increase of absolute slow-beta-band power at anesthetic level as compared to subanesthetic level, again relative power remaining unchanged. No clear differences were seen in either alpha or slow-beta power when S-ketamine levels were compared to the baseline.

Further, Publication **IV** presents the finding that, in propofol anesthesia, power is more concentrated in the delta band, whereas in S-ketamine anesthesia it is concentrated in the theta and gamma bands. In propofol anesthesia, absolute alpha power is higher than what is seen in S-ketamine anesthesia.

Ketamine at concentrations of 0.5 mg/kg and higher has an additive anesthetic effect

Table 3.5: Quantitative EEG and Entropy variables at awake baseline level and in S-ketamine anesthesia; the values presented are mean (SD). The EMG power is calculated for the frequency range 105–145 Hz. As observed, the power in the high frequency range of EEG activity (beta and gamma) remains at the baseline level in S-ketamine anesthesia, whereas the EMG level declines significantly.

EEG/EMG variable	**Awake baseline**	**S-ketamine anesthesia**
EEG 1–70 Hz (μV^2)	18.3 (7.4)	52.8 (29.8)
delta (%)	33.8 (4.8)	24.1 (18.7)
theta (%)	19.6 (15.3)	35.1 (15.9)
alpha (%)	17.8 (7.8)	11.5 (6.2)
beta (%)	14.3 (2.7)	12.8 (14.2)
gamma (%)	14.5 (3.2)	16.5 (12.1)
EMG 105–145 Hz (μV^2)	0.96 (0.58)	0.04 (0.01)
RE	95.7 (2.7)	72.0 (16.7)
SE	85.3 (3.4)	54.6 (18.0)

when administered with propofol; i.e., less propofol is required to obtain OAAS<3 and the loss of eyelash reflex [136]. Yet, these clinical endpoints occur at the higher BIS levels, being inversely proportional to ketamine dosage [136]. In induction of anesthesia with ketamine alone, BIS has been reported to be insensitive to loss of consciousness [166, 199]. The BIS value increases after ketamine administration in propofol+fentanyl anesthesia [59] and in pure propofol anesthesia [175, 187].

Response entropy and state entropy have been reported to be more sensitive for ketamine-induced excitement of EEG than BIS both in propofol+remifentanil [188] and in sevoflurane [53] anesthesia. In sevoflurane anesthesia at BIS, RE, and SE levels of 33, 31, and 30, respectively, a ketamine bolus of 0.5 mg/kg causes an increase of up to 46, 52, and 50 [53]. In the study conducted with propofol+remifentanil anesthesia, all variables were, on the average, at approximately the level of 40 before ketamine administration. Statistically significant increases were observed in both RE and SE after ketamine administration; an average level of about 50 was reached. Mean BIS level increased also following ketamine administration; however, because of wide inter-individual variability in responses, statistical significance was not achieved. Because a fourth of the patients reached burst suppression, the au-

thors suggest that this may be a manifestation of inter-individual variability of BIS at burst suppression level [188].

Publication **IV** clearly shows that the increased high-frequency activity (>20 Hz) induced by S-ketamine explains why Entropy may show high index values during deep S-ketamine anesthesia. Table 3.5 presents results from qEEG analysis and Entropy variables for the baseline and S-ketamine anesthesia. With five subjects in the study, BIS version 3.3 was recorded as a supplementary measure. Neither BIS worked reliably. The mean BIS value during anesthesia was 88 [97].

3.4.3 Dexmedetomidine (V)

Publication **V** is the first study describing the effects of dexmedetomidine on the human EEG. Generally, the EEG in dexmedetomidine sedation resembles the EEG of GABAergic agents, such as propofol. Dexmedetomidine increased total EEG power and the power in the delta and theta bands. When compared to propofol, dexmedetomidine seems to induce characteristically high delta-band power and less power in the alpha band. Additionally, beta power decreased. The dexmedetomidine EEG has been studied in other work as well, where dexmedetomidine was supported with remifentanil [48]. In that study, similar EEG effects were observed: an increase in the relative delta power and EEG slowing captured by a decreasing SEF value.

Data obtained in the study reported upon in Publication **V** have been used later for comparing the dexmedetomidine EEG to a natural-sleep EEG [63]. It was found that the dexmedetomidine EEG indeed resembles natural sleep activity S2, and spindles between the two data sets were similar. The only observed difference was that the duration of single spindles was longer in the dexmedetomidine group. Previous experimental evidence has indicated that endogenous sleep pathways may be involved in dexmedetomidine-induced sedation [109]. Such observations may have great value, because sleep deprivation is recognized as a severe problem in ICU patients, one that may even increase mortality and morbidity rates [86].

In Publication **V**, state and response entropy were shown to rapidly follow the changes in raw EEG and the loss and return of consciousness. At the end of dexmedetomidine infusion and despite most Entropy values being 10–20, subjects were easily and rapidly awakened by a verbal command and light shaking. After that,

Table 3.6: Quantitative EEG and Entropy variables for the five minutes before and after LOC and for one minute before and after ROC in dexmedetomidine sedation. Mean values are shown (SD).

EEG variable	**Before LOC**	**After LOC**	**Before ROC**	**After ROC**
EEG 1–30 Hz (μV^2)	24.5 (8.3)	68.7 (44.1)	356.4 (244.5)	38.0 (29.3)
delta (%)	50.4 (8.9)	67.0 (11.7)	89.1 (7.6)	66.6 (14.1)
theta (%)	20.4 (3.4)	16.5 (4.5)	7.5 (5.3)	13.0 (4.0)
alpha (%)	18.5 (9.4)	12.5 (6.2)	2.8 (2.1)	12.3 (7.8)
beta (%)	10.7 (2.3)	4.0 (2.3)	0.6 (0.4)	8.1 (4.5)
RE	87 (8)	49 (12)	16 (5)	74 (14)
SE	76 (8)	43 (10)	14 (4)	63 (13)

they were left without stimulation and the Entropy values fell again to 10–20. An overview of the results is presented in Table 3.6. Dexmedetomidine is primarily aimed for use in intensive care sedation, where the primary interest is not the prevention of awareness but guiding of sedation and avoiding inadequate levels of sedation, to maximize the comfort of patients and caregivers [174]. Therefore, the low Entropy values of the unstimulated subjects when dexmedetomidine is still in circulation are not a problem.

Bispectral Index values have been applied for the monitoring of post-surgical intensive care patients with propofol supported with dexmedetomidine [174]. In that study, dexmedetomidine reduced the use of propofol from the level seen in the placebo group. For guiding sedation, BIS was found to be useful, because the alternative approach offered by observable sedation scoring systems requires assessments involving acoustic and tactile stimuli. However, certain BIS values cannot be interpreted as corresponding to specific sedation scoring levels. The BIS values in dexmedetomidine+remifentanil sedation have been reported as lower than the values in the corresponding level of midazolam+remifentanil sedation, which may be explained by the characteristically high delta power induced by dexmedetomidine [48]. In addition, this may be explained by the characteristics of dexmedetomidine sedation itself, since sedated patients remain arousable.

3.5 Performance during inhalational anesthesia

3.5.1 Sevoflurane

As studied by Gugino and colleagues [46], sevoflurane effects on EEG are, in general, similar to the influence of propofol. In sevoflurane anesthesia, BIS and Entropy have performed equally well in terms of P_K analysis when compared against LOC information [168, 179] and the estimated effect-site concentration where R^2 analysis is concerned [32]. The results are presented in tables 3.3 and 3.4. Additionally, there is one study describing different slopes in the dose-response curves for sevoflurane with Entropy in the deepening and lightening phase [100]. However, the reason is unclear and might be explained by the estimation technique used.

Recent study investigated correlations of SE and BIS against end-tidal concentrations of sevoflurane [132]. Results demonstrated that overall correlation and correlation at concentrations >1.5% was better for SE, whereas BIS yielded better correlation at concentrations <1.5%. Takamatsu and colleagues [168] compared Entropy and BIS (version 3.4) in end-tidal sevoflurane concentrations 1.3%, 1.7%, 2.1%, and 2.5%. RE and SE decreased significantly with increasing concentrations, whereas BIS did not.

3.5.2 Desflurane

Unlike sevoflurane, desflurane does not produce epileptiform activity [126, 180] and is recommended as a suitable therapy for patients with refractory status epilepticus [154]. Otherwise, the effects of desflurane on EEG activity resemble what is observed with sevoflurane [148]. With increasing concentrations, total power and relative power values in the delta and theta band increased, beta power decreased, and alpha power did not change significantly. In two studies [179, 196] comparing Entropy and BIS in the perioperative period in desflurane anesthesia, no significant differences were observed.

3.5.3 Nitrous oxide

The effects of nitrous oxide on EEG activity depend on the other anesthetic agents used with it. When used alone, it produces frontally dominant high frequency (>30 Hz) activity. When used with halogenated inhalational agents, it can be additive or have antagonist effect. For example, at burst suppression level nitrous oxide has activating effect, reducing suppression periods. When nitrous oxide is given at higher concentrations, it increases delta activity, therefore demonstrating an additive effect.[158] Withdrawal of nitrous oxide causes an increase in delta activity, sometimes referred to as arousal delta [125].

When nitrous oxide is used alone at a concentration below 50%, it does not affect OAAS or BIS [125]. However, if it is supplied at concentrations of 70–75%, causing loss of consciousness and recall, this event is detected by neither BIS [11] nor Entropy [8]. A recent study [163] compared Entropy and BIS in two sets of circumstances: first, when the sevoflurane concentration was held constant and nitrous oxide (end-tidal concentration of >65%) was added and, second, when the sevoflurane level was reduced and nitrous oxide was added. In the first conditions, both BIS and Entropy values decreased, but only Entropy significantly. In the second set of experimental conditions, both BIS and Entropy values increased.

3.5.4 Xenon

Compared to propofol (see Publication **V**), isoflurane, desflurane, and sevoflurane [148], the use of xenon produces a considerably higher increase in the total EEG power, which is mainly concentrated in the delta and theta bands and is frontally dominant [91]. The xenon EEG may be more concentrated in the delta band than an EEG associated with other inhalational agents (isoflurane, desflurane, and sevoflurane) [91, 148]. This is supported by the observation that BIS did not differ between isoflurane and xenon conditions but SEF was significantly lower with xenon [43].

In P_K analysis, Entropy and BIS perform equally in xenon anesthesia (see Table 3.3), although both monitors exhibit a delay at induction, possibly caused by the agitation of the subject. During steady-state xenon anesthesia, Entropy values are lower than BIS values.[91]

3.6 Opioid effect

Despite several comparison studies, a statistically significant difference in P_K analysis favoring BIS over Entropy has been obtained only in the propofol+remifentanil induction by Duncan and colleagues [30]. Vanluchene and colleagues [181] studied the effects of different remifentanil infusion levels in propofol infusion. A remifentanil level of 4 ng/ml was high enough to cause a decrease in P_K values for all BIS, RE, and SE. There were no statistically significant differences between the variables. Table 3.7 presents the P_K values of BIS and Entropy variables in propofol+remifentanil anesthesia.

In a neurosurgical study setting, the propofol+sufentanil anesthesia timeline was divided into three sections, according to the appearance of certain events (the patient stopping counting, loss of blinking reflex, recovery of blinking reflex, following of orders). P_K was assessed against these three levels, and all variables for RE, SE, and BIS displayed high P_K values.[98]

Generally P_K values in propofol+remifentanil anesthesia are lower than in single-agent propofol anesthesia. In today's anesthesia practice opioids are used mainly for analgesia, and single-agent opioid anesthesia is unpredictable and inconsistent [104]. Additionally, opioids affect OAAS scoring, making OAAS a problematic reference [70, 165].

Table 3.7: Prediction probabilities P_K and the corresponding standard errors of BIS, RE, and SE against the OAAS in propofol+remifentanil anesthesia. P_K was assessed against loss of consciousness (i.e., OAAS<3). The number of subjects is denoted by N.

Study	**OAAS**	**N**	**BIS**	**RE**	**SE**
Propofol+remifentanil					
Vanluchene$_{2ng/ml}$ [181]	<3	20	0.93 (0.02)	0.89 (0.03)	0.85 (0.03)
Vanluchene$_{4ng/ml}$ [181]	<3	19	0.89 (0.02)	0.83 (0.03)	0.81 (0.03)
Duncan [30]	<3	31	0.95 (0.02)	0.86 (0.03)	0.82 (0.03)

4 Conclusions

The first aim of this thesis was to develop a method for burst suppression detection and incorporate it into a depth-of-anesthesia monitor. The method's development is described in Publication **I**. The method is based on a nonlinear energy operator, which proved to be better than a simple signal value approach. The method developed constitutes the basis for the burst suppression detection in the Entropy monitor, a system that has been proven more accurate on the burst suppression level than the BIS monitor [32, 179, 182, 193]. Therefore, the method developed, when properly integrated into the Entropy monitor is probably the most accurate technique currently in existence for monitoring anesthetic depth in deep anesthesia.

The second aim of the thesis was to develop a depth-of-anesthesia monitor utilizing both cortical and subcortical information from the patient. Publication **II** describes the algorithm employed in the Entropy monitor, which derives two spectral-entropy-based variables. Response entropy was developed as a rapidly reacting index utilizing information from facial EMG and therefore allowing fast response to impending arousals during surgery. State entropy was developed for monitoring the cortical state of the patient, as a variable less influenced by EMG activity. The studies conducted have indicated that SE is not affected by neuromuscular blocking agents, even though RE and BIS are [96, 188]. RE is more responsive to nociceptive stimulation than BIS or SE [54], therefore presumably reacting more rapidly to impending arousals during surgery than BIS and SE. With hypnotic drugs, Entropy performs as well as BIS in terms of prediction probability. Because one of the primary goals of anesthesia is the prevention of awareness during surgery, one could argue that prediction probability in comparison to the OAAS determined during the induction phase prior to surgery is the primary measure of a depth-of-anesthesia monitor's success. Arousals during surgery may be a result of nociceptive stimulation, and in this kind of study arrangement the Entropy monitor has been proven successful.

The third aim of the thesis was to develop a method for the monitoring of epileptiform activity during anesthesia. In Publication **III**, a novel EEG-derived quantity, wavelet subband entropy, was developed for this purpose. The method is specific to epileptiform activity only, i.e., it does not react to the typical EEG patterns of anesthesia, except for burst suppression. The method succeeded in quantifying

evolutionary patterns of epileptiform activity with high prediction probability and detected misleading readings of the BIS monitor in deep anesthesia with high event-sensitivity. In the future, the method could assist in minimizing the occurrence of epileptiform discharges and seizures in anesthesia and intensive care. Before that, more work is required to identify low WSE values caused by the eye movements and to eliminate the effect of burst suppression without epileptiform activity.

Finally, the project's fourth aim was to investigate the Entropy monitor in S-ketamine anesthesia and in dexmedetomidine sedation. In Publication **IV**, the Entropy monitor's performance in single-agent S-ketamine anesthesia was assessed. Quantitative EEG analysis revealed that high-frequency EEG activity induced by S-ketamine was the reason for high entropy values encountered despite deep anesthesia. The same phenomenon is a probable reason behind results published earlier for studies where quantitative EEG analysis was not conducted [53, 188]. In Publication **V**, the effects of single-agent dexmedetomidine sedation on human EEG signal were reported upon for the first time. High delta activity was characteristic of dexmedetomidine-induced EEG activity. The Entropy monitor proved to be a rapid indicator of the changes between consciousness and unconsciousness.

The last 10 to 15 years have witnessed a revolution in EEG-based depth-of-anesthesia monitoring. However, many important questions remain unresolved. This study was constructed to investigate some of those challenges. In the future, new, more potent drugs probably will be introduced. How those will affect the EEG and the current depth-of-anesthesia indices will be an open question. Dexmedetomidine, although primarily targeted at sedation in intensive care, may be one of these drugs of the future. Opioids influence EEG activity and depth-of-anesthesia monitors, although their primary effect site is in the spinal cord. Thus, monitoring should aim to enhance orthogonalization between cortical and spinal cord effects. The first step in this area already may have been taken, with the recent introduction of a surgical stress index based on hemodynamics [62]. It is hoped that this will improve understanding in EEG monitoring and help to avoid the mistakes made in the early phases of BIS development. At the same time, the future may see automated control of anesthetic drug administration – but many breakthroughs will be required before that point is reached.

References

[1] R. Agarwal, J. Gotman, D. Flanagan, and B. Rosenblatt. 1998. Automatic EEG analysis during long-term monitoring in the ICU. Electroencephalography and Clinical Neurophysiology 107, no. 1, pages 44–58.

[2] M.S. Aho, O.A. Erkola, H. Scheinin, A.-M. Lehtinen, and K.T. Korttila. 1991. Effect of intravenously administered dexmedetomidine on pain after laparoscopic tubal ligation. Anesthesia & Analgesia 73, no. 2, pages 112–118.

[3] I. Aimé, N. Verroust, C. Masson-Lefoll, G. Taylor, P.-A. Laloë, N. Liu, and M. Fischler. 2006. Does monitoring Bispectral Index or spectral entropy reduce sevoflurane use? Anesthesia & Analgesia 103, no. 6, pages 1469–1477.

[4] H.A. Al-Nashash, J.S. Paul, W.C. Ziai, D.F. Hanley, and N.V. Thakor. 2003. Wavelet entropy for subband segmentation of EEG during injury and recovery. Annals of Biomedical Engineering 31, no. 6, pages 653–658.

[5] H.A. Al-Nashash and N.V. Thakor. 2005. Monitoring of global cerebral ischemia using wavelet entropy rate of change. IEEE Transactions on Biomedical Engineering 52, no. 12, pages 2119–2122.

[6] M.T. Alkire, J.R. McReynolds, E.L. Hahn, and A.N. Trivedi. 2007. Thalamic microinjection of nicotine reverses sevoflurane-induced loss of righting reflex in rat. Anesthesiology 107, no. 2, pages 264–272.

[7] F. Amzica and M. Steriade. 1997. The K-complex: Its slow (<1-Hz) rhythmicity and relation to delta waves. Neurology 49, no. 4, pages 952–959.

[8] R.E. Anderson and J.G. Jakobsson. 2004. Entropy of EEG during anaesthetic induction: a comparative study with propofol or nitrous oxide as sole agent. British Journal of Anaesthesia 92, no. 2, pages 167–170.

[9] J.F. Antognini and K. Schwartz. 1993. Exaggarated anesthetic requirements in the preferentially anesthetized brain. Anesthesiology 79, no. 6, pages 1244–1249.

[10] T.P. Barnett, L.C. Johnson, P. Naitoh, N. Hicks, and C. Nute. 1971. Bispectrum analysis of electroencephalogram signals during waking and sleeping. Science 172, no. 3981, pages 401–402.

[11] G. Barr, J.G. Jakobsson, A. Öwall, and R.E. Anderson. 1999. Nitrous oxide does not alter Bispectral Index: a study with nitrous oxide as sole agent and as an adjunct to i.v. anaesthesia. British Journal of Anaesthesia 82, no. 6, pages 827–830.

[12] S.M. Bhananker, J.T. O'Donnell, J.R. Salemi, and M.J. Bishop. 2005. The risk of anaphylactic reactions to rocuronium in the United States is comparable to that of vecuronium: an analysis of Food and Drug Administration reporting of adverse events. Anesthesia & Analgesia 101, no. 3, pages 819–822.

[13] V. Billard, P.L. Gambus, N. Chamoun, D.R. Stanski, and S.L. Shafer. 1997. A comparison of spectral edge, delta power, and Bispectral Index as EEG measures of alfentanil, propofol, and midazolam drug effect. Clinical Pharmacology & Therapeutics 61, no. 1, pages 45–58.

[14] W.T. Blume, P.L. Carlen, E. Starreveld, S. Wiebe, and G.B. Young. 2006. Advances in Neurology, Volume 97, Intractable Epilepsies. Lippincott Williams & Wilkins, Philadelphia, PA, USA.

[15] G. Bodenstein and H.M. Praetorius. 1977. Feature extraction from the electroencephalogram by adaptive segmentation. Proceedings of the IEEE 65, no. 5, pages 642–652.

[16] V. Bonhomme, E. Deflandre, and P. Hans. 2006. Correlation and agreement between Bispectral Index and state entropy of the electroencephalogram during propofol anaesthesia. British Journal of Anaesthesia 97, no. 3, pages 340–346.

[17] J. Bruhn, T.W. Bouillon, and S.L. Shafer. 2000. Bispectral Index (BIS) and burst suppression: revealing a part of the BIS algorithm. Journal of Clinical Monitoring and Computing 16, no. 8, pages 593–596.

[18] J. Bruhn, T.W. Bouillon, and S.L. Shafer. 2000. Electromyographic activity falsely elevates the Bispectral Index. Anesthesiology 92, no. 5, pages 1485–1487.

[19] J. Bruhn, H. Röpcke, and A. Hoeft. 2000. Approximate entropy as an electroencephalographic measure of anesthetic drug effect during desflurane anesthesia. Anesthesiology 92, no. 3, pages 715–726.

[20] J. Bruhn, H. Röpcke, B. Rehberg, T. Bouillon, and A. Hoeft. 2000. Electroencephalogram approximate entropy correctly classifies the occurrence of burst suppression pattern an increasing anesthetic drug effect. Anesthesiology 93, no. 4, pages 981–985.

[21] G. Enlund P. Samuelsson C. Lennmarken, K. Bildfors and R. Sandin. 2002. Victims of awareness. Acta Anaesthesiologica Scandinavica 46, no. 3, pages 229–231.

[22] D.A. Chernik, D. Gillings, H. Laine, J. Hendler, J.M. Silver, A.B. Davidson, E.M. Schwam, and J.M. Siegel. 1990. Validity and reliability of the observer's assessment of alertness/sedation scale: study with intravenous midazolam. Journal of Clinical Psychopharmacology 10, no. 4, pages 244–251.

[23] M. Chinzei, S. Sawamura, M. Hayashida, T. Kitamura, H. Tamai, and K. Hanaoka. 2004. Change in Bispectral Index during epileptiform electrical activity under sevoflurane anesthesia in a patient with epilepsy. Anesthesia & Analgesia 98, no. 6, pages 1734–1736.

[24] A.A. Dahaba. 2005. Different conditions that could result in the Bispectral Index indicating an incorrect hypnotic state. Anesthesia & Analgesia 101, no. 3, pages 765–773.

[25] A.A. Dahaba, M. Mattweber, A. Fuchs, W. Zenz, P.H. Rehak, W.F. List, and H. Metzler. 2004. The effect of different stages of neuromuscular block on the Bispectral Index and the Bispectral Index-XP under remifentanil/propofol anesthesia. Anesthesia & Analgesia 99, no. 3, pages 781–787.

[26] O. Detsch, G. Schneider, E. Kochs, G. Hapfelmeier, and C. Werner. 2000. Increasing isoflurane concentration may cause paradoxical increases in the

EEG Bispectral Index in surgical patients. British Journal of Anaesthesia 84, no. 1, pages 33–37.

[27] O. Dressler, G. Schneider, G. Stockmanns, and E.F. Kochs. 2004. Awareness and the EEG power spectrum: analysis of frequencies. British Journal of Anaesthesia 93, no. 6, pages 806–809.

[28] J.C. Drummond. 2000. Monitoring depth of anesthesia. With emphasis on the application of the Bispetral Index and the middle latency auditory evoked response to the prevention of recall. Anesthesiology 93, no. 3, pages 876–882.

[29] G. Dumermuth, P.J. Huber, B. Kleiner, and T. Gasser. 1971. Analysis of interrelations between frequency bands of the EEG by means of the bispectrum: a preliminary study. Electroencephalography and Clinical Neurophysiology 31, no. 2, pages 137–148.

[30] D. Duncan, K.P. Kelly, and P.J.D. Andrews. 2006. A comparison of Bispectral Index and Entropy monitoring, in patients undergoing embolization of cerebral artery aneurysms after subarachnoid haemorrhage. British Journal of Anaesthesia 96, no. 5, pages 590–596.

[31] T.J. Ebert, J.E. Hall, J.A. Barney, T.D. Uhrich, and M.D. Colinco. 2000. The effects of increasing plasma concentrations of dexmedetomidine in humans. Anesthesiology 93, no. 2, pages 382–394.

[32] R.K. Ellerkmann, V.-M. Liermann, T.M. Alves, I. Wenningmann, S. Kreuer, W. Wilhelm, H. Roepcke, A. Hoeft, and J. Bruhn. 2004. Spectral entropy and Bispectral Index as measures of the electroencephalographic effects of sevoflurane. Anesthesiology 101, no. 6, pages 1275–1282.

[33] R.K. Ellerkmann, M. Soehle, T.M. Alves, V.-M. Liermann, I. Wenningmann, H. Roepcke, S. Kreuer, A. Hoeft, and J. Bruhn. 2006. Spectral entropy and Bispectral Index as measures of the electroencephalographic effects of propofol. Anesthesia & Analgesia 102, no. 5, pages 1456–1462.

[34] M. Ermes, M. Särkelä, M. van Gils, A. Vakkuri, A. Yli-Hankala, and V. Jäntti. 2006. Method for the automatic detection of epileptiform waveforms in sevoflurane-induced anesthesia EEG. In: Proceedings of the 28th

Annual International Conference of the IEEE Engineering in Medicine and Biology Society, pages 6343–6346. New York, NY, USA.

[35] T. Fawcett. 2006. An introduction to ROC analysis. Pattern Recognition Letters 27, no. 8, pages 861–874.

[36] R. Ferenets, A. Vanluchene, T. Lipping, B. Heyse, and M.M.R.F. Struys. 2007. Behavior of entropy/complexity measures of the electroencephalogram during propofol-induced sedation. Anesthesiology 106, no. 4, pages 696–706.

[37] B.J. Fisch. 1999. Fisch and Spehlmann's EEG Primer. Elsevier, Amsterdam, The Netherlands, third edition.

[38] P.L. Gambus, K. Gregg, and S.L. Shafer. 1995. Validation of the alfentanil canonical univariate parameter as a measure of opioid effect on the electroencephalogram. Anesthesiology 83, no. 4, pages 747–756.

[39] T.J. Gan, P.S. Glass, A. Windsor, F. Payne, C. Rosow, P. Sebel, and P. Manberg. 1997. Bispectral Index monitoring allows faster emergence and improved recovery from propofol, alfentanil, and nitrous oxide anesthesia. BIS Utility Study Group. Anesthesiology 87, no. 4, pages 808–815.

[40] M.M. Ghoneim. 2000. Awareness during anesthesia. Anesthesiology 92, no. 2, pages 597–602.

[41] P.S. Glass, M. Bloom, L. Kearse, C. Rosow, P. Sebel, and P. Manberg. 1997. Bispectral analysis measures sedation and memory effects of propofol, midazolam, isoflurane, and alfentanil in healthy volunteers. Anesthesiology 86, no. 4, pages 836–847.

[42] I.I. Goncharova, D.J. McFarland, T.M. Vaughan, and J.R. Wolpaw. 2003. EMG contamination of EEG: spectral and topographical characteristics. Clinical Neurophysiology 114, no. 9, pages 1580–1593.

[43] T. Goto, Y. Nakata, H. Saito, Y. Ishiguro, Y. Niimi, K. Suwa, and S. Morita. 2000. Bispectral analysis of the electroencephalogram does not predict responsiveness to verbal command in patients emerging from xenon anaesthesia. British Journal of Anaesthesia 85, no. 3, pages 359–363.

[44] K.M. Gregg, J.R. Varvel, and S.L. Shafer. 1992. Application of semilinear canonical correlation to the measurement of opiod drug effect. Journal of Pharmacokinetics and Biopharmaceutics 20, no. 6, pages 611–632.

[45] R. Greif, S. Greenwald, E. Schweitzer, S. Laciny, A. Rajek, J.E. Caldwell, and D.I. Sessler. 2002. Muscle relaxant does not alter hypnotic level during propofol anesthesia. Anesthesia & Analgesia 94, no. 3, pages 604–608.

[46] L.D. Gugino, R.J. Chabot, L.S. Prichep, E.R. John, V. Formanek, and L.S. Aglio. 2001. Quantitative EEG changes associated with loss and return of consciousness in healthy adult volunteers anaesthetized with propofol or sevoflurane. British Journal of Anaesthesia 87, no. 3, pages 421–428.

[47] B. Guignard, C. Coste, C. Menigaux, and M. Chauvin. 2001. Reduced isoflurane consumption with Bispectral Index monitoring. Acta Anaesthesiologica Scandinavica 45, no. 3, pages 308–314.

[48] M. Haenggi, H. Yppärilä, K. Hauser, C. Caviezel, I. Korhonen, J. Takala, and S.M. Jakob. 2006. The effects of dexmedetomidine/remifentanil and midazolam/remifentanil on auditory-evoked potentials and electroencephalogram at light-to-moderate sedation levels in healthy subjects. Anesthesia & Analgesia 103, no. 5, pages 1163–1169.

[49] S. Hagihira, M. Takashina, T. Mori, T. Mashimo, and I. Yoshiya. 2001. Practical issues in bispectral analysis of electroencephalographic signals. Anesthesia & Analgesia 93, no. 4, pages 966–970.

[50] S. Hagihira, M. Takashina, T. Mori, T. Mashimo, and I. Yoshiya. 2002. Changes of electroencephalographic bicoherence during isoflurane anesthesia compined with epidural anesthesia. Anesthesiology 97, no. 6, pages 1409–1415.

[51] S. Hagihira, M. Takashina, T. Mori, H. Ueyama, and T. Mashimo. 2004. Electroencephalographic bicoherence is sensitive to noxious stimuli during isoflurane or sevoflurane anesthesia. Anesthesiology 100, no. 4, pages 818–825.

[52] J.E. Hall, T.D. Uhrich, J.A. Barney, S.R. Arain, and T.J. Ebert. 2000. Sedative, amnestic, and analgesic properties of small-dose dexmedetomidine infusions. Anesthesia & Analgesia 90, no. 3, pages 699–705.

[53] P. Hans, P.-Y. Dewandre, J.F. Brichant, and V. Bonhomme. 2005. Comparative effects of ketamine on Bispectral Index and spectral entropy of the electroencephalogram under sevoflurane anaesthesia. British Journal of Anaesthesia 94, no. 3, pages 336–340.

[54] P. Hans, J. Giwer, J.F. Brichant, P.-Y. Dewandre, and V. Bonhomme. 2006. Effect of an intubation dose of rocuronium on spectral entropy and Bispectral Index^{TM} responses to laryngoscopy during propofol anaesthesia. British Journal of Anaesthesia 97, no. 6, pages 842–847.

[55] K. Hayashi, N. Tsuda, T. Sawa, and S. Hagihira. 2007. Ketamine increases the fequency of electroencephalographic bicoherence peak on the α spindle area induced with propofol. British Journal of Anaesthesia 99, no. 3, pages 389–395.

[56] M.H. Hayes. 1996. Statistical Digital Signal Processing and Modeling. John Wiley & Sons, Inc., USA.

[57] W. Hering, G. Geisslinger, H.D. Kamp, M. Dinkel, K. Tschaikowsky, E. Rügheimer, and K. Brune. 1994. Changes in the EEG power spectrum after midazolam anaeshesia combined with racemic or S-(+) ketamine. Acta Anaesthesiologica Scandinavica 38, no. 7, pages 719–723.

[58] C.A. Hilty and J.C. Drummond. 2000. Seizure-like activity on emergence from sevoflurane anesthesia. Anesthesiology 93, no. 5, pages 1357–1359.

[59] K. Hirota, T. Kubota, H. Ishihara, and A. Matsuki. 1999. The effects of nitrous oxide and ketamine on the Bispectral Index and 95% spectral edge frequency during propofol-fentanyl anaesthesia. European Journal of Anaesthesiology 16, no. 11, pages 779–783.

[60] T. Horiuchi, M. Kawaguchi, N. Kurita, S. Inoue, and H. Furuya. 2007. The validity of Bispectral Index values from dislocated sensor: A comparison with values from a sensor located in the commercially recommended position. Anesthesia & Analgesia 104, no. 4, pages 857–859.

[61] Y.-W. Hsu, L.I. Cortinez, K.M. Robertson, J.C. Keifer, S.T. Sum-Ping, E.W. Moretti, C.C. Young, D.R. Wright, D.B. MacLeod, and J. Somma. 2004. Dexmedetomidine pharmacodynamics: Part I: Crossover comparison of the respiratory effects of dexmedetomidine and remifentanil in healthy volunteers. Anesthesiology 101, no. 5, pages 1066–1076.

[62] M. Huiku, K. Uutela, M. van Gils, I. Korhonen, M. Kymäläinen, P. Meriläinen, M. Paloheimo, M. Rantanen, P. Takala, H. Viertiö-Oja, and A. Yli-Hankala. 2007. Assessment of surgical stress during general anesthesia. British Journal of Anaesthesia 98, no. 4, pages 447–455.

[63] E. Huupponen, A. Maksimow, P. Lapinlampi, M. Särkelä, A. Saastamoinen, A. Snapir, H. Scheinin, M. Scheinin, P. Meriläinen, S.-L. Himanen, and S. Jääskeläinen. 2008. Electroencephalogram spindle activity during dexmedetomidine sedation and physiological sleep. Acta Anaesthesiologica Scandinavica 52, no. 2, pages 289–294.

[64] M. Iannuzzi, E. Iannuzzi, F. Rossi, L. Berrino, and M. Chiefari. 2005. Relationship between Bispectral Index, electroencephalographic state entropy and effect-site EC50 for propofol at different clinical endpoints. British Journal of Anaesthesia 94, no. 4, pages 492–495.

[65] T. Iijima, Z. Nakamura, Y. Iwao, and H. Sankawa. 2000. The epileptogenic properties of the volative anesthetics sevoflurane and isoflurane in patients with epilepsy. Anesthesia & Analgesia 91, no. 4, pages 989–995.

[66] T. Inouye, K. Shinosaki, H. Sakamoto, S. Toi, S. Ukai, A. Iyama, Y. Katsuda, and M. Hirano. 1991. Quantification of EEG irregularity by use of the entropy of the power spectrum. Electroencephalography and Clinical Neurophysiology 79, no. 3, pages 204–210.

[67] T. Inouye, K. Shinosaki, H. Sakamoto, S. Toi, S. Ukai, A. Iyama, Y. Katsuda, and M. Hirano. 1992. Abnormality of background EEG determined by the entropy of power spectra in epileptic patients. Electroencephalography and Clinical Neurophysiology 82, no. 3, pages 203–207.

[68] S.K. Jääskeläinen, K. Kaisti, L. Suni, S. Hinkka, and H. Scheinin. 2003. Sevoflurane is epileptogenic in healthy subjects at surgical levels of anesthesia. Neurology 61, no. 8, pages 1073–1078.

[69] C. Jeleazcov, J. Fechner, and H. Schwilden. 2005. Electroencephalogram monitoring during anesthesia with propofol and alfentanil: The impact of second order spectral analysis. Anesthesia & Analgesia 100, no. 5, pages 1365–1369.

[70] E.W. Jensen, H. Litvan, M. Struys, and P. Martinez Vazquez. 2004. Pitfalls and challenges when assessing the depth of hypnosis during general anaesthesia by clinical signs and electronic indices. Acta Anaesthesiologica Scandinavica 48, no. 10, pages 1260–1267.

[71] J.W. Johansen. 2006. Update on Bispectral Index monitoring. Best Practice & Research Clinical Anesthesiology 20, no. 1, pages 81–99.

[72] J.W. Johansen and P.S. Sebel. 2000. Development and clinical application of electroencephalographic bispectrum monitoring. Anesthesiology 93, no. 5, pages 1336–1344.

[73] E.R. John and L.S. Prichep. 2005. The anesthetic cascade. A theory of how anesthesia suppresses consciousness. Anesthesiology 102, no. 2, pages 447–471.

[74] D. Jordan, G. Stockmanns, E.F. Kochs, and G. Schneider. 2007. Median frequency revisited. An approach to improve a classic spectral electroencephalographic parameter for the separation of consciousness from unconsciousness. Anesthesiology 107, no. 3, pages 397–405.

[75] B. Julliac, D. Guehl, F. Chopin, P. Arne, P. Burbaud, F. Sztark, and A.-M. Cros. 2007. Risk factors for the occurrence of electroencephalogram abnormalities during induction of anesthesia with sevoflurane in nonepileptic patients. Anesthesiology 106, no. 2, pages 243–251.

[76] J.F. Kaiser. 1990. On a simple algorithm to calculate the 'energy' of a signal. In: 1990 International Conference on Acoustics, Speech, and Signal Processing, volume 1, pages 381–384. Albuquerque, NM, USA.

[77] K.K. Kaisti, S.K. Jääskeläinen, J.O. Rinne, L. Metsähonkala, and H. Scheinin. 1999. Epileptiform discharges during 2 MAC sevoflurane anesthesia in two healthy volunteers. Anesthesiology 91, no. 6, pages 1952–1955.

[78] T. Katoh, A. Suzuki, and K. Ikeda. 1998. Electroencephalographic derivatives as a tool for predicting the depth of sedation and anesthesia induced by sevoflurane. Anesthesiology 88, no. 3, pages 642–650.

[79] L.A. Kearse, P. Manberg, N. Chamoun, F. deBros, and A. Zaslavsky. 1994. Bispectral analysis of the electroencephalogram correlates with patient movement to skin incision during propofol/nitrous oxide anesthesia. Anesthesiology 81, no. 6, pages 1365–1370.

[80] L.A. Kearse, P. Manberg, F. DeBros, N. Chamoun, and V. Sinai. 1994. Bispectral analysis of the electroencephalogram during induction of anesthesia may predict hemodynamic responses to laryngoscopy and intubation. Electroencephalography and Clinical Neurophysiology 90, no. 3, pages 194–200.

[81] S.D. Kelley. 2003. Monitoring Level of Consciousness during Anesthesia and Sedation. A Clinicians Guide to the Bispectral Index®. Aspect Medical Systems, Norwood, MA, USA, first edition.

[82] E. Kochs, E. Scharein, O. Mollenberg, B. Bromm, and J. Schulte am Esch. 1996. Analgesic efficacy of low-dose ketamine: Somatosensory-evoked responses in relation to subjective pain ratings. Anesthesiology 85, no. 2, pages 304–314.

[83] R. Kohrs and M.E. Duriex. 1998. Ketamine: Teaching an old drug new tricks. Anesthesia & Analgesia 87, no. 5, pages 1186–1193.

[84] M. Koskinen, S. Mustola, and T. Seppänen. 2005. Relation of EEG spectrum progression to loss of responsiveness during induction of anesthesia with propofol. Clinical Neurophysiology 116, no. 9, pages 2069–2076.

[85] M. Koskinen, S. Mustola, and T. Seppänen. 2006. Forecasting the unresponsiveness to verbal command on the basis of EEG frequency pregression during anesthetic induction with propofol. IEEE Transactions on Biomedical Engineering 53, no. 10, pages 2008–2014.

[86] S.L. Krachman, G.E. D'Alonzo, and G.J. Criner. 1995. Sleep in the intensive care unit. Chest 107, no. 6, pages 1713–1720.

[87] S. Kreuer, J. Bruhn, R. Larsen, U. Grundmann, S.L. Shafer, and W. Wilhelm. 2004. Application of Bispectral Index® and Narcotrend® index to the measurement of the electroencephalographic effects of isoflurane with and without burst suppression. Anesthesiology 101, no. 4, pages 847–854.

[88] S. Kreuer, J. Bruhn, C. Stracke, L. Aniset, M. Silomon, R. Larsen, and W. Wilhelm. 2005. Narcotrend or Bispectral Index monitoring during desflurane-remifentanil anesthesia: A comparison with a standard practice protocol. Anesthesia & Analgesia 101, no. 2, pages 427–434.

[89] K. Kuizenga, C.J. Kalkman, and P.J. Hennis. 1998. Quantitative electroencephalographic analysis of the biphasic concentration-effect relationship of propofol in surgical patients during extradural analgesia. British Journal of Anaesthesia 80, no. 6, pages 725–732.

[90] K. Kuizenga, J.M.K.H. Wierda, and C.J. Kalkman. 2001. Biphasic EEG changes in relation to loss of consciousness during induction with thiopental, propofol, etomidate, midazolam or sevoflurane. British Journal of Anaesthesia 86, no. 3, pages 354–360.

[91] R.M. Laitio, K. Kaskinoro, M.O.K. Särkelä, K.K. Kaisti, E. Salmi, A. Maksimow, J.W. Långsjö, R. Aantaa, K. Kangas, S. Jääskeläinen, and H. Scheinin. 2008. Bispectral Index, Entropy and quantitative electroencephalogram during single-agent xenon anesthesia. Anesthesiology 108, no. 1, pages 63–70.

[92] W.L. Lanier, J.H. Milde, and J.D. Michenfelder. 1986. Cerebral stimulation following succinylcholine in dogs. Anesthesiology 64, no. 5, pages 551–559.

[93] K. Leslie, D.I. Sessler, W.D. Smith, M.D. Larson, M. Ozaki, D. Blanchard, and D.P. Crankshaw. 1996. Prediction of movement during propofol/nitrous oxide anesthesia: Performance of concentration, electroencephalographic, pupillary, and hemodynamic indicators. Anesthesiology 84, no. 1, pages 52–63.

[94] W.J. Levy. 1984. Intraoperative EEG patterns: Implications for EEG monitoring. Anesthesiology 60, no. 5, pages 430–434.

[95] T. Lipping, V. Jäntti, A. Yli-Hankala, and K. Hartikainen. 1995. Adaptive segmentation of burst-suppression pattern in isoflurane and enflurane anesthesia. International Journal of Clinical Monitoring and Computing 12, no. 3, pages 161–167.

[96] N. Liu, T. Chazot, I. Huybrechts, J.-D. Law-Koune, L. Barvais, and M. Fischler. 2005. The influence of a muscle relaxant bolus on Bispectral and Datex-Ohmeda Entropy values during propofol-remifentanil induced loss of consciousness. Anesthesia & Analgesia 101, no. 6, pages 1713–1718.

[97] A. Maksimow. 2006. The effects of anesthesia and sedation on EEG spectral entropy and regional cerebral blood flow. Positron emission tomography and EEG studies on healthy male subjects. Ph.D. thesis, University of Turku, Finland.

[98] P.P. Martorano, G. Falzetti, and P. Pelaia. 2006. Bispectral Index and spectral entropy in neuroanesthesia. Journal of Neurosurgical Anesthesiology 18, no. 3, pages 205–210.

[99] D.M. Mathews, P.M. Cirullo, M.M.R.F. Struys, T. De Smet, R.J. Malik, C.L. Chang, and G.G. Neuman. 2007. Feasibility study for the administration of remifentanil based on the difference between response entropy and state entropy. British Journal of Anaesthesia 98, no. 6, pages 785–791.

[100] I.D.H. McKay, L.J. Voss, J.W. Sleigh, J.P. Barnard, and E.K. Johannsen. 2006. Pharmacokinetic-pharmacodynamic modeling the hypnotic effect of sevoflurane using the spectral entropy of the electroencephalogram. Anesthesia & Analgesia 102, no. 1, pages 91–97.

[101] M. Messner, U. Beese, J. Romstöck, M. Dinkel, and K. Tschaikowsky. 2003. The Bispectral Index declines during neuromuscular block in fully awake persons. Anesthesia & Analgesia 97, no. 2, pages 488–491.

[102] D. Michael and J. Houchin. 1979. Automatic EEG analysis: A segmentation procedure based on the autocorrelation function. Electroencephalography and Clinical Neurophysiology 46, no. 2, pages 232–235.

[103] A. Miller, J.W. Sleigh, J. Barnard, and D.A. Steyn-Ross. 2004. Does bispectral analysis of the electroencephalogram add anything but complexity? British Journal of Anaesthesia 92, no. 1, pages 8–13.

[104] R.D. Miller. 2005. Miller's Anesthesia, volume 1. Elsevier Churchill Livingstone, Philadelphia, PA, USA, sixth edition.

[105] Y. Morimoto, S. Hagihira, Y. Koizumi, K. Ishida, M. Matsumoto, and T. Sakabe. 2004. The relationship between Bispectral Index and electroencephalographic parameters during isoflurane anesthesia. Anesthesia & Analgesia 98, no. 5, pages 1336–1340.

[106] Y. Morimoto, S. Hagihira, S. Yamashita, Y. Iida, M. Matsumoto, S. Tsuruta, and T. Sakabe. 2006. Changes in electroencephalographic bicoherence during sevoflurane anesthesia combined with intravenous fentanyl. Anesthesia & Analgesia 103, no. 3, pages 641–645.

[107] P.S. Myles, K. Leslie, J. McNeil, A. Forbes, and M.T.V. Chan. 2004. Bispectral Index monitoring to prevent awareness during anesthesia: the B-Aware randomized controlled trial. Lancet 363, no. 9423, pages 1757–1763.

[108] M. Naguib, A.F. Kopman, and J.E. Ensor. 2007. Neuromuscular monitoring and postoperative residual curarization: a meta-analysis. British Journal of Anaesthesia 98, no. 3, pages 302–316.

[109] L.E. Nelson, J. Lu, T. Guo, C.B. Saper, N.P. Franks, and M. Maze. 2003. The α_2-adrenoreceptor agonist dexmedetomidine converges on an endogenous sleep-promoting pathway to exert its sedative effects. Anesthesiology 98, no. 2, pages 428–436.

[110] E. Niedermeyer and F. Lopes da Silva. 1999. Electroencephalography. Basic Principles, Clinical Applications, and Related Fields. Lippincott Williams & Wilkins, Baltimore, MD, USA, fourth edition.

[111] D.J. Niedhart, H.A. Kaiser, E. Jacobsohn, C.B. Hantler, A.S. Evers, and M.S. Avidan. 2006. Intrapatient reproducibility of the BISxp® monitor. Anesthesiology 104, no. 2, pages 242–248.

[112] C.L. Nikias and M.R. Raghuveer. 1987. Bispectrum estimation: A digital signal processing framework. Proceedings of the IEEE 75, no. 7, pages 869–891.

[113] E. Olofsen, J.W. Sleigh, and A. Dahan. 2002. The influence of remifentanil on the dynamic relationship between sevoflurane and surrogate anesthetic effect measures derived from the EEG. Anesthesiology 96, no. 3, pages 555–564.

[114] J.S. Paul, C.B. Patel, H. Al-Nashash, N. Zhang, W.C. Ziai, M.A. Mirski, and D.L. Sherman. 2003. Prediction of PTZ-induced seizures using wavelet-based residual entropy of cortical and subcortical field potentials. IEEE Transactions on Biomedical Engineering 50, no. 5, pages 640–648.

[115] J.D. Pavlin, K.J. Souter, J.Y. Hong, P.R. Freund, T.A. Bowdle, and J.O. Bower. 2005. Effects of Bispectral Index monitoring on recovery from surgical anesthesia in 1580 inpatients from an academic medical center. Anesthesiology 102, no. 3, pages 566–573.

[116] W.W. Peterson, T.G. Birdsall, and W.C. Fox. 1954. The theory of signal detectability. IEEE Transactions on Information Theory 4, no. 4, pages 171–212.

[117] G. Pfurtscheller and F.H. Lopes da Silva. 1999. Handbook of Electroencephalography and Clinical Neurophysiology. Revised Series, Volume 6. Event-Related Desynchronization. Elsevier Science B.V., Amsterdam, The Netherlands.

[118] S. Pilge, R. Zanner, G. Schneider, J. Blum, M. Kreuzer, and E.F. Kochs. 2006. Time delay of index calculation. Analysis of Cerebral State, Bispectral, and Narcotrend Indices. Anesthesiology 104, no. 3, pages 488–494.

[119] E.I. Plotkin and M.N.S. Swamy. 1998. Signal processing based on parameter structural modeling and separation of highly correlated signals of known structure. Circuits, Systems & Signal Processing 17, no. 1, pages 51–68.

[120] G. Plourde, J. Baribeau, and V. Bonhomme. 1997. Ketamine increases the amplitude of the 40-Hz auditory steady-state response in humans. British Journal of Anaesthesia 78, no. 5, pages 524–529.

[121] G.E. Powell and I.C. Percival. 1979. A spectral entropy method for distinguishing regular and irregular motion of Hamiltonian systems. Journal of Physics A: Mathematical and General 12, no. 11, pages 2053–2071.

[122] R. Quian Quiroga, O.A. Rosso, E. Başar, and M. Schürmann. 2001. Wavelet entropy in event-related potentials: a new method shows ordering EEG oscillations. Biological Cybernetics 84, no. 4, pages 291–299.

[123] I.J. Rampil. 1994. Anesthetic potency is not altered after hypothermic spinal cord transection in rats. Anesthesiology 80, no. 3, pages 606–610.

[124] I.J. Rampil. 1998. A primer for EEG signal processing in anesthesia. Anesthesiology 89, no. 4, pages 980–1002.

[125] I.J. Rampil, J.S. Kim, R. Lenhardt, C. Negishi, and D.I. Sessler. 1998. Bispectral EEG index during nitrous oxide administration. Anesthesiology 89, no. 3, pages 671–677.

[126] I.J. Rampil, S.H. Lockhart, E.I. Eger, N. Yasuda, R.B. Weiskopf, and M.K. Cahalan. 1991. The electroencephalographic effects of desflurane in humans. Anesthesiology 74, no. 3, pages 434–439.

[127] I.J. Rampil, P. Mason, and H. Singh. 1993. Anesthetic potency (MAC) is independent of forebrain structures in the rat. Anesthesiology 78, no. 4, pages 707–712.

[128] I.J. Rampil, R.B. Weiskopf, J.G. Brown, E.I. Eger, B.H. Johnson, M.A. Holmes, and J.H. Donegan. 1988. I653 and isoflurane produce similar dose-related changes in the electroencephalogram of pigs. Anesthesiology 69, no. 3, pages 298–302.

[129] M. Renna, T. Wigmore, A. Mofeez, and C. Gillbe. 2002. Biasing effect of the electromyogram on BIS: A controlled study during high-dose fentanyl induction. Journal of Clinical Monitoring and Computing 17, no. 6, pages 377–381.

[130] I. Rezek, S.J. Roberts, and R. Conradt. 2007. Increasing the depth of anesthesia assessment. Better higher-order statistics with generative polyspectral models. IEEE Engineering in Medicine and Biology 26, no. 2, pages 64–73.

[131] I.A. Rezek and S.J. Roberts. 1998. Stochastic complexity measures for physiological signal analysis. IEEE Transactions on Biomedical Engineering 45, no. 9, pages 1186–1191.

[132] S. Rinaldi, G. Consales, and A.R. de Gaudio. 2007. State entropy and Bispectral Index: correlation with end tidal sevoflurane concentrations. Minerva Anestesiologica 73, no. 1-2, pages 39–48.

[133] H. Röpcke, B. Rehberg, M. Koenen-Bergmann, T. Bouillon, J. Bruhn, and A. Hoeft. 2001. Surgical stimulation shifts EEG concentration-response relationship of desflurane. Anesthesiology 94, no. 3, pages 390–399.

[134] O.A. Rosso, S. Blanco, and A. Rabinowicz. 2003. Wavelet analysis of generalized tonic-clonic epileptic seizures. Signal Processing 83, no. 6, pages 1275–1289.

[135] O.A. Rosso, S. Blanco, J. Yordanova, V. Kolev, A. Figliola, M. Schürmann, and Başar. 2001. Wavelet entropy: a new tool for analysis of short duration brain electrical signals. Journal of Neuroscience Methods 105, no. 1, pages 65–75.

[136] T. Sakai, H. Singh, W.D. Mi, T. Kudo, and A. Matsuki. 1999. The effect of ketamine on clinical endpoints of hypnosis and EEG variables during propofol infusion. Acta Anaesthesiologica Scandinavica 43, no. 2, pages 212–216.

[137] E. Salmi, K.K. Kaisti, L. Metsähonkala, V. Oikonen, S. Aalto, K. Någren, S. Hinkka, J. Hietala, E.R. Korpi, and H. Scheinin. 2004. Sevoflurane and propofol increase ^{11}C-flumazenil binding to gamma-aminobutyric acid$_{\mathrm{A}}$ receptors in humans. Anesthesia & Analgesia 99, no. 5, pages 1420–1426.

[138] R.D. Sanders, N.P. Franks, and M. Maze. 2003. Xenon: no stranger to anaesthesia. British Journal of Anaesthesia 91, no. 5, pages 709–717.

[139] R. Sandin, G. Enlund, P. Samuelsson, and C. Lennmarken. 2000. Awareness during anaesthesia: a prospective case study. Lancet 355, no. 9205, pages 707–711.

[140] G.N. Schmidt, P. Bischoff, T. Standl, A. Hellstern, O. Teuber, and J. Schulte am Esch. 2004. Comparative evaluation of the Datex-Ohmeda S/5 Entropy

module and Bispectral Index® monitor during propofol-remifentanil anesthesia. Anesthesiology 101, no. 6, pages 1283–1290.

[141] G.N. Schmidt, P. Bischoff, T. Standl, K. Jensen, M. Voigt, and J. Schulte am Esch. 2003. Narcotrend® and Bispectral Index® monitor are superior to classic electroencephalographic parameters for the assessment of anesthetic states during propofol-remifentanil anesthesia. Anesthesiology 99, no. 5, pages 1072–1077.

[142] G.N. Schmidt, P. Bischoff, T. Standl, G. Lankenau, M. Hilbert, and J. Schulte am Esch. 2004. Comparative evaluation of Narcotrend™, Bispectral Index™, and classical electroencephalographic variables during induction, maintenance, and emergence of a propofol/remifentanil anesthesia. Anesthesia & Analgesia 98, no. 5, pages 1346–1353.

[143] G. Schneider, A.W. Gelb, B. Schmeller, R. Tschakert, and E. Kochs. 2003. Detection of awareness in surgical patients with EEG-based indices — Bispectral Index and Patient State Index. British Journal of Anaesthesia 91, no. 3, pages 329–335.

[144] T.W. Schnider, C.F. Minto, P. Fiset, K.M. Gregg, and S.L. Shafer. 1996. Semilinear canonical correlation applied to the measurement of the electroencephalographic effects of midazolam and flumazenil reversal. Anesthesiology 84, no. 3, pages 510–519.

[145] T.W. Schnider, C.F. Minto, S.L. Shafer, P.L. Gambus, C. Andresen, D.B. Goodale, and E.J. Youngs. 1999. The influence of age on propofol pharmacodynamics. Anesthesiology 90, no. 6, pages 1502–1516.

[146] A.E. Schwartz, A.T. Navedo, and M.F. Berman. 1992. Pancuronium increases the duration of electroencephalogram burst suppression in dogs anesthetized with isoflurane. Anesthesiology 77, no. 4, pages 686–690.

[147] M.S. Schwartz, S. Virden, and D.F. Scott. 1974. Effects of ketamine on the electroencephalograph. Anaesthesia 29, no. 2, pages 135–140.

[148] D. Schwender, M. Daunderer, S. Klasing, U. Finsterer, and K. Peter. 1998. Power spectral analysis of the electroencephalogram during increasing end-

expiratory concentrations of isoflurane, desflurane and sevoflurane. Anaesthesia 53, no. 4, pages 335–342.

[149] H. Schwilden and C. Jeleazcov. 2002. Does the EEG during isoflurane/alfentanil anesthesia differ from linear random data? Journal of Clinical Monitoring and Computing 17, no. 7-8, pages 449–457.

[150] P.S. Sebel, T.A. Bowdle, M.M. Ghoneim, I.J. Rampil, R.E. Padilla, T.J. Gan, and K.B. Domino. 2004. The incidence of awareness during anesthesia: A multicenter United States study. Anesthesia & Analgesia 99, no. 3, pages 833–839.

[151] P.S. Sebel, S.M. Bowles, V. Saini, and N. Chamoun. 1995. EEG bispectrum predicts movement during thiopental/isoflurane anesthesia. Journal of Clinical Monitoring 11, no. 2, pages 83–91.

[152] E.R.J. Seitsonen, I.K.J. Korhonen, M.J. van Gils, M. Huiku, J.M.P. Lötjönen, K.T. Korttila, and A.M. Yli-Hankala. 2005. EEG spectral entropy, heart rate, photoplethysmography and motor responses to skin incision during sevoflurane anaesthesia. Acta Anaesthesiologica Scandinavica 49, no. 3, pages 284–292.

[153] C.E. Shannon and W. Weaver. 1949. The Mathematical Theory of Communication. University of Illinois Press, Urbana and Chicago, IL, USA, 1998 edition.

[154] M.D. Sharpe, G.B. Young, S. Mirsattari, and C. Harris. 2002. Prolonged desflurane administration for refractory status epilepticus. Anesthesiogy 97, no. 1, pages 261–264.

[155] D.L. Sherman, M.K. Atit, R.G. Geocadin, S. Venkatesha, D.F. Hanley, A.L. Natarajan, and N.V. Thakor. 2002. Diagnostic instrumentation for neurological injury. IEEE Instrumentarium & Measurement Magazine 5, no. 2, pages 28–34.

[156] J.C. Sigl and N.G. Chamoun. 1994. An introduction to bispectral analysis for the electroencephalogram. Journal of Clinical Monitoring 10, no. 6, pages 392–404.

[157] J.W. Sleigh, D.A. Steyn-Ross, M.L. Steyn-Ross, M.L. Williams, and P. Smith. 2001. Comparison of changes in electroencephalographic measures during induction of general anaesthesia: influence of the gamma frequency band and electromyogram signal. British Journal of Anaesthesia 86, no. 1, pages 50–58.

[158] T.B. Sloan. 1998. Anesthetic effects on electrophysiologic recordings. Journal of Clinical Neurophysiology 15, no. 3, pages 217–226.

[159] W.D. Smith, R.C. Dutton, and N.T. Smith. 1996. A measure of association for assessing prediction accuracy that is a generalization of non-parametric ROC area. Statistics in Medicine 15, no. 11, pages 1199–1215.

[160] W.D. Smith, R.C. Dutton, and N.T. Smith. 1996. Measuring the performance of anesthetic depth indicators. Anesthesiology 84, no. 1, pages 38–51.

[161] D. Song, G. Joshi, and P. White. 1997. Titration of volatile anesthetics using Bispectral Index facilitates recovery after ambulatory anesthesia. Anesthesiology 87, no. 4, pages 842–848.

[162] L. Sörnmo and P. Laguna. 2005. Bioelectrical Signal Processing in Cardiac and Neurological Applications. Elsevier Academic Press, San Diego, CA, USA.

[163] R.G. Soto, R.A. Smith, A.L. Zaccaria, and R.V. Miguel. 2006. The effect of addition of nitrous oxide to a sevoflurane anesthetic on BIS, PSI, and Entropy. Journal of Clinical Monitoring and Computing 20, no. 3, pages 145–150.

[164] M. Struys, L. Versichelen, E. Mortier, D. Ryckaert, J.C. De Mey, C. De Deyne, and G. Rolly. 1998. Comparison of spontaneous frontal EMG, EEG power spectrum and Bispectral Index to monitor propofol drug effect and emergence. Acta Anaesthesiologica Scandinavica 42, no. 6, pages 628–636.

[165] M.M.R.F. Struys, H. Vereecke, A. Moerman, E.W. Jensen, D. Verhaegen, N. De Neve, F.J.E. Dumortier, and E.P. Mortier. 2003. Ability of Bispectral Index, autoregressive modelling with exogenous input-derived auditory evoked potentials, and predicted propofol concentrations to measure patient

responsiveness during anesthesia with propofol and remifentanil. Anesthesiology 99, no. 4, pages 802–812.

[166] M. Suzuki, H.L. Edmonds, K. Tsueda, A.L. Malkani, and C.S. Roberts. 1998. Effect of ketamine on Bispectral Index and levels of sedation. Journal of Clinical Monitoring and Computing 14, no. 5, page 373.

[167] A. Swami, J.M. Mendel, and C.L. Nikias. 1998. Higher-Order Spectral Analysis Toolbox User's Guide, Version 2. The Mathworks, Inc., Natick, MA, USA, third edition.

[168] I. Takamatsu, M. Ozaki, and T. Kazama. 2006. Entropy indices vs the Bispectral Index^{TM} for estimating nociception during sevoflurane anesthesia. British Journal of Anaesthesia 96, no. 5, pages 620–626.

[169] TaskForce. 2006. Practice advisory for intraoperative awareness and brain function monitoring. Anesthesiology 104, no. 4, pages 847–864.

[170] C.E. Thomsen and P.F. Prior. 1996. Quantitative EEG in assessment of anaesthetic depth: comparative study of methodology. British Journal of Anaesthesia 77, no. 2, pages 172–178.

[171] P.H. Tonner, C. Wei, B. Bein, N. Weiler, A. Paris, and J. Scholz. 2005. Comparison of two Bispectral Index algorithms in monitoring sedation in postoperative intensive care patients. Critical Care Medicine 33, no. 3, pages 580–584.

[172] D.M. Treiman. 1995. Electroclinical features of status epilepticus. Journal of Clinical Neurophysiology 12, no. 4, pages 343–362.

[173] D.M. Treiman, N.Y. Walton, and C. Kendrick. 1990. A progressive sequence of electroencephalographic changes during generalized convulsive status epilepticus. Epilepsy Research 5, no. 1, pages 49–60.

[174] A.E. Triltsch, M. Welte, P. von Homeyer, J. Große, A. Genähr, M. Moshirzadeh, A. Sidiropoulos, W. Konertz, W.J. Kox, and C.D. Spies. 2002. Bispectral Index-guided sedation with dexmedetomidine in intensive care: A prospective, randomized, double blind, placebo-controlled phase II study. Critical Care Medicine 30, no. 5, pages 1007–1014.

[175] N. Tsuda, K. Hayashi, S. Hagihira, and T. Sawa. 2007. Ketamine, an NMDA-antagonist, increases the oscillatory frequencies of α-peaks on the electroencephalographic power spectrum. Acta Anaesthesiologica Scandinavica 51, no. 4, pages 472–481.

[176] A. Vakkuri, V. Jäntti, M. Särkelä, L. Lindgren, K. Korttila, and A. Yli-Hankala. 2000. Epileptiform EEG during sevoflurane mask induction: Effect of delaying the onset of hyperventilation. Acta Anaesthesiologica Scandinavica 44, no. 6, pages 713–719.

[177] A. Vakkuri, A. Yli-Hankala, R. Sandin, S. Mustola, S. Høymork, S. Nyblom, P. Talja, T. Sampson, M. van Gils, and H. Viertiö-Oja. 2005. Spectral entropy monitoring is associated with reduced propofol use and faster emergence in propofol-nitrous oxide-alfentanil anesthesia. Anesthesiology 103, no. 2, pages 274–279.

[178] A. Vakkuri, A. Yli-Hankala, M. Särkelä, L. Lindgren, S. Mennander, K. Korttila, L. Saarnivaara, and V. Jäntti. 2001. Sevoflurane mask induction of anaesthesia is associated with epileptiform EEG in children. Acta Anaesthesiologica Scandinavica 45, no. 7, pages 805–811.

[179] A. Vakkuri, A. Yli-Hankala, P. Talja, S. Mustola, H. Tolvanen-Laakso, T. Sampson, and H. Viertiö-Oja. 2004. Time-frequency balanced spectral entropy as a measure of anesthetic drug effect in central nervous system during sevoflurane, propofol, and thiopental anesthesia. Acta Anaesthesiologica Scandinavica 48, no. 2, pages 145–153.

[180] A.P. Vakkuri, E.R. Seitsonen, V.H. Jäntti, M. Särkelä, K.T. Korttila, M.P.J. Paloheimo, and A.M. Yli-Hankala. 2005. A rapid increase in the inspired concentration of desflurane is not associated with epileptiform encephalogram. Anesthesia & Analgesia 101, no. 2, pages 396–400.

[181] A.L.G. Vanluchene, M.M.R.F. Struys, B.E.K. Heyse, and E.P. Mortier. 2004. Spectral entropy measurement of patient responsiveness during propofol and remifentanil. A comparison with the Bispectral Index. British Journal of Anaesthesia 93, no. 5, pages 645–654.

[182] A.L.G. Vanluchene, H. Vereecke, O. Thas, E.P. Mortier, S.L. Shafer, and M.M.R.F. Struys. 2004. Spectral entropy as an electroencephalographic measure of anesthetic drug effect. A comparison with Bispectral Index and processed midlatency auditory evoked response. Anesthesiology 101, no. 1, pages 34–42.

[183] F.C. Vasella, P. Frascarolo, D.R. Sandin, and L. Magnusson. 2005. Antagonism of neuromuscular blockade but not muscle relaxation affects depth of anesthesia. British Journal of Anaesthesia 94, no. 6, pages 742–747.

[184] L.J. Velly, M.F. Rey, N.J. Bruder, F.A. Gouvitsos, T. Witjas, J.M. Regis, J.C. Peragut, and F.M. Gouin. 2007. Differential dynamic of action on cortical and subcortical structures of anesthetic agents during induction of anesthesia. Anesthesiology 107, no. 2, pages 202–212.

[185] R.M. Venn and R.M. Grounds. 2001. Comparison between dexmedetomidine and propofol for sedation in the intensive care unit: patient and clinician perceptions. British Journal of Anaesthesia 87, no. 5, pages 684–690.

[186] R.M. Venn, J. Hell, and R.M. Grounds. 2000. Respiratory effects of dexmedetomidine in the surgical patient requiring intensive care. Critical Care 4, no. 5, pages 302–308.

[187] H.E.M. Vereecke, M.M.R.F. Struys, and E.P. Mortier. 2003. A comparison of Bispectral Index and ARX-derived auditory evoked potential index in measuring the clinical interaction between ketamine and propofol anaesthesia. Anaesthesia 58, no. 10, pages 957–961.

[188] H.E.M. Vereecke, A.L. Vanluchene, E.P. Mortier, K. Everaert, and M.M.R.F. Struys. 2006. The effects of ketamine and rocuronium on the A-line® auditory evoked potential index, Bispectral Index, and spectral entropy monitor during steady state propofol and remifentanil anesthesia. Anesthesiology 105, no. 6, pages 1122–1134.

[189] H.E.M. Vereecke, P.M. Vasquez, E.W. Jensen, O. Thas, R. Vandenbroecke, E.P. Mortier, and M.M.R.F. Struys. 2005. New composite index based on midlatency auditory evoked potential and electroencephalographic parameters to optimize correlation with propofol effect site concentration. Com-

parison with Bispectral Index and solitary used extracting auditory evoked potential index. Anesthesiology 103, no. 3, pages 500–507.

[190] J.M. Vernon, E. Lang, P.S. Sebel, and P. Manberg. 1995. Prediction of movement using bispectral electroencephalographic analysis during propofol/alfentanil or isoflurane/alfentanil anesthesia. Anesthesia & Analgesia 80, no. 4, pages 780–785.

[191] B. Walder, M.R. Tramèr, and M. Seeck. 2002. Seizure-like phenomena and propofol: A systematic review. Neurology 58, no. 9, pages 1327–1332.

[192] T.S. Walsh, P. Ramsay, T.P. Lapinlampi, M.O.K. Särkelä, H.E. Viertiö-Oja, and P.T. Meriläinen. 2008. An assessment of the validity of spectral entropy as a measure of sedation state in mechanically ventilated critically ill patients. Intensive Care Medicine 34, no. 2, pages 308–315.

[193] J. Wennervirta, T. Salmi, M. Hynynen, A. Yli-Hankala, A.-M. Koivusalo, M. van Gils, R. Pöyhiä, and A. Vakkuri. 2007. Entropy is more resistant to artifacts than Bispectral Index in brain-dead organ donors. Intensive Care Medicine 33, no. 1, pages 133–136.

[194] P. Wheeler, W.E. Hoffman, V.L. Baughman, and H. Koenig. 2005. Response entropy increases during painful stimulation. Journal of Neurosurgical Anesthesiology 17, no. 2, pages 86–90.

[195] P.F. White, W.L. Way, and A.J. Trevor. 1982. Ketamine - its pharmacology and therapeutic uses. Anesthesiology 56, no. 2, pages 119–136.

[196] R.F. White, J. Tang, G.F. Romero, R.H. Wender, R. Naruse, A. Sloninsky, and R. Kariger. 2006. A comparison of state and response entropy versus Bispectral Index values during the perioperative period. Anesthesia & Analgesia 102, no. 1, pages 160–167.

[197] H. Witte, C. Schelenz, M. Specht, H. Jäger, P. Putsche, M. Arnold, L. Leistritz, and K. Reinhart. 1999. Interrelations between EEG frequency components in sedated intensive care patients during burst-suppression period. Neuroscience Letters 260, no. 1, pages 53–56.

[198] I.J. Woodforth, R.G. Hicks, M.R. Crawford, J.P.H. Stephen, and D.J. Burke. 1997. Electroencephalographic evidence of seizure activity under deep sevoflurane anesthesia in a nonepileptic patient. Anesthesiology 87, no. 6, pages 1579–1582.

[199] C.C. Wu, M.S. Mok, C.S. Lin, and S.R. Han. 2001. EEG-Bispectral Index changes with ketamine versus thiamylal induction of anesthesia. Acta anaesthesiologica Sinica 39, no. 1, pages 11–15.

[200] A. Yli-Hankala, A. Vakkuri, M. Särkelä, L. Lindgren, K. Korttila, and V. Jäntti. 1999. Epileptiform electroencephalogram during mask induction of anesthesia with sevoflurane. Anesthesiology 91, no. 6, pages 1596–1603.

[201] G.B. Young. 2000. The EEG in coma. Journal of Clinical Neurophysiology 17, no. 5, pages 473–485.

ISBN 978-951-22-9288-2
ISBN 978-951-22-9289-9 (PDF)
ISSN 1795-2239
ISSN 1795-4584 (PDF)